DESIGNING CONTACT LENSES FOR EPITHELIAL CELL TRANSFER: EFFECT OF SURFACE GEOMETRY, SURFACE COATING AND CELL MOTILITY

By

Christopher James Pino

Dissertation

Submitted to the Faculty of the

Graduate School of Vanderbilt University

in partial fulfillment of the requirements

for the degree of

DOCTOR OF PHILOSOPHY

in

Biomedical Engineering

December, 2006

Nashville, Tennessee

Approved:	Date:
Frederick Haselton	11/29/2006
Min S. Chang	11/22/2006
V. Prasad Shastri	11/29/2006
Franz Baudenbacher	11/29/2006
Uyen Tran	11/29/2006

ACKNOWLEDGEMENTS

I would like to thank the many people at Vanderbilt University who have made the completion of this dissertation possible. I thank my committee members, Dr. Rick Haselton, Dr. Min Chang, Dr. Prasad Shastri, Dr. Franz Baudenbaucher, and Dr. Uyen Tran, for their insight, advice, and support. I particularly want to thank Dr. Haselton, my primary advisor, for his time and effort on this project. I admire his ability to adapt to different types of projects outside his primary expertise. His patience and personable demeanor made our lab an enjoyable work environment. I would like to thank Dr. Chang for his encouragement and commitment to this project and my education. I thank Dr. Shastri for his enthusiasm and "big idea" mentality, which has helped this work to come to fruition. I would also like to thank Dr. Tran and Dr. Baudenbacher for their practical expertise, which was invaluable. I thank Elizabeth Dworska for her patient teaching of cell technique, and for her diligent and constant help with cell line upkeep. Ash, Greg, and Elizabeth, you are like family to me. Thanks for making this time in my life more enjoyable and for your daily encouragement. I would like to acknowledge the financial support of two great institutions: NIH and Vanderbilt University whose investment in me is greatly appreciated.

I would like to thank the members of Vandy GCF and Fellowship Bible Church for their fellowship and prayers. I thank my parents for their love and education as my teachers in life. I couldn't have studied with better people! I thank my wife, Trish, for her unconditional love and guidance as my partner in life. Most importantly, I thank God for His constant presence in my life.

TABLE OF CONTENTS

LIST OF FIGURES

LIST OF EQUATIONS

LIST OF ABBREVIATIONS

Abbreviation	Definition
AJ	Adherens junction
AM	Amniotic membrane
C-Bves	Chick - Blood vessel epicardial substance
C-Bves HCE	C-Bves transfected human corneal epithelia
CCD	Charge-coupled device
CTG	Cell Tracker green
CTR	Cell Tracker red
D	DESMOSOME
DKSFM	Defined keratinocyte serum free medium
DMEM	Dulbecco's modified Eagle medium
ECM	Extracellular matrix
EGF	Epithelial growth factor
EMT	Epithelial-Mesenchymal Transition
FN	Fibronectin
GFP	Green fluorescence protein
HCEC	Human corneal epithelial cells
HLA	Human leukocyte antigen
LASEK	LASER assisted epithelial keratomileusis
LASIK	LASER assisted in situ keratomileusis
NaFl	Sodium fluorescein
PBS	Phosphate buffered saline
PDMS	Polydimethylsiloxane
PK	Penetrating keratectomy
PRK	Photorefractive keratectomy
PTK	Phototherapeutic keratectomy
RFP	Red fluorescence protein
t-Bves	Truncated - Blood vessel epicardial substance
t-Bves HCE	Truncated Bves transfected human corneal epithelia
TCL	Therapeutic contact lens
TJ	Tight junction
UV	Ultra violet

CHAPTER I

INTRODUCTION

Normal wound healing is a complex and highly coordinated process of cell-cell signaling, cell spreading, migration, proliferation, and cell-ECM interaction. However, the main limitation in natural wound healing is that cells can mainly fill in the wound void from the wound margin. We hypothesize that epithelial cells applied to the interior of a wound will attach to the exposed extracellular matrix of the wound, and may contribute to the healing process. Our objective was to design and evaluate a therapeutic contact lens that could deliver epithelial cells to wounds. We set out to develop a cell transfer contact lens that could keep cells in close proximity to the cornea and allow cell movement onto wounded regions. Lens designs were chosen by the following criteria: 1) The lens material must allow for primary epithelial cell attachment and *in vitro* culture growth. 2) Lens application must result in the transfer of a portion of these cells to wound areas to aid in re-epithelialization of corneal injuries. 3) The lens must function as a bandage lens after cell transfer in order to protect both applied and endogenous cell populations on the corneal surface.

We hypothesized that cell transfer from PDMS contact lenses to wound ECM was a function of both cell motility and adhesion. In order to test this hypothesis, we developed in vitro assays for the assessment of cell transfer, and evaluated contact lens designs in increasingly complex model systems with an iterative design approach to enhance cell transfer. In this design process we used surface patterns to induce migration and surface coatings to effect cell adhesion. Surface patterns such as grooved channels

have been shown to direct cell movement (Evans, McFarland et al. 2005). Utilizing this idea, post and hole topographies were fabricated on contact lens surfaces to encourage cell movement along these structures. Cell attachment surface coatings such as fibronectin, collagen and matrigel were also used to test the effect of cell adhesion on the process of cell transfer.

In order to enhance cell transfer through the modulation cell motility and adhesion, we explored some of the underlying biological mechanisms of these two inter-related cellular behaviors. Though there were many potential molecular targets to alter cellular adhesion and aaugment motility, we specifically explored the regulation of cell-cell contacts, which have a profound impact on cell phenotype and migration. Previous studies have shown that cell adhesion to different substrates can effect on cell-cell adhesion (Monier-Gavelle and Duband 1995; Weaver, Petersen et al. 1997) and cell–cell adhesion can also influence motility (Huttenlocher, Lakonishok et al. 1998). When cells form cell–cell contacts, cells exhibit reduced migration rates, form fewer cell protrusions such as lamellae and filopodia, and cells decrease their microtubule and actin cytoskeleton dynamics (Waterman-Storer, Salmon et al. 2000). All of these processes involved in migration are affected by cell-cell adhesion. The mechanisms of crosstalk between cell adhesion and motility are not fully understood, however, since Rho and other small GTPase proteins are essential for both cell adhesion and cell migration (Bishop and Hall 2000), these are likely key proteins in the crosstalk pathways.

Normal corneal epithelial cells are motile cells that move slowly as a sheet. In contrast, fibroblasts move more quickly as individual cells. When epithelial cells exist as individual cells at very low cell density, they are more motile and more closely resemble

fibroblast cells. Individual epithelial cells do not exhibit cell junction proteins. In this investigation we altered Bves, a protein we have shown is associated with tight junctions (TJ), in an effort to make epithelial cells become more like fibroblasts regardless of cell density. This transition from an epithelial cell type to a fibroblastic cell type is called epithelial-mesenchymal transition (EMT), and has broad reaching implications for other fields such as metastasis in cancer biology.

This dissertation is divided into six chapters. This Chapter is an introduction to the work that states the objectives and summarizes the organization of the document. Chapter II contains the background and motivation for the research, including an overview of corneal physiology, normal corneal wound healing, epithelial-mesenchymal transition and cell junctions, and a literature review of re-epithelialization methods and using polydimethylsiloxane (PDMS) as a cell culture material. Chapter III is the first manuscript published in Cell Transplantation, which decribes our in vitro cell transfer assay and the effect of post surface patterns on epithelial cell transfer entitled: "Seeding of corneal wounds by epithelial cell transfer from micropatterned PDMS contact lenses." Chapter IV is a manuscript that explores the use of differrent surface geometries and surface coatings to enhance the transfer of primary cells entitled: "Cell transfer contact lenses deliver primary corneal epithelial cells to wounded organ cultured corneas." Chapter V probes cell adhesion and motility characteristics of epithelial cells by disrupting cell junctions in the manuscript "Loss of proper Bves function promotes epithelial-mesenchymal transition (EMT) and enhanced cell motility in corneal epithelial cells." All manuscripts include background, methods, results, discussion, and references. Chapter VI is the overall summary of the body of work, which consists of a general

discussion and directions for future work. Chapter VII includes the measures taken for the protection of research subjects and a statement of the societal implications of the research. Appendix A describes the role of the student on the manuscripts. Appendix B is supplemental information on surface modifications of Polydimethylsiloxane, which was not written in a finalized manuscript form. Appendix C is the manuscript: "Method to produce precise and reproducible epithelial wounds for in vitro studies of corneal wound healing."

CHAPTER II

BACKGROUND

Physiology of the cornea

The cornea is the transparent central portion of the eye surface that serves as a barrier defense for the inner eye, and as a critical refractive element in normal vision (Kaufman 1998). The cornea is made up of three main layers, the epithelium, the stroma, and the endothelium. The innermost layer is called the endothelium, which is a monolayer of cells responsible for the water and nutrient balance of the cornea. Endothelium maintain corneal clarity by pumping water out of the corneal stroma (Lim and Ussing 1982; Fischbarg, Hernandez et al. 1985; Wiederholt, Jentsch et al. 1985). Endothelial cells cannot replicate, so if too many of these cells die the cornea losses its way to regulate water balance. When this happens the cornea becomes edematous, which reduces corneal clarity and causes vision impairment (Kaufman 1998).

The middle layer of the cornea, the stroma, provides mechanical strength. The stroma constitutes 90% of the total corneal tissue and most of the cornea's 0.5 mm thickness (Kaufman 1998). Stromal clarity is dependent on the endothelium keeping the stroma in a dehydrated state. Mechanical support is provided by strong intertwined collagen fibrils maintained by fibroblast-like cells called keratocytes.

The outermost layer, the epithelium, is the corneal layer that is most responsible for sustaining protective and optical functions. Because the epithelium is directly exposed to the ambient environment, it is the first line of defense from injury and disease. This external layer is hardy and has a high healing capacity. In addition, because much

of the eye's focusing power comes from the refraction of light at the corneal surface, a smooth superficial epithelial layer with evenly distributed tear film is required for visual acuity.

The human corneal epithelium is comprised of 5-7 cell layers, with a total thickness of 50 microns. Morphologically these layers can be split up into 3 types of epithelium: basal cells, wing cells, and superficial cells. The cells types have distinct cell sizes and shapes, as well as exhibit different organelles and cell-cell junctions.

Basal cells are the only cell type of the cornea capable of cell division and are responsible for adhesion to, and maintenance of, the basal membrane. These mitogenically active columnar cells are roughly 20 microns thick and 10 microns in diameter. Basal cells exhibit many more cytoplasmic organelles than the other epithelial cell types, and notably many more glycogen granuoles to provide energy during cellular stress. These cells express zonula adherens and gap junctions with other basal cells, and adhere to an underlying basement membrane by connections called hemidesmosomes, which are normal long-term adhesion structures between intermediate filaments and basement membrane. Cells of the basal layer secrete materials such as laminin to form the basal lamina, which helps to separate and organize the epithelium on top of the stroma and maintain mitogenic capacity (Vracko and Benditt 1972).

Suprabasal cells, called wing cells, reside in the 2-3 middle layers of the corneal epithelium. Wing cells are transitional cells, which demonstrate an intermediate morphology between basal cells and superficial cells. Wing cells are filled with intermediate filaments, which help them to maintain their shape, and exhibit both desmosomes and gap junctions.

The Superficial cell layer is the topmost cell layer on the corneal surface, and normally is 2 cell layers thick. Superficial cells are thin, terminally differentiated cells bathed in tear film (Nichols, Dawson et al. 1983). These cells are flattened, squamous epithelium that are approximately 50 microns in diameter, 5 microns thick centrally, and 2 microns thick peripherally. Superfical cells express junctional proteins that lead to a contiguous cell layer interconnected by tight junctions. Tight junctions allow for effective barrier function and maintenance of a stable, smooth, external corneal surface for proper vision.

Corneal Injury

Corneal injuries are the most common of all eye injuries. The Schepens Eye Research Institute recently reported that corneal injury and disease constitute over 60% of all reported eye related patient visits in the U.S. health care system. The causes of corneal epithelial defects and disorders are numerous. Symptoms normally include vision impairment (corneal opacity), or pain (stimulation of the many corneal nerves). Nearly 10% of all eye related hospital visits are due to abrasions and ~8% of these cases suffer from complications that lead to delayed wound healing or at least one episode of recurrent epithelial erosion (Weene 1985).

In addition to the fact that abrasions are common, there are many other complications that can lead to delayed wound healing. Bacterial or viral infections such as herpes simplex virus infection, which has an incidence of 1 in less than 1,000 Americans (Liesegang, Melton et al. 1989), can cause severe persistent ulcerations. Autoimmune diseases such as Stevenson-Johnson Syndrome, and wound-healing

disorders such as diabetes, cause alterations in the cornea resulting in decreased sensitivity, recurrent epithelial erosions, and abnormal wound repair (Sanchez-Thorin 1998; Rosenberg, Tervo et al. 2000). According to the American Diabetes Association, 18.2 million people are diabetic, and this population is rapidly growing. It is expected that roughly one in ten diabetic patients during some point in their life will experience corneal wound healing problems, and those that are affected will be prone to recurrences (Ben Osman, Jeddi et al. 1995; Inoue, Kato et al. 2001).

The most severe form of persistent corneal wounds is caused by limbal stem cell deficiency (LSCD). However, LSCD is relatively rare in the United States. Only a few thousand people suffer from diseases or injuries such as acid or base burns that cause LSCD. Corneal deficiencies are much greater in developing nations where malnutrition and infectious diseases of the eye commonly cause delayed wound healing and lead to corneal blindness. Despite the wide range in corneal wound severity, clearly there is a large patient population, which suffers from delayed wound healing that would benefit from enhanced re-epithelialization therapies.

Normal Corneal Wound Healing

Corneal wound healing is a complex, coordinated cellular process. The paradigm of corneal wound healing is that it takes place in separate phases: the latent phase, the cell adhesion and migration phase, and the cell proliferation phase. In the first phase of wound healing, existing basal epithelial cells remain inactive for the first 4-6 hours after wounding (Crosson, Klyce et al. 1986). During this time, polymorphonuclear leukocytes (PMN) found in tears, remove dead cells at the wound margin (Pahlitzsch and Sinha

1985). Viable cells around the wound margin retract and round up, and lose surface microvilli (Haik and Zimny 1977) and hemidesmosomes (Gipson 1992). These cells then flatten to quickly cover the area around the wound margin, and start to form filopodia, which are spike-like projections also called microspikes, and lamellapodia, which appear as ruffled cell edges (Haik and Zimny 1977; Brewitt 1979). This step marks the onset of the second phase of wound healing, cell migration, which is also referred to as the linear cell healing phase.

During the cell migration phase, basal cells migrate from the wound edge into the central area of the wound region by the formation and contraction of actin filaments (Anderson 1977). Actin filaments are concentrated in the leading edge of migrating cells, especially in filopodia and lamellipodia. Migration is a cyclical process of actin synthesis to extend the cell cytoskeleton, focal adhesion formation to temporarily anchor the cell, then actin is contracted to draw the cell forward (Soong 1987; Soong, Dass et al. 1990). The focal adhesions in the trailing edge of the cell are then cleaved, and the adjoining actin is disassembled. Once these migrating cells have filed the wound region to create a monolayer, cells begin to attach more firmly to the underlying basement membrane by synthesizing new hemidesmosomes. Restoration of hemidesmosomes to normal levels after wounding can take weeks to months (Gipson, Spurr-Michaud et al. 1989).

The next healing phase, epithelial cell proliferation, is a process of cell division to create new cells to restore the cornea's normal 5-7 cell-layer thickness. All self-regenerating tissues, such as epithelium, are thought to be maintained by stem cells. In the cornea, it is believed that these stem cells are found only in the basal epithelial layer, and more specifically reside in the limbus, a region at the corneal-scleral junction. These

limbal stem cells are required for corneal epithelialization. Limbal stem cells have low, but unlimited, mitotic activity and are inactive most of the time (Cotsarelis, Cheng et al. 1989; Pellegrini, Golisano et al. 1999). However, stem cells become active after wounding, giving rise to new epithelium (Schwab and Isseroff 2000). Limbal stem cells asymmetrically divide to generate a daughter stem cell and a transient amplifying cell (Schermer, Galvin et al. 1986; Cotsarelis, Cheng et al. 1989), and it is these transient amplifying cells that give rise to differentiated corneal epithelium. The transient amplifying cell population is highly varied in replication potential and differentiation status. It has been shown that cell replication potential can be correlated to a transient amplifying cell's radial position in the basal layer (Nagasaki and Zhao 2003). Cells capable of the highest number of divisions reside in the outer-most region, adjacent to the stem cells, whereas those with the lowest mitogenic potential are located at the center of the basal layer.

Transient amplifying cells of the basal layer divide into more differentiated cells of the middle wing cell layer and superficial layer. Newly formed daughter cells, post mitotic cells, push anteriorily and differentiate, exhibiting different morphology and protein expression. Epithelial proliferation is so efficient in the cornea that every cell of the epithelium can be completely replaced in less than 7 days (Hanna, Bicknell et al. 1961; Kourenkov, Mytiagina et al. 1999; Fagerholm 2000).

Cell Adhesion Junctions

Normal epithelial cells form uniform sheets, which are maintained by cell adhersion junctions. These multi-protein complexes are found at cell-cell boundaries and

regulate the interactions between adjacent cells. These adhesion molecules between cells provide structural integrity that is necessary for both development and maintenance of tissues (Gumbiner 1996). Proper cell junction expression and function are crucial to normal physiology, and disorders involving cell junctions cause serious pathologies such as skin blistering diseases(Amagai, Klaus-Kovtun et al. 1991), and in the cornea, bullous keratopathy (Kenney and Chwa 1990).

Epithelial cells are polarized, having apical and basolateral regions delineated by junctions on the lateral surface. These cell junctions include tight junctions (TJ) (Gonzalez-Mariscal, Betanzos et al. 2003), adherens junctions (AJ) (Nagafuchi 2001) and desmosomes (Garrod, Chidgey et al. 1996). These cell junctions are very different in terms of function, cell membrane location, and protein components.

Tight Junctions

Tight junctions are the most apically located of the three adhesion junctions, and are involved in establishing and maintaining cell polarity. Tight junctions also create a barier by sealing the space between cells, which prevents the passage of molecules through a contiguous cell layer (Balda, Flores-Maldonado et al. 2000). Transmembrane proteins such as occludin (Furuse, Hirase et al. 1993) and the claudins (Furuse, Fujita et al. 1998) make up tight junctions, with peripheral associated proteins ZO-1 (Stevenson, Siliciano et al. 1986), ZO-2 (Gumbiner, Lowenkopf et al. 1991) and ZO-3 (Haskins, Gu et al. 1998).

Interestingly, blood vessel/epicardial substance (Bves), which was originally identified in epicardium (Reese, Zavaljevski et al. 1999), is also expressed in corneal

epithelial cells (Ripley, Chang et al. 2004), and is suspected of having a role at the tight junction. Though the molecular structure of Bves is well characterized on the cellular level, little is known regarding its molecular role. Bves is composed of approximately 357-amino acids containing three hydrophobic regions with two glycosylation sites. Knight and others later verified Bves to be an integral 3-pass transmembrane protein that forms homodimers (Knight, Bader et al. 2003). Bves localizes to the lateral membrane of various epithelium, and is highly conserved across species (DiAngelo, Vasavada et al. 2001; Wada, Reese et al. 2001; Ripley, Chang et al. 2004; Osler, Chang et al. 2005). Because of its subcellular localization and the fact that Bves transfection of non-adherent cell lines confers adhesive properties, Bves is considered an adhesion molecule. However, Bves does not contain any motifs or domains found in known classes of adhesion molecules.

Bves does share domains with two other related genes now considered to be part of the popeye domain-containing gene family (Osler, Smith et al. 2006). Brand and colleagues identified the three related genes with the domain in common, which they named popeye (Brand 2005). Despite being a part of this newly identified family of genes, Bves remains the accepted name for the gene product of popdd.

Based on antisense morpholino oligonucleotide (MO) knockdown, loss of Bves has been shown to lead to epithelial disorganization and a decrease of transepithelial electrical resistance (TER), a functional measurement of TJ. Recently it has been shown that Bves localizes with components of tight junctions, ZO-1 and occludin in corneal epithelia (Osler, Chang et al. 2005). Bves function appears to be coupled to tight junction localization. Immunoprecipitation studies have shown that Bves interacts with ZO-1, which further indicates that Bves is a component of the TJ. In summary, Bves is a transmembrane component of TJ and is necessary for epithelial sheet integrity.

Epithelial-Mesenchymal Transition

In normal physiology, during embryonic development and in pathological conditions such as in epithelial-based cancers (carcinomas), epithelial cells adopt a mesenchymal phenotype with reduced intercellular interactions and increased migratory capacity (Arias 2001). This is a process known as epithelial-mesenchymal transition (EMT). During EMT, epithelial cells actively down-regulate cell-cell adhesion molecules and lose their polarity. The opposite process, mesenchymal-epithelial transition (MET), has been observed in development as well. Mesenchymal cells can also form epithelial tissues by forming cell-cell contacts. In order to better characterize cellular transition, researchers have sought to identify molecular events that lead to EMT in disease progression. It is now widely accepted that loss of E-cadherin function is a primary event in EMT, which demonstrates the importance of cell junctions in this process (Hirohashi 1998; Hanahan and Weinberg 2000). Since E-cadherin is associated with adherens junctions, previously EMT studies have focused on the role of adherens junctions in cancer progression. However, during recent studies in our lab we have found that the loss of functional Bves associated with tight junctions may initiate EMT for corneal epithelial cells. This finding may be used to encourage cell migration for re-epithelialization applications, as well as provide a framework for understanding the possible role of Bves as a tumor suppressor and its loss as a possible trigger for EMT.

Novel methods to facilitate re-epithelialization of wounds

There are a number of re-epithelialization strategies that have been pursued by both corneal and dermal researchers. Though the epidermis and corneal epithelium are

similar in that they are both composed of epithelial layers maintained by stem cells, they differ in many ways and therefore re-epithelialization therapies must take these differences into account. Skin is vascularized and highly keratinized, where as the cornea lacks blood vessels and is optically transparent. In epidermal wound healing, scar formation and hypervascularization are more acceptable than in the cornea, where scars or blood vessel in-growth may hinder proper vision.

In many forms of delayed wound healing it is thought epithelial cell migration is hindered, so various extracellular matrix (ECM) proteins such as collagen, fibrin, and fibronectin (Nakamura, Sato et al. 1997) have all been applied to the cornea to enhance epithelialization. However these therapies have had mixed results. Other groups have tried to use MMPs and aldose reductase inhibitors (Datiles, Kador et al. 1983; Ohashi, Matsuda et al. 1988) to modify the wound area's ECM. Epithelial growth factors and chemotactic agents have been used to try to encourage cell migration into epithelial void regions. Other therapeutic agents such as aminocaprioc acid, lecithin, superdismutase, aprotinin (plasmin inhibitor), and hyaluranic acid have been used in attempt to augment corneal wound healing.

Cell based therapies for the cornea

Instead of delivering therapeutic molecules to the cornea, another approach to re-epithelialize the cornea is to culture epithelial cells and apply them to wounds. This technology in the past has been used to treat the most severe cases of delayed healing and persistent wounds that we associated with limbal stem cell deficiency. Stem cell deficient corneas lack the ability to heal because the proliferative cell population is

compromised. In order to treat total limbal stem cell deficiency, a limbal stem cell transplant method was developed to replenish corneas with cells capable of proliferation. Limbal stem cell deficient corneas are usually highly scarred and opaque. These problems must be addressed before limbal transplant. Keratectomy and conventional corneal transplant procedures may accompany limbal transplants to prepare the eye in stages, however, these procedures alone are unable to treat limbal stem cell deficiency independently (Tsubota, Satake et al. 1999). A source of new limbal stem cells in the form of a transplant are needed to re-epithelialize the cornea by replenishing it's supply of proliferative cells.

Limbal transplants may differ depending on the source of donor cells, the amount of tissue used, and the method of delivery to the deficient eye. A limbal autograft is a transplantation of stem cells into a patient's deficient eye from their contra-lateral healthy eye. A portion of the stem cell-sufficient limbus is harvested from the healthy eye, and is surgically placed in the affected eye. Tseng and Kenyon conducted the first trial of autologous limbal transplants on patients in 1987. They found that this technique could be effective in the treatment of patients with previously failed corneal transplants, demonstrating an initial success rate of 85% (Kenyon and Tseng 1989). Many causes of corneal stem cell deficiency are bilateral, affecting both eyes. In these cases, limbal allografts are used instead of autografts. In an allograft, transplanted tissue comes from a donor. The stem cell populated donor graft is then implanted into the deficient patient's limbus. These patients are then required to use immunosuppressive drugs such as cyclosporin. The process of taking ocular tissue from the limbus can be dangerous for a living donor if too much tissue is removed, leaving them with too few stem cells (Schwab

and Isseroff 2000). This risk to the donor eye has been minimized by *ex vivo*-expanding limbal stem cells on growth substrates using cell culture techniques.

Michele DeLuca and his research team at the University of Genova have pioneered and popularized *ex vivo* expansion for limbal stem cell transplants. They demonstrated that efficient expansion of corneal stem cells was possible, requiring fewer cells to be harvested from donor tissues. They found that 1 mm^2 sections harvested from the limbus were adequate to provide enough proliferative cells to re-epithelialize the cornea. Originally, implanted epithelial cultures were placed directly into the eye using surgical gauze as a substrate, which was covered by a bandage contact to hold the gauze in place (Pellegrini, Traverso et al. 1997). Tseng and Kim found that amniotic membrane, which had been used in the past half century in ocular surgeries, could be used as a cell carrying substrate for limbal transplants (Kim and Tseng 1995). When limbal tissue is implanted, the membrane is sutured onto the eye's surface. The innate characteristics of the membrane have been reported to prevent vascularization of the new cornea and reduce immune response (Tseng, Prabhasawat et al. 1998). This is thought to limit tissue rejection problems of limbal allograft transplants. However, patients still require the same regiment of immunosuppressive drugs. The immunological and anti-vascularization roles of amniotic membrane are still being investigated. Research groups in Taiwan, Japan, Germany, Italy, and the U.S. have combined the use of *ex vivo* expansion of corneal epithelial cells with the amniotic membrane transplant procedure . Limbal stem cells are now cultured directly on amniotic membrane in vitro, which creates 100-fold more cells to be implanted into a deficient eye (Quantock, Koizumi et al. 2002).

Limbal transplant methods have been shown to be effective treatment for corneal stem cell deficiency. However, it is difficult to assess the overall success rate of each of these different types of cell transplantation surgeries because each patient's case has a different clinical outlook with varying amounts of stem cell deficiency, conjunctival invasion, blindness, and past history of surgeries. Because preparation before limbal stem cell transplantation is different for many cases involving keratectomy or conventional corneal transplants, there is further heterogeneity to trial groups.

Despite the advances produced by limbal stem cell transplantation methods, the methodology still suffers from a few drawbacks. The stem cell population that is most therapeutic to patients is difficult to isolate and purify from donor tissues because there is no identified stem cell surface marker. A stem cell marker would allow clinicians to locate stem cells for harvest and a way to track them to ensure their delivery and preservation in treated corneas. Researchers have been trying to develop ways to visualize limbal stem cells since the early 1990's. One of the first attempts to identify limbal stem cells was to analyze expression of keratins in corneal cells. Differentiated corneal epithelial cells, such as transient amplifying cells, were found to express a 64K keratin, whereas corneal stem cells of the basal limbus layer express 50K/58K keratins. The 64K keratins were used as markers of differentiated epithelial cells visualized by labeled antibody AE5 (Schermer, Galvin et al. 1986). BrdU has been used to label slow cycling cells of the limbus, which are likely to be stem cells (Grueterich, Scheffer et al. 2002). However, these methods for identifying limbal stem cells were poor because they identified many cells that were not stem cells or the staining needed to be done on fixed cells, so the method couldn't be used to sort cells to be used therapeutically.

Recently, there have been great strides in this area, however, these is still no way to positively identify limbal stem cells (Shimazaki, Aiba et al. 2002). Researchers have developed mouse lines that express GFP in corneal epithelium, so that the limbal stem cells and their progeny can be visualized (Nagasaki and Zhao 2003). In addition many new stem cell marker candidates have been identified including δNp63 (Vascotto and Griffith 2006) and negative surface markers such as connexin 43 (Chen, Evans et al. 2006).

Other drawbacks to limbal stem cell therapy exist, including the practical limitations of cell administration methods and also subsequent cell rejection and inflammation issues. Some practical issues of using collagen and amniotic membrane to support ex vivo expansion include handling problems. These materials are delicate, and difficult to work with. They require technical surgical skill to properly affix the corneal stroma surface and efficacy can be adversely impacted. In addition, amniotic membrane and collagen sheet materials are not off-the-shelf products. Amniotic membrane is a biomaterial that degrades with time and is prone to tearing, requiring special shipping considerations. Amniotic membrane (AM) is used as a substrate for ex vivo expansion of limbal stem cells because it is a biologically inert degradable matrix. AM is an avascular stromal matrix with a basement membrane composed of collagen type IV and laminin. These extracellular matrix materials make amniotic membrane an amenable material for cultivating stem cells. Corneal stem cells grow well on the membrane *in vitro*. The preparation process most commonly used by clinicians working with AM is modified from the methods originally proposed by Kim and Tseng (Kim and Tseng 1995). Amniotic membranes are harvested placentas from disease-free consenting mothers who

have delivered by caesarian section. The membrane is then separated via blunt dissection, washed, cut up, and stored submerged in 50% DMEM/glycerol at -80ºC. Freeze dried amniotic membrane is now commercially available, which ships well, but is relatively expensive. In order to make corneal cell therapy economically viable, cost should be minimized without reducing efficacy. Nishida et al have developed a method to prepare full epithelial sheets for implantation without a substrate material. Limbal explants were cultivated on a temperature-sensitive polymer growth surface. After weeks of culture time, hardy epithelium composed of multiple cell layers were released from the polymer by a temperature change (Nishida, Yamato et al. 2004). This type of approach would eliminate the need for carrier materials, however there are still surgical and technical issues that remain. Limbal explant expansion to be confluent sheets is time consuming and, in some cases, may delay patient treatment. In addition, many limbal transplant procedures require sutures, which can have complications. Lastly, these methods are poorly suited to treat less severe cases of wound healing deficiency. Therefore, they have limited application. In summary, the current limbal transplant procedures are cumbersome, expensive in cost and in time, and are limited to the treatment of complete limbal stem cell deficiency.

Therapeutic contact lenses (TCL)

Therapeutic contact lenses, also known as bandage contact lenses, are used to treat many ophthalmic conditions including corneal abrasions, erosions, persistent defects, chemical injuries, and postoperatively after vitrectomy, penetrating keratoplasty, epikeratoplasty, lamellar grafts, PRK, LASIK, and cataract extraction. These contact

lenses differ from vision correction lenses in that their primary function is to protect the corneal epithelium, rather than correct refractive error. The most serious complications of TCL wear are infections such as microbial keratitis and anoxia, which can result in neovascularization. To combat infection, prophylactic antibiotics may be used for a short period.

Contact lenses may be made of a wide range of materials, which include: thermoplastic polymers, elastic polymers, rigid gas permeable materials and hydrogels (Sariri and Sabbaghzadeh 2001). The most common material for making contact lenses are polymethylmethacrylate (PMMA) and polyhydroxyethylmethacrylate (PHEMA). However, polydimethylsilxane (PDMS) is an elastic polymer with an oxygen permeability 1000x PMMA. This is one of many important material considerations, which also include biocompatibility, protein absorption, chemical stability, optical clarity, water content and water interaction.

Motivation behind an epithelial transfer lens

Simplifying the etiologies causing delayed corneal healing, we could roughly divide the disorders into 2 different groups; those where cellular migration is hindered so that epithelial cells fail to spread over the wound area, and those where epithelial cells fail to proliferate. We propose to treat both of these groups by developing a therapeutic transfer device to deliver primary corneal epithelial cells directly within the persistent wound site. As limbal transplant groups have shown in the past, replacing the stem cell population with cells from a donor can treat limbal stem cell deficiency (Pellegrini, Traverso et al. 1997; Tseng, Prabhasawat et al. 1998; Tsubota, Satake et al. 1999;

Nishida, Yamato et al. 2004). Likewise, our therapeutic contact lenses are meant to deliver primary cells to re-supply stem cell deficient corneas as well as to completely re-epithelialize the corneal surface. However, in the cases of non-stem cell related corneal wound healing disorders, delivered primary cells may instead serve as a transient epithelial patch instead of a permanent source of proliferative cells. Because these corneas have a stem cell reserve, their own cells will probably replace transferred cells after corneal remodeling. In addition, non-stem cell related persistent wounds are likely to have extracellular matrix modification so that cells can't attach or migrate into the interior wound area. In order to prepare the wound site for epithelial attachment and enhance wound closure, past groups have used fibronectin drops (Nakamura, Sato et al. 1997). We plan to prepare the wound region by application of fibronectin as well, to prime the wound area to accept transferred cells from our contact lens.

The main advantages of this therapeutic cell transfer contact lens device would be the ease of active re-epithelialization therapy administration for a number of corneal disorders and reduction in the time to superficial epithelial coverage. This project builds from a strong background in the literature on limbal stem cell therapy, bandage contacts, and other novel treatments of wound healing disorders. Our proposed cell transfer contact lens approach has numerous advantages over currently available therapies. We are designing these therapeutic contact lenses to be simple, inexpensive to fabricate, and easy to apply. By delivering individual, or small groups of, donor harvested corneal cells to the interior of corneal wounds, we will be able to provide a quick, flexible, and active re-epithelialization therapy to treat moderate and severe persistent corneal wounds.

Design criteria for epithelial cell delivery systems for use on the cornea include cornea basal cell growth on the carrier device in culture, cell transfer from the carrier to the wound region, and protection of applied cells from blink shear and tear film washing for long term retention.

Polydimethylsiloxane (PDMS) as a cell growth surface

Polydimethylsiloxane (PDMS) is a very useful polymer that has been used in many different fields including biomedical devices, gas exchangers, insultators, microfabrication and microfluidics. Investigators have recently started to use PDMS as a cell culture material (van Kooten, Whitesides et al. 1998; Deutsch, Motlagh et al. 2000). PDMS is an interesting cell substrate in that it can be micropatterned using standard photolithographic technologies to create surfaces with surface microtextures that can influence cell behavior (Mata, Boehm et al. 2002; Matsuzaka, Walboomers et al. 2003).

Cell attachment to untreated PDMS surfaces has been contested in the literature, however, several investigators have reported successful cell culture (Mata, Boehm et al. 2002). PDMS is made up of a chain of silicon that has two methyl groups. These methyl groups makes the surface of PDMS highly hydrophobic, which means that it strongly repels water. A measure of hydrophobicity, surface contact angle (SCA), can be measured by placing a bead of deionized water on PDMS. Materials that are hydrophilic have low SCA and those that are hydrophobic have SCA of >70°. Many researchers have measured PDMS to have a SCA of 108°. Despite many advantages of PDMS' material properties, its hydrophobic nature translates into poor wettability, which is a significant problem for cell attachment. Previous studies suggest that cell adhesion is

maximized on surfaces with moderate SCA from 60° to 80° (Lee, Park et al. 2003), which is an intermediate hydrophobic/hydrophilic property.

In order to make PDMS more amenable to cell attachment, the surface needs to be modified either by hydrophilization of PDMS or by surface coating with adhesive proteins. Several investigators have reported treating PDMS with oxygen plasma to reduce its hydrophobicity. The chemical structure of PDMS is a chain of silicon interconnected by oxygen with two methyl groups attached to silicon. Experimental evidence indicates that PDMS is made more hydrophilic when oxidized in plasma because oxygen in the form of hydrophilic silanol groups (Si-OH) replace hydrophobic methyl groups ($Si\text{-}CH_3$) at the surface (Morra, Occhiello et al. 1990). However, PDMS surfaces treated by oxygen plasma do not remain hydrophilic permanently. Mobile, low-molecular weight monomers are able to migrate from the bulk of the PDMS to the air-surface interface causing hydrophobic recovery a few hours following plasma treatment. To retain the hydrophilic nature of plasma treated PDMS, several investigators have found that storage in water reduces the rate of hydrophobic recovery (Ng, Gitlin et al. 2002; Lee, Park et al. 2003)

CHAPTER III

SEEDING OF CORNEAL WOUNDS BY EPITHELIAL CELL TRANSFER FROM MICROPATTERNED PDMS CONTACT LENSES

Christopher J. Pino[1]

Frederick R. Haselton[1,2]

Min S. Chang[2]

[1]Biomedical Engineering

and

[2] Ophthalmology and Visual Sciences

Vanderbilt University

Nashville, Tennessee 37232

Address for Correspondence:
Rick Haselton
Box 1510 Station B
Vanderbilt University
Nashville TN, 37235, USA
(615) 322-6622 office
(615) 343-7919 fax
rick.haselton@vanderbilt.edu

Abstract

Persistent corneal wounds result from numerous eye disorders, and to date, available treatments often fail to accelerate re-epithelialization, the key initial step in wound healing. To speed re-epithelialization, we explored a cell-transfer transplant method utilizing polydimethylsiloxane (PDMS) contact lenses to deliver epithelial cells derived from limbal explants directly within a corneal wound. Human primary epithelial cells and an immortalized corneal epithelial cell line (HCE-SV40) grew well on PDMS contact lenses and their morphology and growth rates where similar to cells grown on tissue culture polystyrene. To initially study cell transfer from PDMS, HCE-SV40 cells were seeded onto PDMS with or without micropatterned posts. After a day in culture, HCE-SV40 cells attached to the unpatterned PDMS uniformally, whereas on micropatterned PDMS, they appeared to attach primarily between posts. The cell-covered PDMS contacts were then placed cell side down onto tissue culture plastic and after one, two, or three days, the PDMS contact was removed and the transferred cells were trypsinized and counted. Micropatterned PDMS contact lenses with 100-micron-diameter posts, and a post height of 40 microns, transferred four times as many cells as unpatterned PDMS. Cell transfer to a wounded cornea was tested in a pig cornea organ-culture model de-epithelialized by alkali treatment. Post micropatterned PDMS contact lenses were seeded with labeled HCE-SV40 cells at a density 50,000 cells/cm^2 and applied to the wounded pig corneas. After 24, 48, or 96 hours of application, PDMS contact lenses were removed, corneas fixed with formaldehyde, and sectioned. After 24 hours, epithelial cells transferred from post micropatterned contact lenses to provide 35% epithelial coverage of denuded pig corneas; after 96 hours, coverage was 65%. We

conclude that cell transfer from epithelial-coated PDMS contact lenses micropatterned with posts provides a promising approach to re-epithelialize corneal surfaces.

Key Words: cornea, wound healing, primary epithelial cells, transfer, contact lens

Introduction

Persistent corneal epithelial wounds pose a serious risk to patient vision and a dilemma to clinicians attempting to treat them. Corneal defects result from a variety of causes, including viral and bacterial infections, chemical, thermal or UV burns, autoimmune disorders, diabetic ulcerations, epithelial abrasion, foreign body impact, and ophthalmic surgeries (Kenyon and Tseng 1989; Reim, Kottek et al. 1997; Sanchez-Thorin 1998). Due to the diverse causes and etiologies of persistent corneal wounds, there are currently many different treatments used to augment healing. Some conservative treatments for persistent corneal wound conditions include anti-inflammatory agents, antibiotics, and antiviral therapies to prevent infection and inflammatory damage. Clinicians also routinely use lubrication, hypertonic ointments, mechanical debridement, cauterization or PTK. Therapeutic soft contact lenses, collagen shields, patching or tarsorrhapy may be used to cover the eye, which increases lubrication and protects the cornea from external forces (Ali and Insler 1986; Le Sage, Verreault et al. 2001). However, none of these therapies directly stimulate re-epithelialization of corneal epithelial defects nor prevent recurrent epithelial erosions. As a result, ulcerations may persist for many weeks and can lead to corneal perforation (Larouche, Leclerc et al. 2000). Aggressive treatments such as conjunctival flap, amniotic

membrane transplant, and corneal transplants procedures are considered when large area of the epithelium is affected or the underlying stromal layer is compromised.

The goal of persistent corneal wound treatment is to promote coverage of the corneal stroma with healthy epithelial cells. Currently there are a few treatments available that utilize epithelial cell transplants to treat corneal disorders, which include penetrating keratoplasty, limbal stem cell transplantation (Grueterich, Scheffer et al. 1996; Pellegrini, Traverso et al. 1997; Meller, Dabul et al. 2002), and *ex vivo* expanded epithelial sheets (Nishida, Yamato et al. 2004). *Ex vivo* cell preparation methods for these procedures require long culture periods exceeding 2 weeks to expand cells from $1mm^2$ limbal explants (Nishida, Yamato et al. 2004). In addition, these grafts or epithelial sheets must be sutured onto the eye. Our proposed alternative approach transfers individual or small groups of epithelial cells from a therapeutic contact lens, instead of requiring a confluent sheet or sutures. In this way we may decrease the lag time between cell harvest and cell transplant application and initiate earlier epithelial coverage, while simplifying the cell transplant application process. Thus, we may be able to achieve quicker epithelial coverage with fewer harvested cells.

Methods

Lens fabrication

Cell growth surfaces of two different styles (smooth without posts and micropatterned with posts) were fabricated using Sylgard® 184, a polydimethylsiloxane (PDMS), obtained from Dow Corning (Midland, Michigan, U.S.A.). PDMS was mixed

according to the manufacturer's instructions, in a 10:1 mixture of polymer to curative agent. Air bubbles were removed by vacuum pump and PDMS was polymerized at 37°C. Unpatterned PDMS surfaces were fabricated using a 2 cm diameter cork bore to cut out circular regions of a thin layer of PDMS. Similarly, micropatterned surfaces were cut out of a PDMS layer cured on a photolithography patterned silicon master, which created 40-micron tall, 100-micron diameter posts with 200-micron center-to-center post spacing.

A multi-step procedure was used to mold curved contact lenses, which resemble commercially available bandage contact lenses. Using a 2 cm concave drop slide (Cat # 12-565A, Fisher Scientific, Pittsburgh, PA), a convex dome was made out of PDMS to serve as a mold for the concave side of the contact lens. When this mold was fully polymerized and hardened, a contact lens was fabricated by pouring PDMS between the drop slide and the convex PDMS mold raised by a spacer. The resulting contact lenses were 2 cm in diameter, less than 1 mm thick, transparent, sturdy, and elastic. A thin layer (~0.5 mm) of micropatterned PDMS was added to the inside concave surface to produce the micropatterned cell-transfer contact lenses used for transfer to pig corneas. Contact lenses were autoclaved for 25 minutes before seeding epithelial cells.

Primary corneal culture expansion of limbal explants on PDMS

Human corneas from two male donors, 46 and 51 years of age, were obtained from Vanderbilt University's Eye Bank. Limbal ribbons were cut from each cornea, and the ribbons were cut into approximately $1mm^2$ explant squares. These explants were grown on 100mm diameter Petri dishes coated with a layer of PDMS. Corneal explant

cultures were maintained with EpiLife medium with corneal growth factor supplement (Cascade Biologics, Portland, OR), and incubated at 37°C in 5% CO_2.

Corneal epithelial growth on PDMS contact lenses

Human corneal epithelial cells (HCE-SV40 cells) immortalized with SV40 adenovirus developed by Araki-Sasaki (Araki-Sasaki, Ohashi et al. 1995), were used to test the cell growth and transfer characteristics of corneal epithelium on PDMS. This immortalized human corneal epithelial cell line has been shown to have similar characteristics to *in vivo* corneal epithelial cells (Araki-Sasaki, Ohashi et al. 1995). HCE-SV40 cells exhibit a cobblestone-like appearance in culture, express cornea specific proteins, and differentiate into stratified tissue when grown on extracellular matrix material such as collagen type I (Araki-Sasaki, Ohashi et al. 1995). Cultures were initiated at a seeding density of 5,000 cells per cm^2 on the contact lenses. Defined keratinocyte-serum free medium with growth supplement (Kit # 10744019, Invitrogen/Gibco, Grand Island, NY), along with trypsin and defined trypsin inhibitor for use in serum free culture conditions, were used to maintain and passage cells. Growth medium was changed twice weekly.

Growth comparison study

The growth of HCE-SV40 cells on PDMS was compared to growth on standard tissue culture plastic. PDMS components were mixed and poured into each well of sterile 6-well tissue culture treated plates (Cat.# 353046, Falcon™/Becton Dickinson, Franklin Lakes, NJ). Each well received 1 ml of PDMS, which spread out and

polymerized into a thin layer (~2 mm thick) coating the bottom. Plates without PDMS were used for growth comparison. Forty-eight thousand cells (5,000 cells per cm^2) were added to each of the wells. At 2, 5 and 9 days after seeding, cells were trypsinized with a serum free trypsin/EDTA solution (Cat.# R-001-100, Cascade Biologics, Portland, OR), neutralized by defined trypsin inhibitor (Cat.# R-007-100, Cascade Biologics™, Portland, OR) and counted with a cell counter (Coulter Counter model ZF, Coulter Corp., Miami, FL).

Quantification of HCE migration

Smooth unpatterned and micropatterned PDMS was seeded at 50,000 cells per cm^2 (200,000 cells over approximately a 4 cm^2 area). To initiate cell transfer, the PDMS was flipped cell-side down onto a 12-well plate, with a thin layer of defined keratinocyte serum free medium coating the bottom surface. After 1, 2, or 3 days, the PDMS was removed from the wells, and cells were trypsinized from both the PDMS and 12-well plastic surfaces and counted. Digital images of the contact lenses and corresponding wells were taken prior to trypsinization and cell counts from these images were used as a check for the number of transferred cells obtained by trypsinization.

Migration of HCE from a PDMS contact lens onto a pig cornea *in vitro*

Enucleated pig eyes (SiouxPreme Packing Co., Sioux Center, Iowa) were dissected upon receipt to harvest corneas. Corneas were de-epithelialized by application of a ~50 mm^2 trimmed polyester foam biopsy pad (Cat.# 21150-088, VWR, West Chester, PA) soaked in 0.5 M NaOH for 15 minutes (Chuck, Behrens et al. 2001),

followed by washing in sterile PBS to remove injured cells. In addition, some corneas were completely denuded by blunt dissection. Sodium fluorescein staining as well as histological sectioning was used to confirm the removal of epithelial layers. HCE-SV40 cells to be used for transfer were labeled using 5 μM CellTracker™ Red CMTPX (Cat.# C-34552, Molecular Probes, Inc., Eugene, OR) applied for 30 minutes. Micropatterned PDMS contact lenses were then seeded with these labeled cells at a density of 50,000 cells/cm^2. The fluorescence of the cells on the PDMS contact lenses was verified before the start of the transfer experiment. The contact lenses were then placed cell-side down on the pig cornea, and held in place by a transwell insert. Control wounds received a contact lens without HCE cells. After 48 hours contact lenses were removed to take photographs of the cell-transfer treated and control corneas using a Nikon Eclipse TE2000U microscope (Nikon USA, Melville, NY) equipped with a Hamamatsu C7780 CCD camera (Hamamatsu Corporation, Bridgewater, NJ) and a Nikon D100 digital camera (Nikon USA, Melville, NY). After imaging, corneas were immediately fixed in 10% formaldehyde for 30 minutes and stored in 70% ethanol before sectioning. Corneas with transferred HCE-SV40 cells were bisected through the wound area, and embedded in paraffin on edge so that cross-sections could be taken. Tissues were sectioned into 7μm thick slices and deparaffinized. Alternating slides were H&E stained to visualize cell bodies, nuclei and extracellular matrix.

Histological cross-sections of transfer regions were evaluated by comparing denuded control corneas to corneas treated with micropatterned PDMS contact lenses carrying cultured cells. Histological cross-sectional images of the whole corneal surface were acquired by a high-resolution microarray scanner (GenePix 4000B, Axon

Instruments, Union City, CA) and analyzed by the Image Pro software package (IPP version 5.0, Media Cybernetics, Silver Spring, MD). Transferred cells with fluorescent labels were visualized with high contrast to background by this fluorescent scanner. Analysis consisted of drawing a free-hand line-profile within Image Pro along the surface of cornea, adjacent to the stroma. Pixel intensities of the superficial layer were then extracted for spreadsheet computations. To quantify the epithelial cell coverage on a corneal surface, a minimum pixel threshold value for pixels to be counted as part of a cell was determined by sampling equivalent scans with patches of control cells. Epithelial coverage was computed as a percent of the total number of pixels sampled that had intensity values above the minimum cell value. Representative high magnification phase contrast micrographs were also taken of each corneal surface in cross-section to show cellular detail.

Statistical analysis

Cell growth and transfer data were analyzed using SigmaStat (SPSS Inc, Build 3). Analysis of variance (ANOVA) was used to examine trends between groups and over the time course of the experiments. Because some groups had unequal N, the Holm-Sidak method was used to assess significance. A value of $p < 0.05$ was accepted as significant.

Results

PDMS supports the growth of primary and immortalized corneal epithelial cells

Primary corneal cells migrated from the limbal explants to form cell islands on

PDMS within a week. These primary cells were then trypsinized from the PDMS surface and passaged onto another PDMS coated 100mm diameter Petri dish. This first passage of corneal primary cells reached confluence approximately 3 days after passaging. EpiLife medium with corneal supplements appeared to favor epithelial growth because many of the primary cells observed had epithelial rather than fibroblastic morphology (Figure 1). These results indicate that PDMS is a suitable biomaterial to support the growth of primary corneal epithelial cells.

Corneal epithelial growth on PDMS contact lenses

Human corneal epithelial cells (HCE-SV40 cells) also adhere to and populate the untreated surfaces of smooth and micropatterned polydimethylsiloxane (PDMS) contact lenses shown in Figure 2. When grown on PDMS, immortalized HCE-SV40 cells exhibit similar morphology to normal corneal epithelial cells in culture, which has been described as cobblestone-like by Araki-Sasaki (Araki-Sasaki, Ohashi et al. 1995). The cells attach to PDMS within two hours, a time comparable to attachment to tissue culture plastic.

Growth comparison study

HCE-SV40 cells grown on PDMS and standard tissue culture plastic exhibit similar growth characteristics (Figure 2). Mean cell densities with accompanying standard deviations were obtained for PDMS for a sample size of 12 cultures. A growth delay of approximately 1 day was observed after seeding at 5,000 cells/cm^2. By day 2, HCE-SV40 cells recovered and exceeded the seeding density. Cell density had

quadrupled by day 5, and by day 9 the population was expanded by over 20-fold. Corneal cell densities grown on PDMS were equal to the densities of the cells grown on the tissue culture plastic control surface, with no statistical significance. In both cases, seeding at 5,000 cells/cm^2 produced a high density layer of ~100,000 cells/cm^2 after 9 days. From these growth curves, the cell doubling time was estimated to be approximately one day for HCE-SV40 on both PDMS and on plastic. This value is similar to the 24.4 hour doubling time reported by the originators of this cell line (Araki-Sasaki, Ohashi et al. 1995).

Quantification of HCE migration

In cell transfer experiments from smooth unpatterned PDMS, an increasing number of HCE-SV40 cells were found to transfer to tissue culture plastic on each of the three successive days. Approximately 20% of the original number of seeded epithelial cells transferred from the contacts after day1, 40% after 2 days, and 60% after 3 days (n=10). This was considered to be a moderate transfer rate because many cells remained on the contacts and continued to proliferate. In order to enhance epithelial surface-to-surface transfer, a micropatterned PDMS disk design was tested (Figure 3). The 100-micron diameter post micropatterned PDMS disks were found to transfer a statistically significant, greater number of cells compared to smooth PDMS disks at each time point (n=3). The transfer rate of micropatterned PDMS was approximately three times the rate of smooth unpatterned PDMS.

Migration of HCE-SV40 cells from a PDMS contact lens onto a pig cornea *in vitro*

In the *in vitro* pig cornea wound model experiment, 0.5 M NaOH administered to the central cornea for 15-30 minutes damaged local regions of the corneal epithelium. After washing, cells in the central treated region sloughed off, and this region appeared to be more opaque. The cornea also increased in total thickness due to stromal swelling. In a phase contrast image of a corneal surface, a rectangular epithelial wound area is seen where the NaOH soaked biopsy pad was applied (Figure 4 A). The wound edge is a sharp boundary between an intact epithelial layer and a region without epithelium. After 48 hours in our organ culture system, there is no indication of indigenous pig epithelial healing taking place in the NaOH treated region, and an irregular collagen surface is exposed. Based on preliminary findings of enhanced transfer *in vitro*, PDMS micropatterned contact lenses with posts were chosen for cell transfer to pig corneas. Figure 4 B shows the wound region with attached CellTracker red-labeled HCE-SV40 cells, which were delivered to the corneal surface by direct transfer from PDMS contact lenses after 48 hours. The majority of the red fluorescence appears to have originated from within the rectangular NaOH treated region, demonstrating preferential epithelial attachment to the NaOH treated area. Transfer regions were inspected after histological sectioning. Paraffin embedded fixed tissue cross-sections were taken from denuded corneas that were treated with a micropatterned PDMS contact lens carrying cultured cells. These sections were compared to sections taken from a wounded pig cornea covered with a contact lens without cells. Image analysis of the corneal surfaces was performed using pixel intensities of the superficial layer to determine the epithelial coverage after contact lens transfer determined that ~35% of the corneal surface had been

covered after 2 days and ~65% was covered after 4 days. The control de-epithelialized cornea was determined to have less than one percent remaining epithelium. Phase contrast images of pig cornea after transfer are shown in Figure 5 (middle panels). HCE-SV40 cells appear to have transferred from the micropatterned contact lens with posts onto the native pig cornea collagen at both day 2 and day 4. Transferred HCE-SV40 cells growing on the corneal surface appear have a healthier morphology, and comprise a more contiguous and better-organized epithelium at 4 days (Figure 5, middle right) than when observed at 2 days (Figure 5, middle left). The denuded corneal surface shows no remaining porcine epithelial cells on the exposed stromal collagen (Figure 5, far left). Normal pig cornea with healthy, well-organized cellular strata is shown for comparison (Figure 5, far right).

Discussion

Polydimethylsiloxane (PDMS) appears to be an excellent material for an epithelial cell transfer contact lens. The material is nontoxic, has high oxygen permeability, contact lenses can be easily fabricated and autoclaved, and its surface properties promote cell attachment and growth *in vitro*. PDMS proved to be an excellent primary cell growth surface for limbal explants, performing comparably to amniotic membrane (Grueterich, Scheffer et al. 1996). In addition, the HCE-SV40 cell line grew well on PDMS, allowing for their use in preliminary transfer experiments.

In order to initially test cell transfer from PDMS to an adjacent surface, the HCE-SV40 cell line was chosen because of its availability, ease of use, and well characterized comparison with *in vivo* corneal cells. In this way we were able to address some design

considerations without the added complexity of repeated eye procurement and limbal harvesting. In this simplified system we were able to quantify cell transfer using both optical and Coulter counter based methods. This method also allowed for a quick way to compare transfer efficiencies of the smooth and micropatterned contact lens designs. Successful cell transfer was seen in cell transfer experiments from both patterned and unpatterned PDMS onto tissue culture plastic (Figure 3). However, we have found that micropatterned PDMS delivers approximately four times more viable cells to a recipient surface than smooth unpatterned PDMS. We speculate that transfer of epithelial cells is dominated by single cell trans-surface migration via filopodia, rather than cell release into suspension, and subsequent attachment to the opposing surface. Unpatterned contacts have a surface area contact advantage, in that their whole surface is in close proximity to the opposing transfer target surface, which could allow for filopodial attachment after extension. However, we propose 3 possible mechanisms to explain the enhanced transfer by micropatterned posts: directed migration, cell loss due to contact application and removal, and culture medium exclusion. Posts may allow for filopodia-mediated cell migration up the posts between the surfaces. Alternatively, it may be the case that similar amounts of cells transfer, but fewer intial viable cells are reside on unpatterned contact at transfer onset due to some cells being crushed upon contact lens application. Posts on the patterned PDMS contact lenses, may prevent cell crushing. Upon unpatterned contact lens removal, fewer cells may remain on the transfer surface because transferred cells may still have some points of adhesion on contact lens due to its proximity to the recipient surface. These cells may be pulled off with the PDMS contacts instead of remaining on the target surface. However, in the case of the micropatterned

posts, cells may reside on the plastic transfer surface between the regions where the PDMS posts are making physical contact. Therefore, when micropatterned PDMS is peeled off, fewer cells may be lost. A final explanation may be attributed to cell death triggered by nutrient limitations imposed by smooth contact lenses that are overcome by micropatterned PDMS with posts. The posts may cause a slightly larger void space between the PDMS and recipient surface, allowing for faster nutrient diffusion from fresh culture medium. Unpatterned contact lenses make a closer fit to the recipient surface, and may exclude fresh medium, which is confined to the rim region. Cell culture medium nutrient limitations are more probable than oxygen deficiency, because PDMS has a high oxygen permeability coefficient (~781 cm^3 (STP) cm/cm^2 s cmHg) (Kuriana 2003), allowing for good oxygen diffusion through the lens. This oxygen barrier was also minimized by spin casting thin layers of PDMS.

Micropatterned PDMS with posts were successful in transferring HCE-SV40 cells to denuded pig corneas (Figures 6), shown qualitatively by phase contrast micrographs in which cells appear to be attached and growing on the collagen of the corneal stroma at day 2, and become more confluent by day 4. At this later time point, it appears that there is some epithelial cell layer organization. Transfer to the pig cornea was evaluated quantitatively by utilizing a denuded cornea model used to quantify epithelial coverage rates, and the specificity of transfer was tested by the regional de-epithelialization by sodium hydroxide. We conjecture that transferred HCE-SV40 cells preferentially attach to de-epithelialized regions with exposed stromal collagen, because collagen matrix is a better cell anchorage substrate than the surrounding confluent pig epithelial cells. This is supported by rhodamine fluorescence imaging of Celltracker Red CMPTX labeled HCE-

SV40 cells, which suggests that the superficial epithelium growing in the injured region originated from the epithelial-coated PDMS contact lens and that few transferred HCE-SV40 cells reside outside this wound region (Figure 4). We believe that this positive result is accurate because the labeling of HCE-SV40 cells with Celltracker Red CMPTX was specific, without any pig epithelium staining. HCEC-SV40 cells were directly labeled and washed prior to corneal introduction, and the hydrophobic nature of PDMS restricts harboring of unsequestered Celltracker. Celltracker Red CMPTX is only cell membrane permeable in its delivered form, which was only exposed to HCE-SV40 cells. After being internalized by a cell and cleaved by an intracellular esterase into its fluorescence emitting form, it is no longer membrane permeable (MolecularProbes 2003). If this form of the tracer was released during lysis of transferred cells on the corneal surface, pig epithelial cells would not be able to take up the activated Celltracker Red. According to the manufacturer's literature, Celltracker Red stays resident in viable cells for 72 hours (MolecularProbes 2003), making it an adequate cell label for use in this pig cornea model of epithelial wounding. Celltracker Green CMFDA also worked well in this application (data not shown). However, its use was limited by the fact that sodium fluorescein, the most common dye indicator of corneal surface defects, has similar emission wavelengths, making the utilization of both incompatible.

The findings of this study suggest that epithelial-coated PDMS contact lenses are a promising means to re-epithelialize the cornea. In addition, using standard photolithography, silicon masters can be produced to allow for the micropatterning of PDMS contact lenses, which has been observed to increase epithelial transfer. Our *in vitro* epithelial cell transfer experiment is a means of quick micropatterned contact lens

prototype evaluation to optimize design. Altering the dimensions or geometry of post structures may result in a design that better utilizes filopodia-mediated migration. By changing post size and spacing, we may also optimize the surface area for both effective cell attachment in culture and transfer to the cornea. PDMS is a versatile material, which can be easily modified (Aucoin, Griffith et al. 2002; Merrett, Griffith et al. 2003; Monge, Mas et al. 2003), which may provide for periods of cell retention and cell transfer.

Acknowledgments

We thank Dr. Patricia Russ for her troubleshooting and editing, and Sai-han Presley for her support as a cell technician. Special thanks to David Schaffer and the Vanderbilt Institute for Integrative Biosystems Research and Education for fabrication of silicon masters. We especially thank Elizabeth Dworska, for her work as this project's primary cell technician. This work was sponsored in part by NIH grants: EY 13593, EY 13451, HL 07751, and by a Vanderbilt University discovery grant.

References

Ali Z and Insler MS. A comparison of therapeutic bandage lenses, tarsorrhaphy, and antibiotic and hypertonic saline on corneal epithelial wound healing. Ann Ophthalmol 18: 22-24, 1986.

Araki-Sasaki K, Ohashi Y, Sasabe T, Hayashi K, Watanabe H, Tano Y, and Handa H. An SV40-immortalized human corneal epithelial cell line and its characterization. Invest Ophthalmol Vis Sci 36: 614-621, 1995.

Aucoin L, Griffith CM, Pleizier G, Deslandes Y, and Sheardown H. Interactions of corneal epithelial cells and surfaces modified with cell adhesion peptide combinations. Journal of Biomaterials Science-Polymer Edition 13: 447-462, 2002.

Chuck RS, Behrens A, and McDonnell PJ. Microkeratome-based limbal harvester for limbal stem cell transplantation: preliminary studies. American Journal of Ophthalmology 131: 377-378, 2001.

Grueterich, Scheffer, and Tseng. Human limbal progenitor cells expanded on intact amniotic membrane ex vivo. Archives of Ophthalmology 120: 783-791, 1996.

Kenyon K and Tseng S. Limbal autograft transplantation forocular surface disorders. Ophthalmology 96: 709-723, 1989.

Kuriana P, B. Kasibhatlaa, J. Dauma, C.A. Burnsb, M. Moosac, K.S. Rosenthald, J.P. Kennedya. Synthesis, permeability and biocompatibility of tricomponent membranes containing polyethylene glycol, polydimethylsiloxane and polypentamethylcyclopentasiloxane domains. Biomaterials 24: 3493–3503, 2003.

Larouche K, Leclerc S, Salesse C, and Guerin SL. Expression of the alpha 5 integrin subunit gene promoter is positively regulated by the extracellular matrix component fibronectin through the transcription factor Sp1 in corneal epithelial cells in vitro. J Biol Chem 275: 39182-39192, 2000.

Le Sage N, Verreault R, and Rochette L. Efficacy of eye patching for traumatic corneal abrasions: a controlled clinical trial. Ann Emerg Med 38: 129-134, 2001.

Meller D, Dabul V, and Tseng SC. Expansion of conjunctival epithelial progenitor cells on amniotic membrane. Exp Eye Res 74: 537-545, 2002.

Meller D, Pires RT, and Tseng SC. Ex vivo preservation and expansion of human limbal epithelial stem cells on amniotic membrane cultures. Br J Ophthalmol 86: 463-471, 2002.

Merrett K, Griffith CM, Deslandes Y, Pleizier G, Dube MA, and Sheardown H. Interactions of corneal cells with transforming growth factor beta 2-modified poly dimethyl siloxane surfaces. Journal of Biomedical Materials Research Part A 67A: 981-993, 2003.

MolecularProbes. Follow that cell. BioProbes, 2003.

Monge S, Mas A, Hamzaoui A, Kassis CM, Desimone JM, and Schue F. Improvement of silicone endothelialization by treatment with allylamine and/or acrylic acid low-pressure plasma. Journal of Applied Polymer Science 87: 1794-1802, 2003.

Nishida K, Yamato M, Hayashida Y, Watanabe K, Maeda N, Watanabe H, Yamamoto K, Nagai S, Kikuchi A, Tano Y, and Okano T. Functional bioengineered corneal epithelial sheet grafts from corneal stem cells expanded ex vivo on a temperature-responsieve cell culture surface. Transplantation 77: 379-385, 2004.

Pellegrini G, Traverso CE, Franzi AT, Mario Zingirian, Cancedda R, and De Luca M. Long-term restoration of damaged corneal surfaces with autologous cultivated corneal epithelium. The Lancet 349: 990-993, 1997.

Reim M, Kottek A, and Schrage N. The cornea surface and wound healing. Progress in Retinal and Eye Research 16: 183-225, 1997.

Sanchez-Thorin JC. The cornea in diabetes mellitus. Int Ophthalmol Clin 38: 19-36, 1998.

Figures

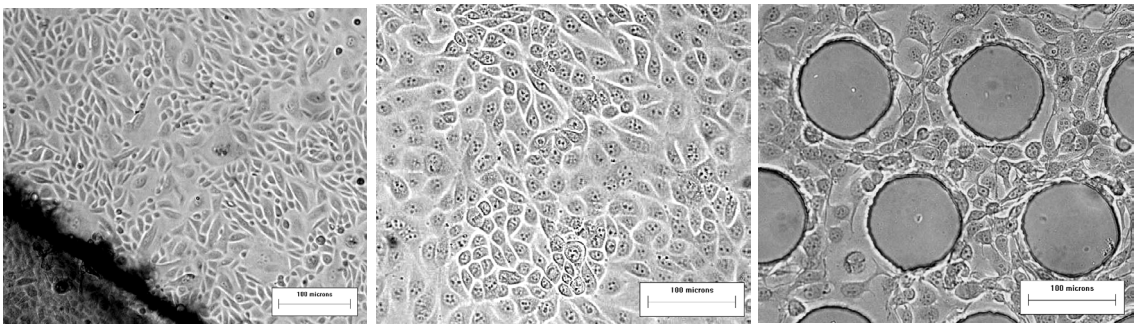

Figure 1. Human limbal explant expansion on PDMS (left). The explant is shown in the bottom left corner, and the outer limit of cell migration is shown in the top right corner. HCE-SV40 cells cultured on an unpatterned PDMS contact lens without posts (middle) and on a micropatterned PDMS contact lens with 100-micron diameter posts (right). Scale bars are 100 microns.

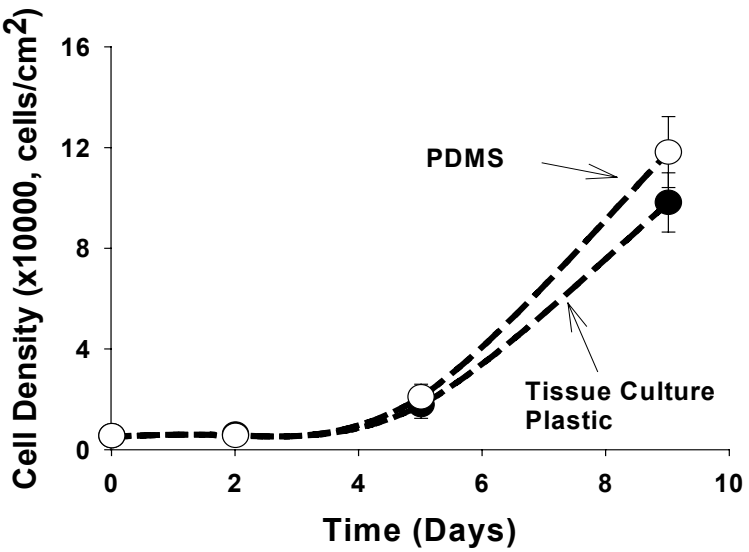

Figure 2. HCE-SV40 growth on PDMS is similar to growth on tissue culture polystyrene (mean ± s.d., n=10, Error bars are shown, but for early time points errors are too small to be discerned from the data points). The difference between groups is statistically insignificant.

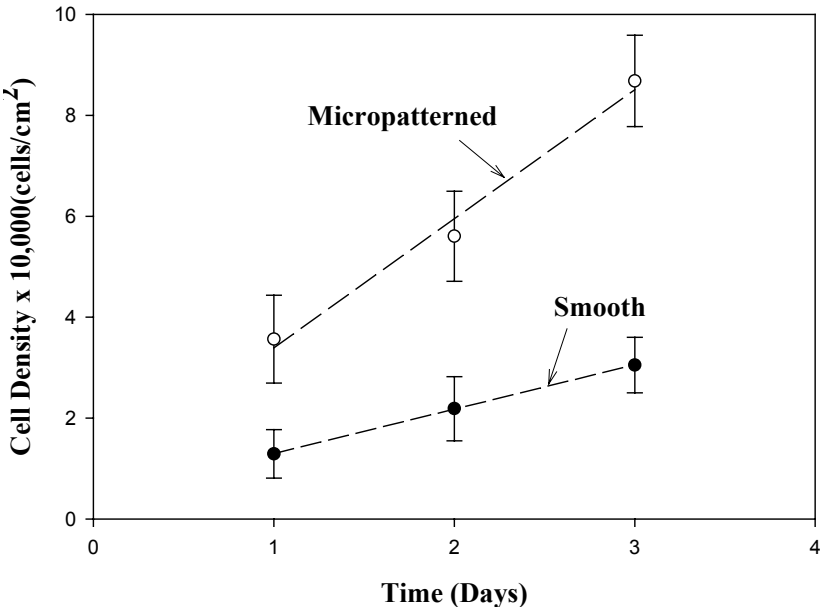

Figure 3. Transfer comparison from unpatterned (mean±s.d., n=10) and micropatterned PDMS (mean±s.d ,n=3). Micropatterned PDMS speed the transfer rate by 3-fold, which was statistically significant ($p < .05$).

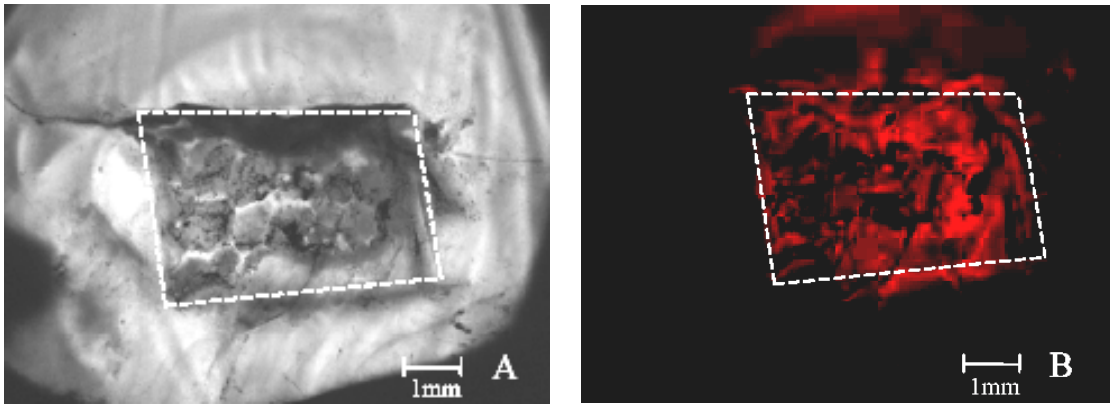

Figure 4. Epithelial transfer to a corneal wound region. Photographs of a whole cornea where the dotted box indicates the area of NAOH application. Phase contrast image of a NaOH treated regionally de-epithelialized pig cornea before application of a micropatterned PDMS cell-transfer contact lens (A). Rhodamine fluorescence image showing Celltracker Red-labeled HCE-SV40 cells attached in the wounded area after 48 hours of contact lens treatment (B).

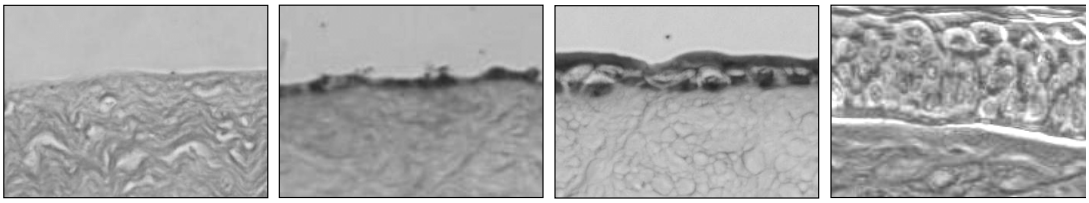

Figure 5. Epithelial cell transfer progression. Denuded cornea (far left), 2 day application (middle left), 4 day application (middle right), healthy cornea (far right). All images widths are 100 microns.

CHAPTER IV

CELL TRANSFER CONTACT LENSES DELIVER PRIMARY CORNEAL EPITHELIAL CELLS TO WOUNDED ORGAN CULTURED CORNEAS

Christopher J. Pino[1]

Min S. Chang[2]

Frederick R. Haselton[1,2]

[1]Biomedical Engineering

and

[2]Ophthalmology and Visual Sciences

Vanderbilt University

Nashville, Tennessee

Address for Correspondence:
Rick Haselton
Box 1510 Station B
Vanderbilt University
Nashville TN, 37235, USA
(615) 322-6622 office
(615) 343-7919 fax
rick.haselton@vanderbilt.edu

Abstract

Corneal wounds naturally heal from the outside wound margin. However we hypothesize that cells applied to the interior of wounds will augment healing. In our previous work, we found that PDMS contact lenses could be used as carrier devices to transfer immortalized human corneal epithelial cells to extracellular matrix materials. However, in the process to apply primary epithelial cells to wounded corneas we found that some of our past designs suffered from two main problems: limited primary cell transfer and limited cell viability/retention after transfer. In this work, we build on the previous findings that patterned carrier surfaces promote increased cell delivery, and explore the limitations of cell transfer in separate experiments. In order to demonstrate the feasibility of using cell carriers to seed wounds and to estimate the number of cells needed to enhance healing, cells were transferred to in vitro wounds using cytodex 3 beads. We found that cell-covered cytodex 3 bead treated wounds healed in a dose dependent manner, and that these wounds healed significantly faster than untreated control wounds. Using this in vitro model to investigate surface pattern topographies and coatings that enhance cell transfer, primary epithelial cells were seeded on cell carrier devices and transferred to matrigel well plates. We found that post patterning and fibronectin coating were the most beneficial to the delivery of primary cells. Cell carrier designs were developed as contact lenses and Cell Tracker Red labeled primary epithelia were applied to wounded organ culture corneas. However, during this process we found that some lenses partially removed healthy epithelium outside the wound region. In order to evaluate healthy epithelial removal, PDMS contact lenses with various surface coatings were applied to healthy organ culture corneas for 24 hours. After lens removal,

the remaining epithelium was stained and the coverage area was quantified. We have demonstrated that PDMS contact lenses coated with fibronectin can be used to deliver primary epithelial cells to injured corneal surfaces.

Introduction

Corneal wound healing is a complex, and highly coordinated process of cell-cell signaling, cell spreading, migration, proliferation, and cell-ECM interaction. The main limitation in natural wound healing is that cells can only fill in the wound void from the outside wound margin. We hypothesize that by administering primary epithelial cells to the interior of a corneal wound that cells will attach to the wound region and augment the healing process.

Building on two well-established technologies, therapeutic contact lenses and limbal stem cell transplantation, we set out to design and evaluate an epithelial cell transfer contact lens to seed persistent corneal wounds. Our objective was to design and evaluate contact lens that could deliver epithelial cells to wounds. We set out to develop a cell transfer contact lens that could keep cells in close proximity to the cornea and allow cell movement onto wounded regions. Promising lens designs were chosen by the following criteria: the lens material must allow for primary epithelial cell attachment and *in vitro* culture growth. Application of the cell-coated contact lens must result in the transfer of a portion of these cells to wound areas to aid in re-epithelialization of corneal injuries. Lastly, the lens must then function as a bandage lens after cell transfer in order to protect both applied and endogenous cell populations on the corneal surface.

In limbal stem cell tranplant therapy, adult stem cells are harvested from the limbus of a donor cornea and transplanted onto patient's stem-cell deficient cornea. This therapy is variable, depending on the source of donor cells, the amount of tissue used, and the method of delivery to the deficient eye. A limbal autograft is a transplantation of stem cells into a patient's deficient eye from their contra-lateral healthy eye. A portion of the stem cell-sufficient limbus is harvested from the healthy eye, and is surgically placed in the affected eye. Tseng and Kenyon conducted the first trial of autologous limbal transplants on patients in 1987. They found that this technique could be effective in the treatment of patients with previously failed corneal transplants, demonstrating an initial success rate of 85% (Kenyon and Tseng 1989). In cases of bilateral corneal stem cell deficiency, limbal allografts are used instead of autografts. In an allograft, transplanted tissue comes from a donor. The stem cell populated donor graft is then implanted into the deficient patient's limbus. These patients are then required to use immunosuppressive drugs such as cyclosporin. The process of taking ocular tissue from the limbus can be dangerous for a living donor if too much tissue is removed, leaving them with too few stem cells (Schwab and Isseroff 2000). This risk to the donor eye has been minimized by *ex vivo*-expanding limbal stem cells on growth substrates using cell culture techniques.

Michele DeLuca and his research team at the University of Genova have demonstrated that efficient *in vitro* expansion of corneal stem cells was possible, requiring fewer cells to be harvested from donor tissues. They found that 1 mm^2 sections harvested from the limbus were adequate to provide enough proliferative cells to re-epithelialize the cornea. Originally, implanted epithelial cultures were placed directly

into the eye using surgical gauze as a substrate, which was covered by a bandage contact to hold the gauze in place (Pellegrini, Traverso et al. 1997). Tseng and Kim found that amniotic membrane, which had been used in the past half century in ocular surgeries, could be used as a cell carrying substrate for limbal transplants (Kim and Tseng 1995). Limbal stem cells are now cultured directly on amniotic membrane in vitro, which creates 100-fold more cells to be implanted into a deficient eye (Quantock, Koizumi et al. 2002). However, Nishida et al have developed a method to prepare full epithelial sheets for implantation without a substrate material. Limbal explants were cultivated on a temperature-sensitive polymer growth surface. After weeks of culture time, hardy epithelium composed of multiple cell layers were released from the polymer by a temperature change (Nishida, Yamato et al. 2004). Research groups in Taiwan, Japan, Germany, Italy, and the U.S. have demonstrated the efficacy of *ex vivo* expansion of corneal epithelial cells for transplant procedures to treat limbal stem cell deficiency .

Therapeutic contact lenses, also known as bandage contact lenses, are used to treat many ophthalmic conditions including corneal abrasions, erosions, persistent defects, chemical injuries and postoperatively after vitrectomy, penetrating keratoplasty, epikeratoplasty, lamellar grafts, PRK, LASIK and cataract extraction. These contact lenses differ from vision correction lenses in that their primary function is to protect the corneal epithelium, rather than correct refractive error. They have been shown to help stabilize the corneal surface after trauma and allow for re-epithelialization. The most serious complications of TCL wear include infections such as microbial keratitis and giant papillary conjunctivitis and anoxia, which can result in neovascularization. To

prevent infection, antibiotics may be used for a short period, however, it is important to choose an antibiotic that will not adversely effect wound healing.

In our previous work, we demonstrated that PDMS contact lenses could be used as carrier devices to grow and transfer immortalized human corneal epithelial cells to extracellular matrix materials (Pino, Haselton et al. 2005). However, in the process to apply primary epithelial cells to wounded corneas we found that some of our past designs suffered from two main problems: limited initial cell transfer, and limited cell viability and retention after transfer. In this work, we have set out to characterize these limitations, and evaluate primary cell transfer from therapeutic contact lenses to organ culture corneas.

Materials and Methods

Precision epithelial drill press

The drill was assembled using a rotational motor, interchangeable drill bits and a micromanipulator. Interchangeable teflon drill bits shaped like chisel points were cut using a scalpel while observing through a microscope, and smoothed by standard machining techniques. The bits were slip-fit onto the motor shaft, and the motor was mounted on a Drummond micromanipulator (Marzhauser MM33, Catalogue #3-000-024) for fine control over the x, y, and z positioning.

Wounding cell culture monolayers

An immortalized human cornea epithelial cell line (HCE-SV40 cells) developed by Araki-Sasaki (Araki-Sasaki, Ohashi et al. 1995), was seeded at 100 cells/cm^2 on 21 cm^2 tissue culture dishes coated with Collagen I (B.D. Biosciences). Cells were cultured in defined keratinocyte serum free media (Gibco/Invitrogen, Grand Island, NY) and maintained for over 3 days to insure confluence and recovery from trypsinization.

To create wounds in these monolayers, autoclaved drill bits were affixed to the precision drill press in a sterile laminar flow hood. The height adjustment screw of the micromanipulator was used to slowly lower the spinning drill bit down to the cell surface. Removed cells were washed away in sterile phosphate buffered saline (PBS).

Culture media was changed every day after wounding. Wounds were viewed using a Nikon Eclipse TE2000U inverted microscope (Nikon USA, Melville, NY), and images were recorded with a Hamamatsu C7780 CCD (Hamamatsu Corporation, Bridgewater, NJ) and Nikon D100 (Nikon USA, Melville, NY) camera every 24 hours.

Preparation of HCEC on Cytodex3 beads

One milliliter of cytodex 3 beads and one million cells were added to 100 milliters of medium in a small spinner flask. For one day the spinner flask was automated to spin for 2 minutes intervals with 30 minutes between each spin cycle. Thereafter, the flask was constantly mixed. After 3 days of cell attachment, beads were pipetted from the spinner flask into wells that had monolayer wounds. Well plates with cell-coated beads were not disturbed for 2 days to allow for cells on beads to attach to wound areas. Daily medium changes and imaging of the wound areas resumed on day 3.

Analysis of cell transfer from Cytodex 3 beads to monolayer wounds

All image analysis was done using the Image Pro software package (IPP version 5.0, Media Cybernetics, Silver Spring, MD). Images were calibrated using a stage micrometer. Before analysis, each image was contrast enhanced by boosting the contrast to 75% and adjusting the overall brightness so that the background pixels had zero values. Using Image Pro's measurement tools, the automated free hand tool was used to identify the wound margin for cell culture monolayers after initial wounding. Image Pro reported the area of the wound regions in square microns, which were converted into corresponding areas in square millimeters. For cell-coated bead treated wounds, a wound area was determined by identifying the outermost wound margin in the same way as the control wounds, but then interior areas of cell transfer from beads were subtracted from this area. All initial wound areas, control wound healing areas, and cell-coated Cytodex 3 treated areas were entered into Excel (Microsoft Office) spreadsheets for statistical analysis. In order to calculate average wound closure rate for each period, the wound diameter at the end of a time interval was subtracted from the initial wound diameter.

Cell transfer to matrigel

See Protocol in Pino et al in Cell Tansplantation (Pino, Haselton et al. 2005). Briefly, Immortalized HCE were seeded on PDMS disks with embedded Cytodex 3 beads at approximately 50,000 cells/cm^2. After 1 day of cell attachment, the PDMS disks were turned cell side down onto fresh matrigel-coated wells, and ~400 microliters of medium was added. Every 24 hours thereafter, selected disks were removed, and wells were

washed prior to imaging of well plates and trypsinization to determine cell transfer. Transferred cell density was quantified using a Coulter-Beckman Multisizer 2 and then verified by cell counts from image analysis. Other wells with cells on PDMS disks that were not ready to be counted received medium changes daily.

For primary epithelial cell transfer experiments, cells from primary explants were harvested using trypsin and a cell scraper. The total number of primary cells isolated determined cell seeding density. Once again, cells were allowed 24 hours for attachment on PDMS disks in 24 well plates. Then the disks were placed cell side down into a fresh 12-well plate coated with matrigel. Cell transfer was determined by imaging and trypsinized cell counts after 3 days.

Epithelial retention assay for organ culture corneas treated with contact lenses

Fresh tissue samples were obtained from euthanized animals that were used for other research at Vanderbilt University in accordance with IUCAC guidelines. Rabbit, goat, or pig eyes were enucleated and transported in sterile PBS with 1% antibiotic. Corneas were isolated by cutting the sclera to form a corneal button. A millimeter rim of the sclera was kept all around the corneal button, which was found to help maintain corneal clarity and integrity in organ culture.

Corneas were washed in PBS and placed into 6 well plates for culture on agar/DMEM plugs. Corneas to be treated had contact lenses applied, and then Defined Keratinocyte Serum-Free Medium was added to the wells until the medium level washed over the top of the contact lens.

Rose Bengal (100 mg/10mL) was applied to organ culture corneas to visualize regions with retained epithelial cells (Feenstra and Tseng 1992). After 30 seconds, excess rhodamine was washed off with PBS, and the corneas were placed on clear domes for imaging. Corneas were photographed with a Nikon D100 camera coupled to a Zeiss surgical microscope. Regions with bound epithelium appeared bright red, and denuded regions appeared clear.

Preparation of PDMS contact lenses and patterned disks

Poly(dimethylsiloxane) (PDMS) obtained from Dow Corning (Sylgard® 184, Midland, Michigan, U.S.A) was mixed according to the manufacturer's instructions, in a 10:1 mixture of monomer to curative agent. To make contact lenses, the mixture was poured into a concave mold with a radius of curvature of 8.8mm. Air bubbles were removed from the PDMS by application of a vacuum pump for 10 minutes. Then the top part of the mold, a ball bearing with a radius of curvature of 9 mm, was placed on top of the bottom mold. After a few hours at 65°C, PDMS contact lenses were fully cured, and were released from the mold. Contact lenses with Cytodex 3 embedded beads were fabricated by partially curing the PDMS and then adding Cytodex beads to the PDMS through a sifter. Lastly, patterned disks were fabricated by pouring the monomer and curative agent mixture onto prefabricated polyurethane surfaces, and curing under the same conditions.

PDMS contact lenses and disks were then sterilized by either soaking in 70% ethanol while under UV overnight, or by autoclave treatment at 135°C for 30 minutes.

Fibronectin surface coating at a concentration of 5 micrograms per milliliter was applied to sterile contacts so that the coating completely covered the PDMS surface.

Results

Cell transfer from Cytodex 3 beads

When added to the culture plate wells with wounded epithelial monolayers, cell covered cytodex3 beads immediately settled to the bottom of the wells. After 24 hours, cell migration from few beads to bottom culture surface was evident. And at 48 hours, the majority of cell-coated beads exhibited cell transfer. Medium was changed after 48 hours to avoid bead movement before cell migration could occur. Images of cell-covered bead treated wounds and control wounds were imaged at 36 hours and each day thereafter to access wound coverage by epithelial cells Figure 2. .Steady cell migration from cytodex 3 beads was exhibited from day 3 to day 7, which enhanced coverage of the treated wound regions. As shown in Figure 7, cell-covered bead treated wounds had significantly lower remaining wound areas each day after treatment compared to the untreated monolayer wounds.

In addition to cell transfer from beads to wounded regions, cell-coated beads also adhered to contiguous healthy regions of the monolayer. Though the cell-coated bead solution was well mixed when added to the culture plate, cell attachment to all areas of the culture plate was random and heterogenous. Some areas of the plate exhibited more bead attachment than others, and therefore some wounds received cell transfer from a higher density of beads. In order to determine if monolayer wound healing was cell-

transfer dose dependent, the number of beads within each wound were counted, and classified as having high bead concentration (>10 beads/mm^2) or low bead concentration (<10 beads/mm^2), and uncovered wound areas were quantified using image analysis software. We found that wounded regions treated with more than 10 beads per square millimeter healed significantly faster, as demonstrated by lower wound areas each day during bead treatment (Figure 8). From the images obtained, we estimate that approximately 5,000-10,000 cells/cm^2 were seeded when ~10 beads/mm^2 were applied within the first 3 days of treatment. Using this cell transfer density as a benchmark for enhancing the healing of wounds, we sought to design an easy to apply contact lens transfer device to transfer primary cells to corneal wounds.

Cell transfer from Cytodex 3 beads embedded in PDMS

In previous work with an immortalized human corneal epithelial cell line, we found that transferred cell densities in excess of 10,000 cells/cm^2 could be obtained by seeding cells at a density of over 50,0000 cells/cm^2. When Cytodex 3 beads embedded in PDMS were seeded with 50,000 cells/cm^2, cells adhered to both the Cytodex 3 beads as well as on the PDMS between beads. When flipped onto matrigel, an increasing number of cells transferred from the PDMS disks onto the bottom matrigel surface on each consecutive day. After one day, 7108 ± 1459 cells transferred, on the second day, 14802 ± 3849, and on the third day 45383 ± 16558 transferred to matrigel as shown in Figure 9. However, when this experiment was repeated with primary cells seeded at approximately 50,000 cells/cm^2, only 13,000 cells/cm^2 transferred to matrigel by day three.

Primary cell transfer from patterned PDMS to matrigel

Patterned cell substrates have been used to direct cell movement (Matsuzaka, Walboomers et al. 2003), and in our previous work, we showed that micropatterned posts improve epithelial cell transfer. Since these findings, we have fabricated many other types of surface pattern designs that we tested which are summarized in Figure 10: flat, posts, ridges, through-holes, and wells.

In evaluating PDMS surface designs to augment primary cell delivery, we observed that surface features that stick up off of the culture surface, such as posts and ridges, are most beneficial to primary cell transfer to matrigel.

Primary cell transfer from ECM-coated PDMS to various types of ECM

When 25,000 cells/cm^2 were added to autoclaved PDMS disks, and other disks coated with fibronectin and matrigel, primary cells attached to each material. As expected, matrigel, a matrix material made up of collagen and laminin, allowed for slightly greater primary cell attachment than autoclaved PDMS. However, we found that the differences in cell attachment were too small to be statistically significant. Of 25,000 cells/cm^2 seeded, 23,896 ± 8647 cells/cm^2 attached to autoclaved PDMS, 22,695 ± 5713 cells/cm^2 attached to fibronectin coated PDMS and 26,422 ± 9412 attached to matrigel.

Primary cell transfer to organ culture corneas

After 24 hours of application, primary cells transferred from contact lenses to wound regions of injured organ cultured corneas. Cornea surfaces were imaged by both epi-fluorescence and confocal microscopy, where transferred epithelial cells were stained

with Cell Tracker red (red), and the wound region was stained with sodium fluorescein (green). The confocal images in Figure 13 show that autoclaved PDMS contact lenses were able to deliver cells to corneal wounds.

We noted that primary cells that were directly pipetted on the corneal surface and allowed to attach for 24 hours, appeared qualitatively similar to cells transferred from the cell transfer lens. In a quantatative assessment of primary cell transfer from ECM coated contact lenses to damaged corneas, we found similar reults to our previous transfer to matrigel. We found that fibronectin coated lenses delivered significantly more cells than did collagen or matrigel coated lenses Figure 14.

We also observed that when an autoclaved PDMS cell transfer contact lens was removed, some healthy corneal epithelium from outside the wound region was also removed. This finding prompted us to investigate if surface protect normal healthy epithelium from being peeled off after lens removal.

Healthy epithelial cell removal was minimized by fibronectin coating

In order to identify contact lens designs that might transfer cells to wound regions, but leave healthy epithelium in tact, we developed an assay to determine the extent of healthy epithelial removal after contact lens application. Autoclaved PDMS, and PDMS with fibronectin and bovine serum albumin coatings on contact lenses, were tested by applying the contact lenses for 24 hours, and assessing the remaining epithelium. We found that fibronectin coated lenses allowed for the greatest amount of epithelial retention (Figure 15). Lenses coated with BSA removed the most epithelium when peeled off healthy corneas.

Discussion

In order to estimate cell transfer mediated by cell motility from a carrier to a wound, an in vitro model was used. Cytodex 3 beads were used in this model system because they supported HCE cells growth, and allowed for cell transfer when they settled onto another cell growth surface. In this model, we did not have to worry about the possible effect of apoxia encountered when using a contiguous large device, such as a contact lens for delivery. In addition, media was changed liberally, so as to remove nutrient limitation as a confounding factor. This model gave us some proof that cells applied to the interior of wounds would speed time to complete re-epithelialization. From this model we also estimate that 5-10 thousand cells/cm^2 are required to be delivered in order to have a therapeutic effect.

In this work, we have advanced a cell transfer technology, which had previously only been explored with an immortalized epithelial cell line. In the process of moving to primary epithelial cells isolated from corneal explants from an SV40 adenovirus immortalized human corneal epithelial cell line, we knew that there would be many technical hurdles to overcome. Using well-established cell isolation techniques, we were able to harvest mixed population of primary corneal epithelial cells for use in transfer experiments. We did not attempt to purify the cultured cells to obtain a cell population that enriched in limbal stem cells. Rather we used the mixed population of epithelial cells that consisted of a stem cell like population that Pelligrini et al. termed holoclones, and differentiated population called paraclones (Pellegrini, Ranno et al. 1999). Based on morphology observations, both cell populations were able to attach and transfer from

PDMS. However, in comparison to immortalized HCE, the mixed population of primary epithelial cells was less able to transfer from PDMS onto both matrigel and wounded corneas. The amount of primary cell transfer was lower in both cell density and percent efficiency of transfer. This result is unsurprising, since generally immortalized cell lines are hardier, more adhesive and more proliferative. However, in order to optimize cell transfer for therapy, it would be ideal to improve the cell migration characteristics of the primary cell line. This could be done by cell selection from the primary isolates. In normal corneal wound healing, it is the basal cells, which migrate into wound areas from the margin. These cells are characterized as being more stem cell like. Therefore by removing cells that are terminally differentiated, we may enhance primary cell transfer. This, in addition, will enhance therapy since delivery of a pure stem cell population is more beneficial than delivering terminally differentiated cell, which die and slough off.

Primary cells that were transferred to damaged corneas by PDMS contact lenses were protected by the fibronectin-coated contact lens after transfer. When this contact lens was removed, transferred epithelium and endogenous healthy epithelium clearly remained shown by Rose Bengal staining. This stain was used because it gave good contrast to the remaining epithelial cell regions, as opposed to diffuse staining of sodium fluorescein, which we previously used to identify regions lacking epithelium. Many clinicians use Rose Bengal to stain for devitalized corneal epithelial cells in vivo. However, in organ culture, all healthy rabbit corneal epithelial cells stain positively with Rose Bengal, as demonstrated by Feenstra et al. This is because in vivo, it is a healthy tearfilm interaction with healthy cells, which prevents Rose Bengal staining. However,

when organ cultured there is no remaining tear film components to hinder the epithelial stain, and therefore all cells are labeled.

After cell transfer to a damaged corneal surface, when shear was added to this unprotected cornea by repeated washings, some transferred cells were lost. This is a major technical hurdle this technology faces before it could be implemented as a therapy. In vivo, shear exerted on the transferred cells may prevent strong cell adhesion to wound ECM, which in turn would prevent cell proliferation and re-epithelialization at the corneal surface.

Acknowledgements

We would like to thank Elizabeth Dworska, for her work as this project's primary cell technician. Special thanks to David Schaffer and the Vanderbilt Institute for Integrative Biosystems Research and Education for fabrication of silicon masters. This work was sponsored in part by NIH grants: EY 13593, EY 13451, HL 07751, and by a Vanderbilt University discovery grant.

References

Araki-Sasaki, K., Y. Ohashi, et al. (1995). "An SV40-immortalized human corneal epithelial cell line and its characterization." Invest. Ophthalmol. Vis. Sci. 36(3): 614-621.

Feenstra, R. P. and S. C. Tseng (1992). "What is actually stained by rose bengal?" Arch Ophthalmol 110(7): 984-93.

Kenyon, K. and S. Tseng (1989). "Limbal autograft transplantation for ocular surface disorders." Ophthalmology 96: 709-23.

Kim, J. and S. Tseng (1995). "Transplantation of preserved human amniotic membrane for surface reconstruction in severely damaged rabbit corneas." Cornea 14: 473-484.

Koizumi, N., T. Inatomi, et al. (2001). "Cultivated corneal epithelial stem cell transplantation in ocular surface disorders." Ophthalmology 108(9): 1569-1574.

Meller, D., V. Dabul, et al. (2002). "Expansion of conjunctival epithelial progenitor cells on amniotic membrane." Exp Eye Res 74(4): 537-45.

Nishida, K., M. Yamato, et al. (2004). "Functional bioengineered corneal epithelial sheet grafts from corneal stem cells expanded ex vivo on a temperature-responsieve cell culture surface." Transplantation 77(3): 379-385.

Pan, Z., W. Zhang, et al. (2002). "Transplantation of corneal stem cells cultured on amniotic membrane for corneal burn: experimental and clinical study." Chin Med J (Engl) 115(5): 767-9.

Pellegrini, G., R. Ranno, et al. (1999). "The control of epidermal stem cells (holoclones) in the treatment of massive full-thickness burns with autologous keratinocytes cultured on fibrin." Transplantation 68(6): 868-79.

Pellegrini, G., C. E. Traverso, et al. (1997). "Long-term restoration of damaged corneal surfaces with autologous cultivated corneal epithelium." The Lancet 349(9057): 990-993.

Pino, C. J., F. R. Haselton, et al. (2005). "Seeding of corneal wounds by epithelial cell transfer from micropatterned PDMS contact lenses." Cell Transplant 14(8): 565-71.

Quantock, A. J., N. Koizumi, et al. (2002). "Limbal stem cell deficiencies and ocular surface reconstruction." Optometry Today(July 12th): 27-30.

Schwab, I. R. and R. R. Isseroff (2000). "Bioengineered Corneas -- The Promise and the Challenge." N Engl J Med 343(2): 136-138.

Shimazaki, J., M. Aiba, et al. (2002). "Transplantation of human limbal epithelium cultivated on amniotic membrane for the treatment of severe ocular surface disorders." Ophthalmology 109(7): 1285-1290.

Figures

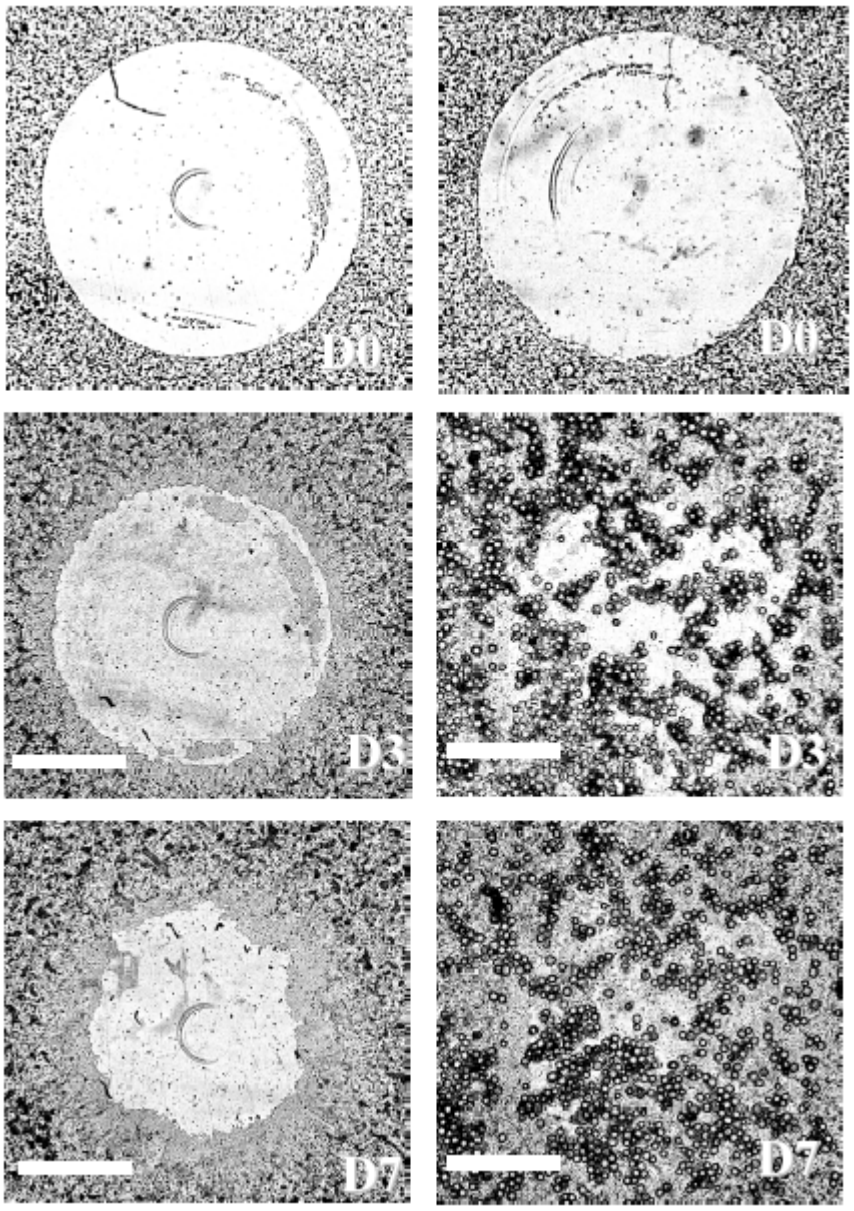

Figure 6.Monolayer wounds created with a 6mm drill bit heal more quickly when cells are administered from Cytodex 3 beads. Wound areas for bead treated wounds were not measured on days 1 and 2 to allow for cell transfer without disturbance, however at all measured time points, wound area differences are statistically significant ($p < 0.05$).

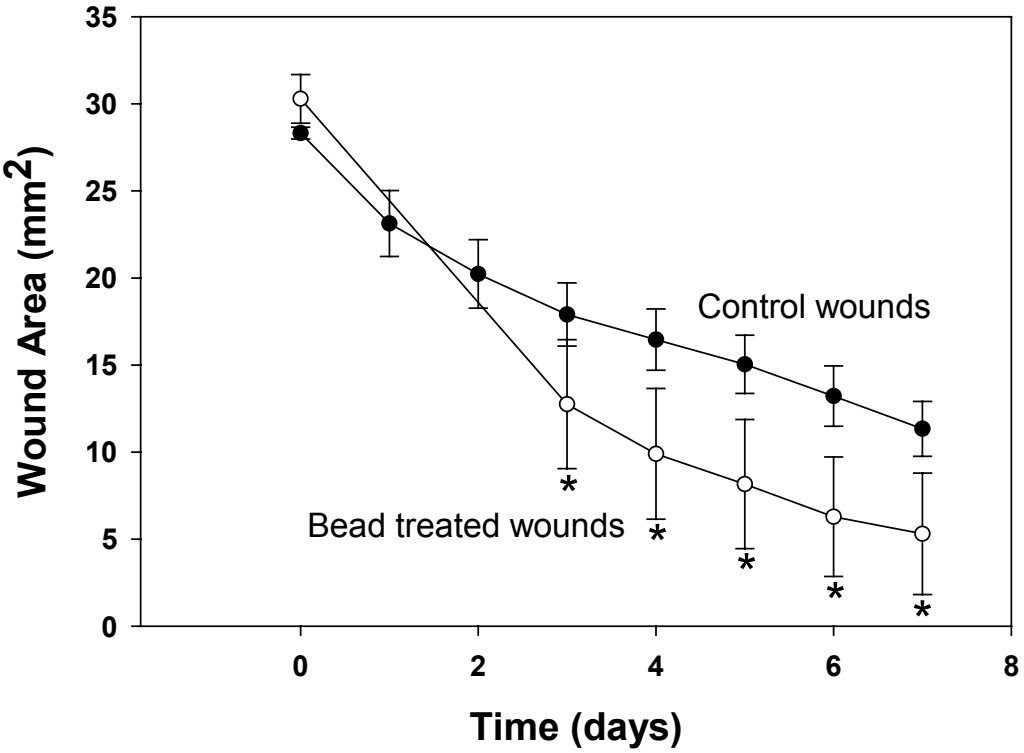

Figure 7. Monolayer wounds created with a 6mm drill bit heal more quickly when cells are administered from Cytodex 3 beads. Wound areas for bead treated wounds were not measured on days 1 and 2 to allow for cell transfer without disturbance, however at all measured time points, wound area differences are statistically significant ($p < 0.05$).

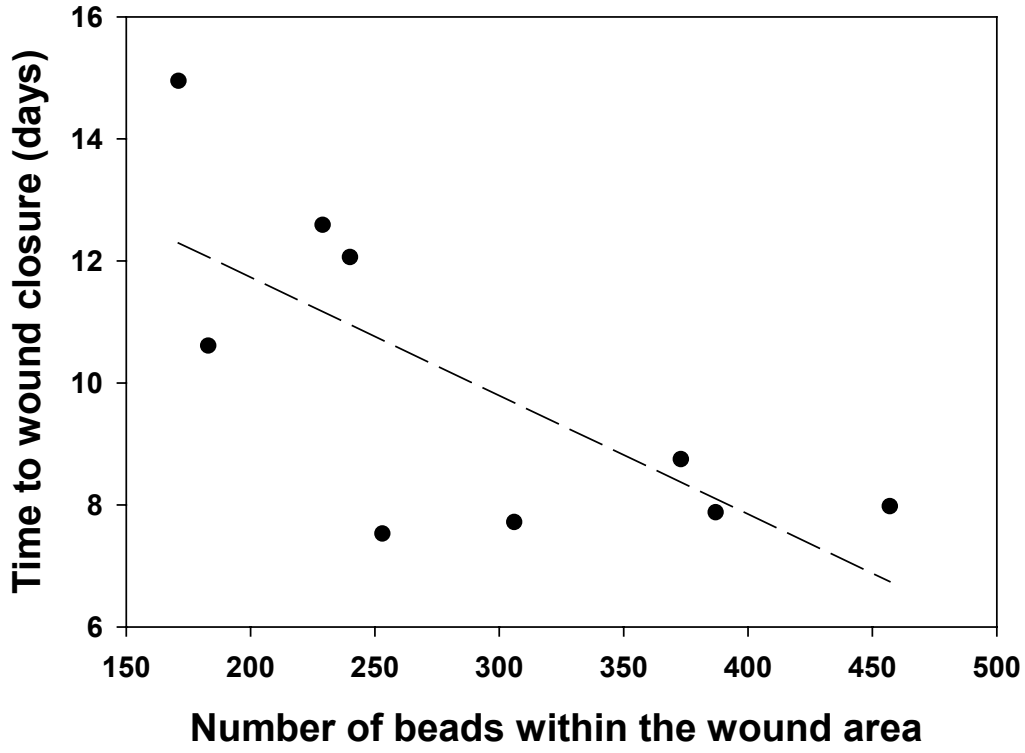

Figure 8. Monolayer wounds exhibit enhanced wound healing when treated with higher concentrations of cell-covered beads. Each point shown in the graph is one wound treated with cells on beads with an associated number of beads in the wound region and a time to wound closure. The dotted line shown is a linear regression trend line for the wound healing data.

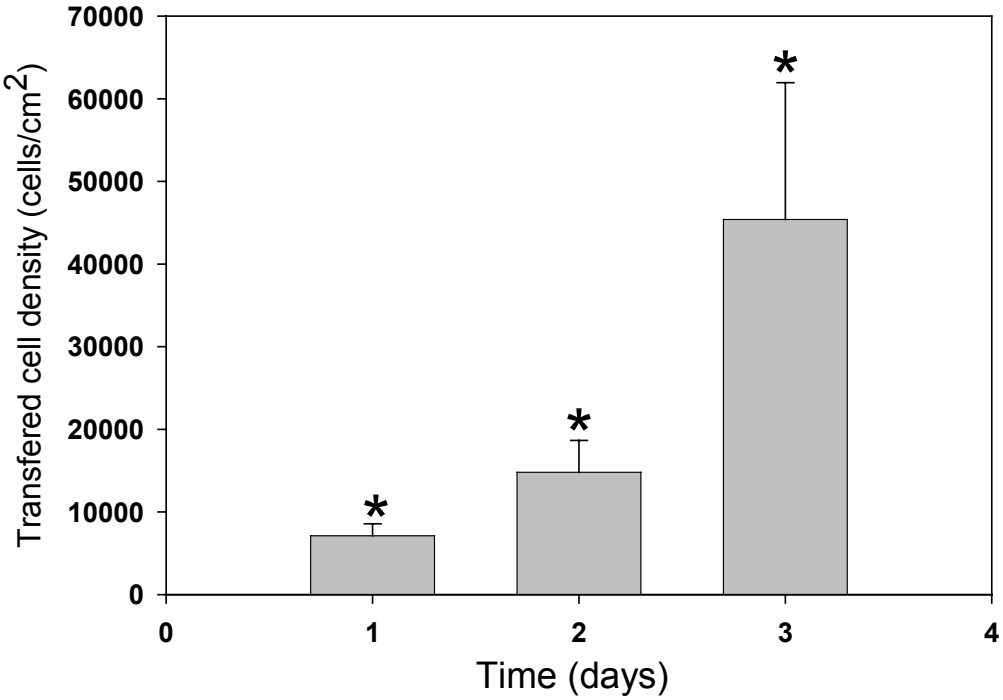

Figure 9. HCE cell transfer from cytodex3 beads embedded in PDMS to matrigel-coated well plates. Original seeding density was approximately 50,000 cells/cm^2.

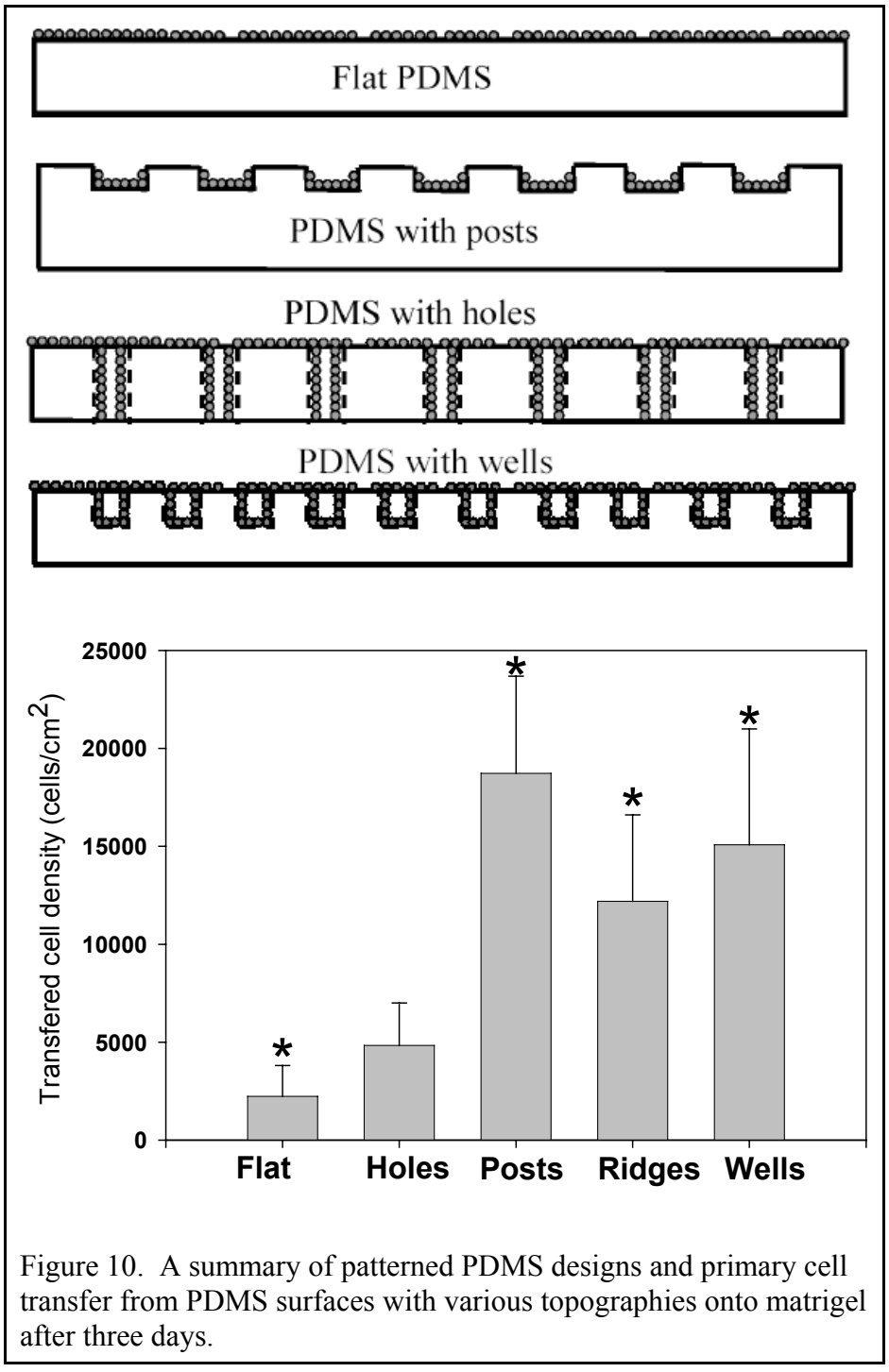

Figure 10. A summary of patterned PDMS designs and primary cell transfer from PDMS surfaces with various topographies onto matrigel after three days.

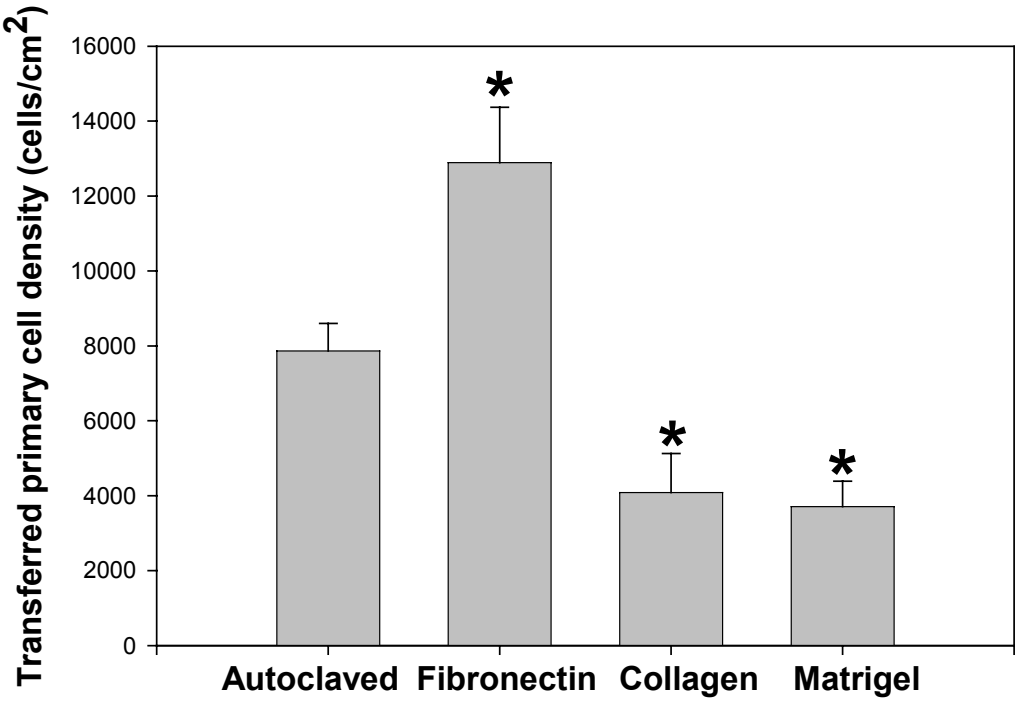

Figure 11. Primary cell transfer from coated contact lenses to tissue culture polystyrene (TCPS). Fibronectin coated lenses facilitated the greatest amount of cell transfer.

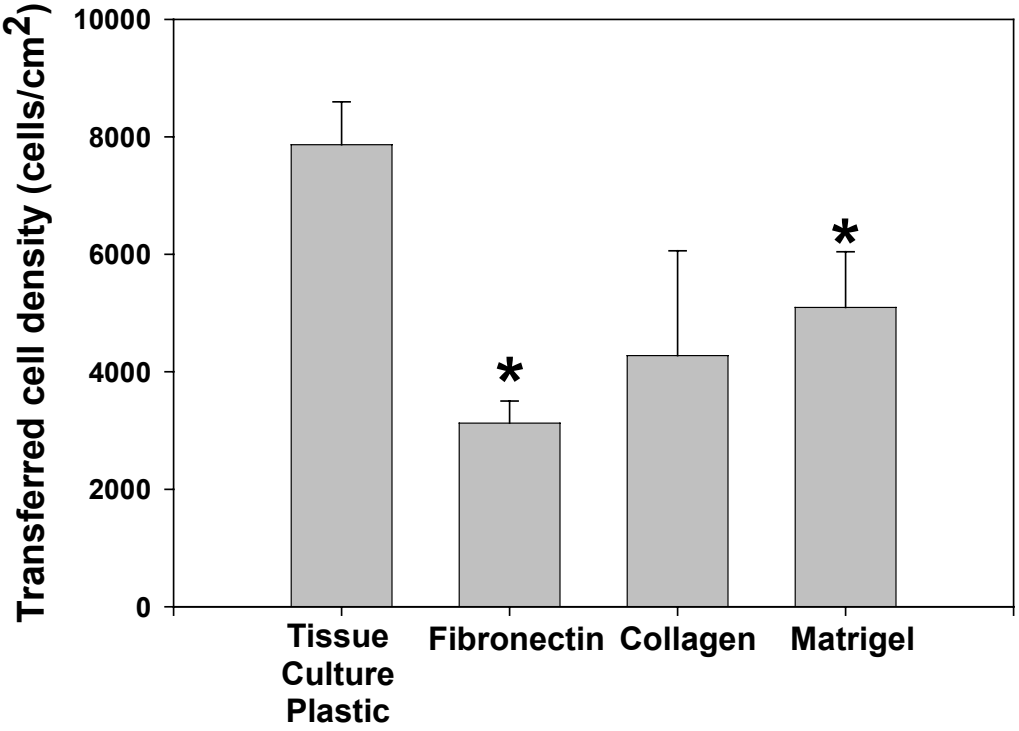

Figure 12. Primary cell transfer from autoclaved PDMS contact lenses to various types of ECM. Autoclaved PDMS displayed the greatest amount of cell transfer to poly L-lysine tissue culture polystyrene (TCPS), however, of the ECM materials, matrigel surfaces were the best recipient surfaces.

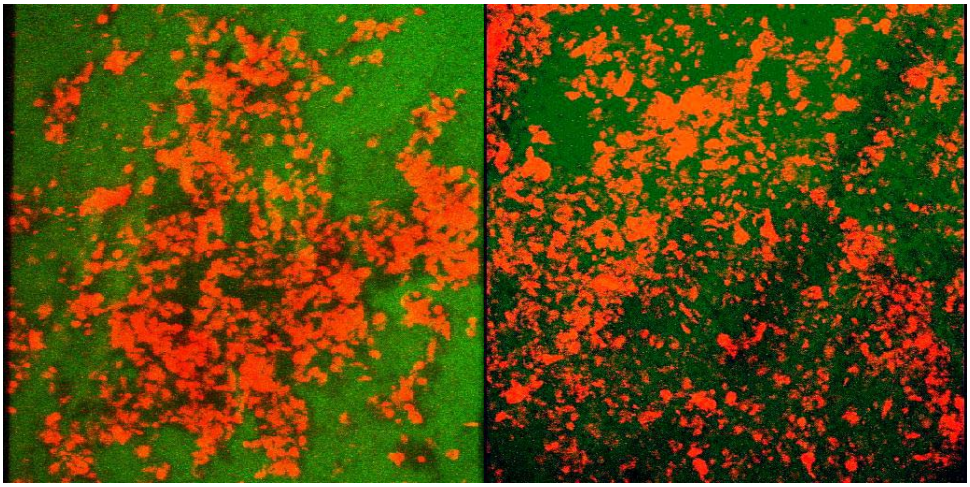

Figure 13. Confocal microscope images of organ cultured cornea wound regions treated with primary cells directly pipetted into place (A) and transferred by an autoclaved PDMS cell-transfer contact lens. Primary cells were stained with Cell Tracker red and the ECM of the wound region was stained green with sodium fluorescein. Scale bar is 100 microns.

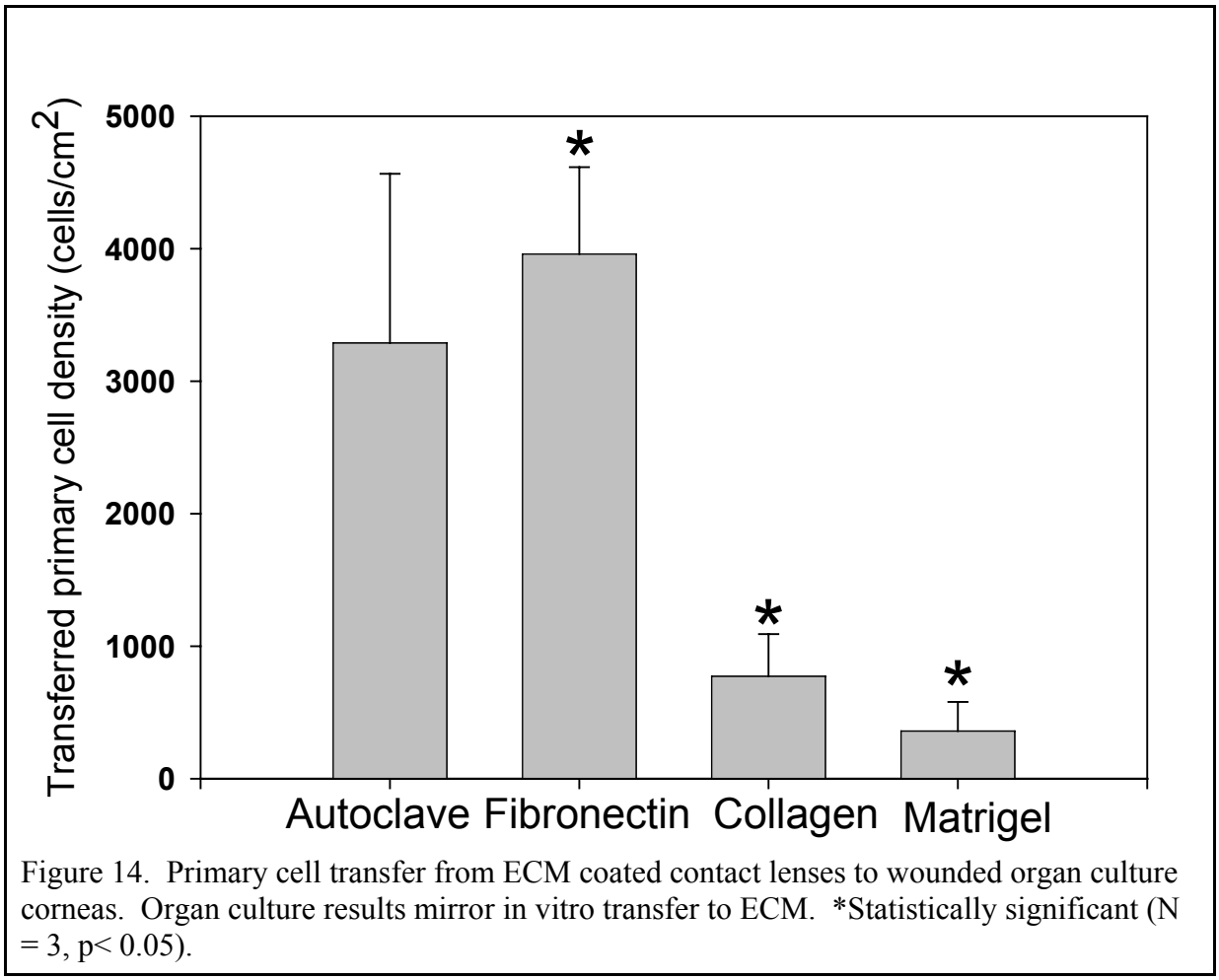

Figure 14. Primary cell transfer from ECM coated contact lenses to wounded organ culture corneas. Organ culture results mirror in vitro transfer to ECM. *Statistically significant (N = 3, $p < 0.05$).

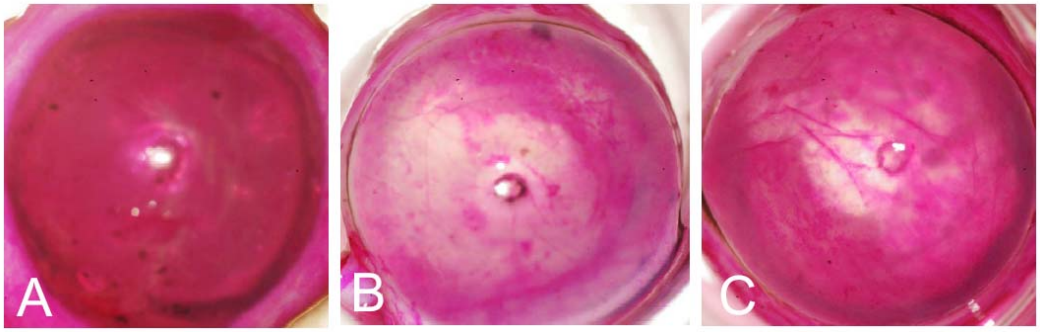

Figure 15. Remaining epithelium stained pink by rose bengal after contact lens treatment. Corneas with no contact lens treatment showed no signs of epithelial loss (A). However autoclaved PDMS contact lens treated corneas showed substantial epithelial removal (B) and fibronectin coated lenses minimized cell removal (C). Remaining epithelial coverage is ~100% (A), ~50% (B), ~85% (C).

CHAPTER V

LOSS OF PROPER BVES FUNCTION PROMOTES EPITHELIAL-MESENCHYMAL TRANSITION (EMT) AND ENHANCED CELL MOTILITY IN CORNEAL EPITHELIAL CELLS

Christopher J. Pino[1]

Frederick R. Haselton[1,2]

Min S. Chang[2]

[1]Biomedical Engineering

and

[2] Ophthalmology and Visual Sciences

Vanderbilt University

Nashville, Tennessee 37232

Address for Correspondence:
Min S. Chang
Vanderbilt University
Nashville, TN,
Phone: (615) 936-6413 (office)
min.s.chang@vanderbilt.edu

Abstract

Normal epithelial cells form a continuous layer of polarized cells, which have cell-cell contacts and distinct apical and basolateral domains. However during the process of Epithelial-Mesenchymal Transition (EMT), epithelial cells lose cell-cell contacts with an accompanying loss of polarity and the ability to form continuous sheets. These cells have mesenchymal properties such as increased motility, and the ability to proliferate and reside within matrix materials, which are invasive characteristics similar to cancer cells. It is widely accepted that functional loss of the adherens junction protein E-cadherin, is a primary event in EMT, which demonstrates the importance of cell junctions in EMT. We hypothesize that the loss of blood vessel/epicardial substance (Bves), a gene product that localizes to tight junctions and maintains epithelial sheet integrity, may also lead to EMT. In order to study the role of Bves in EMT, an SV40 immortalized human corneal epithelial cell line (parental HCE) was stably transfected to over-express chick-Bves (c-Bves), a fully functional form of Bves. A second line of cells were transfected with a truncated, Bves mutant (t-Bves), which does not properly localize to tight junctions to create a dominant negative cell line (t-Bves HCE). Changes in epithelial morphology, cell migration, and proliferation within a 3-dimenstional matrix in c-Bves and t-Bves cells were characterized and compared to the parental (HCE) cells. In these studies we have demonstrated epithelial cells undertake a mesenchymal phenotype when Bves trafficking to the cell membrane is disrupted by over-expressing t-Bves. These cells were not able to form a continuous monolayer. Furthermore, t-Bves HCE have acquired a fibroblast-like morphology with spindle like projections, along with greatly enhanced motility with a migration rate of nearly twice the parental HCE.

Dominant negative Bves cells also exhibited ~40% enhanced proliferation within a 3-dimensional nutrient matrix (soft agar). Though the molecular mechanisms for these observations are not fully understood, our findings suggest that the loss of proper trafficking of Bves to the cell membrane induces cell changes similar to those used to characterize EMT, whereas over-expression of Bves maintains and enhances epithelial characteristics.

Introduction

A defining characteristic of epithelial cells is their ability to a form a continuous monolayer, or multiple layers, of polarized cells. The cells within a monolayer are more than just a grouping of adherent cells. In addition, they typically exhibit uniform morphology with coordinated cellular proliferation and differentiation. Points of cell-cell adhesion within a monolayer provide both structural integrity and sites for cellular interaction so that groups of cells can function as a tissue. However, epithelial cells can acquire mesenchymal cell properties marked by a loss of cell-cell contacts and cellular polarity, accompanied by increased motility and invasive potential through a process known as epithelial-mesenchymal transition (EMT). Regulation of EMT is an important cellular function involved in both normal development and cancer (Bates and Mercurio 2005). Understanding the molecular mechanisms regulating EMT will provide insight into physiologic and pathologic phenomena.

EMT was originally described in embryonic development and defined by the formation of mesenchymal cells originating form primitive epithelia. Given the proper cues, a number of different adult and embryonic epithelial cells have been found to lose

polarity and migrate as individuals when cultured within collagen growth matrix (Greenburg and Hay 1982; Greenburg and Hay 1986). When treated with conditioned medium from fibroblasts, Madin-Darby canine kidney cells have been shown to acquire a migratory fibroblast-like phenotype (Stoker 1989). The molecular basis of EMT is complex and involves a growing number of signaling pathways, which include: transforming growth factor beta (TGF-B), tyrosine kinase surface-receptor-asscociated pathways, transcriptional regulation, small GTPases, and cell-cell adhesions. It is widely accepted that functional loss of the adherens junction protein E-cadherin, is a primary event in EMT, which demonstrates the importance of cell junctions in this process (Hirohashi 1998; Hanahan and Weinberg 2000).

Blood vessel/epicardial substance (Bves) is a novel adhesion molecule that has been demonstrated to be an integral component of tight junctions (Osler, Chang et al. 2005). Bves expression was originally observed, and the protein was isolated from epithelial cells at the surface of the developing chick embryo heart (Reese and Bader 1999; Reese, Zavaljevski et al. 1999). During cardiac development, a subpopulation of pro-epicardial cells exhibit loss of cell-cell contact, which coincides with the loss of Bves expression at the cell surface. It has also been shown that Bves confers cellular adhesion properties to non-adhesive L-cells when transfected to over-express Bves(Wada and others 2001). These findings led authors to classify Bves as an adhesion molecule and hypothesize that Bves is involved cell-cell contact and cellular migration during organogenesis. Ripley et al verified the critical role of Bves in cell migrations and epithelial rearrangement during development in *Xenopus laevis* by injecting an antisense

mopholino to knock down Bves expression in two-celled embryos. Morphologenesis was disrupted by deregulation of epithelial movements (Ripley, Osler et al. 2006).

When various epithelial cell lines were stably transfected to over-express a full-length chicken Bves (C-Bves), we observed increased levels of TJ proteins and increase transepithelial electrical resistance (TER), a functional measurement TJ formation. However, when using an anti-sense-morpholino knock down strategy to disrupt Bves expression, TJ formation was reduced as demonstrated by reduction in TER and TJ proteins. These findings indicate that Bves is important in regulating the barrier functions of epithelial TJs (Osler, Chang et al. 2005).

During disruption of Bves expression by morpholino treatment, we also noted an increase in epithelial cell migration. When a normal epithelial monolayer is injured, wound closure occurs as a sheet of cells from the wound edge migrates to cover the injured area. This unified migration of the wound front is observed both in vivo and in vitro. However, when Bves expression is disrupted, we noted that more cells delaminated away from the healing wound margin, which led to faster wound coverage. In addition, these cells took on more fibroblast-like morphology (Ripley, Chang et al. 2004). This observation led to us to hypothesize that Bves also regulates EMT.

The function of Bves in epithelial TJs is not fully understood, but Bves appears to play an important role in the formation and maintenance of TJ in epithelial cells. However, it is becoming increasingly evident that TJ in epithelial cells have other cellular functions beyond cellular adhesion. TJs are also involved in regulating epithelial cellular differentiation. The most obvious mechanism of how TJs regulate differentiation is based on the physical property of TJs. TJs are composed of continuous adhesive strands

encircling the upper portions of cells within an epithelial sheet, which separate the cells into two distinct apical and basal portions. The protein contents within the cell lipid layer are prevented from freely diffusing between these two portions by the encircling strands of TJ and cellular polarity is maintained. However, if TJs become compromised, the apical and basal regions will not have the required separation leading to loss of cellular polarity, a hallmark of EMT.

Methods

Development of c-Bves and t-Bves HCE lines

Immortalized human corneal epithelial cells (Araki-Sasaki, Ohashi et al. 1995) were stably transfected using lipofectamine and plasmid. Plasmid with Chick Bves (c-Bves) was used in order to create a Bves over-expressing cell line where the exogenous Bves is trafficked in the same way as endogenous Bves, which is dependent on the Bves-Bves interaction of the cytoplasmic carboxyl terminus (Andree, Hillemann et al. 2000). These findings led us to hypothesize that the expression of a truncated Bves at the carboxyl terminus (t-Bves) will lead to hetero-oligomerization between endogenous Bves and t-Bves resulting in abnormal trafficking. We used a truncated sequence plasmid construct to create a dominant negative cell line with disrupted Bves.

Measurement of cell packing

Cell lines were seeded at 5,000 cell/ cm^2 on transwell inserts (Falcon), and maintained with Defined Keratinocyte Serum free Medium until confluence. Cells were

then fixed with methanol and stained with DAPI. Cells were imaged, and neighboring cell distances were measured from the center of one cell nucleus to the center of the neighboring cell nucleus. These measurements were repeated for all cells within a field of view.

Measurement of cell migration by time-lapse microscopy

In separate studies of individual cell migration rates, well plates were seeded with various cell lines at low density (< 5,000 cells/cm^2). We allowed for three days after trypsinization to allow for recovery of membrane proteins before time-lapse studies. Individual cells were imaged hourly over 24 hours using a Hamamatsu C7780 CCD (Hamamatsu Corporation, Bridgewater, NJ) camera attached to a Nikon Eclipse TE2000U inverted microscope (Nikon USA, Melville, NY). A stage incubator was used to supply CO_2 and steady heat to maintain the temperature at 37° and Image Pro Plus 5 (Media Cybernetics) controlled time-lapse image acquisition at one-hour intervals.

Analysis of cell migration

Using Image Pro Plus 5, individual cells in each field were identified using pixel intensity and object area histograms, and were selected for tracking. Using the "Track objects" dialogue, cell movement tracking from one frame to the next was automated. For each cell, center-to-center movement measurements for the whole time-lapse sequence were exported into Excel for numerical analysis. Since each image in the sequence was taken at an interval of one hour, the migration rate (microns/hour) for that time period was the distance moved. Migration rate for each individual cell was

averaged for the time-lapse sequence, and the migration rate reported for each cell line was the average and standard deviation of the individual cell migration rates.

Cell viability in soft agar

In order to assess cell survival and proliferation in a three-dimensional nutrient matrix, each cell line was grown in soft agar. Six well plates with soft agar were prepared with a bottom dense layer of agarose and a top cell growth agarose layer. Agarose of two different concentrations were prepared: 1% agarose (100mg agarose in 10ml Defined Keratinocyte Serum Free Medium without growth supplement) for the base layer and 0.5% Agarose (50mg agarose in 10ml Defined Keratinocyte Serum Free Medium (DKSFM) without growth supplement) for the top cell growth layer. Each solution of agarose was heated and well mixed before autoclaving. Agarose solutions were sterilized in a steam autoclave at 121 ˚C for 10 minutes, then at a dry setting for 30 minutes. Both agarose mixtures were then cooled to 37˚C in water bath. Epithelial growth supplement provided by Gibco in the DKSFM kit was added to each (20µl into 10ml agarose). First, 1 ml of 1% agarose was poured into the bottom of each six-well plate well. The gel was then cooled for 5 minutes in a refrigerator at 4˚C. The top cell growth layer of agarose was then prepared. Cells were added to warm 0.5% agarose at a seeding density of 5,000 cells/cm² for each 9.62 cm² well. The agarose growth layer (1 ml in each well) was added on top of the gelled 1% agarose layer. Both layers were then cooled at room temperature, until fully gelled. Each well then received 1ml of DKSFM with supplement, and the soft agar plates were incubated at 37˚C, 5% CO_2 and 95% humidity.

Cells were maintained for two full weeks, with media changes every 2-3 days. On day 14, cells were treated with 20 μg/ml fluorescein diacetate and 4 μg/ml ethidium bromide in Hank's Buffered Saline, a live/dead viability stain, to assess the amount of viable cell colonies within the soft agar. Images of low power fields (2x, 4x) were taken, and colonies were counted.

Statistical Analysis

SigmaStat for Windows version 3.0 was used for all statistical analysis. Analysis of variances (ANOVA) was applied for c-Bves and t-Bves data versus the control parental HCE line. Statistical significance was set at $p<0.05$.

Results

Subcellular localization of Bves in stably transfected cells:

Bves trafficking to the cell membrane has been demonstrated to be dependent on the Bves-Bves interaction of the cytoplasmic carboxyl terminus (Andree, Hillemann et al. 2000). These findings led us to hypothesize that the expression of a truncated Bves at the carboxyl terminus (t-Bves) will lead to hetero-oligomerization between endogenous Bves and t-Bves resulting in abnormal trafficking of Bves to the cell surface. Immunohistochemical staining in cells stably expressing transfected Bves with Flag epitope (Figure 16) appears to support this hypothesis. Bves antibody, B846, recognizes both the endogenouse and stably expressed c-Bves (wild type chick Bves with Flag epitope). Immunofluorescence straining of c-Bves cells with B846 revealed prominent localization at the cell border at sites of cell-cell contact and none at a free cell edge

(Figure 16 G). When the Flag image (H) is merged with B846 image (Figure 16 I), there is corresponding overlap, which indicates that the stably transfected c-Bves is trafficked in the HCE cells in a similar manner as endogenous Bves, and the Flag epitope does not interfere with endogenous Bves trafficking.

Bves antibody, B846, recognizes an intercellular epitope not present in truncated t-Bves, and therefore will only detect endogenous Bves in the t-Bves cells. Endogenous Bves localization is mainly in a cytoplasmic pattern and rarely at the cell borders (Figure 16D). Staining with Flag antibody also revealed mainly cytoplasmic localization of t-Bves (Figure 16E). When merged, there is incomplete overlap between endogenous and t-Bves, and no Flag localization at cell borders (Figure 16F). We also observe rare scattered regions where endogenous Bves is seen in linear pattern indicating the localization at the cell membrane borders. These regions do not correspond to Flag localization. These observations indicate that endogenous Bves is interacting with the transfected truncated form, and this interaction results in disrupted trafficking to the cell membrane.

Altered monolayer formation in stably transfected t-Bves cells

We previously demonstrated that both parental and c-Bves HCE cells form an organized monolayer, and Bves over-expression led to increased TJ formation as reflected in the doubling of TER in the C-Bves cells (Osler, Chang et al. 2005). Our present study confirmed these findings. Parent and C-Bves cell readily establish cell-cell contact and form islands of epithelial cells. The C-Bves islands are typically larger and coalesce with each other forming a complete monolayer quicker than parental cells. Both

parental and C-Bves cells form complete well-organized monolayers with uniform cell size and shape. However, C-Bves cell layers appear to be more tightly packed, and individual cells appear to be even more regular. There is also a doubling of TER in the C-Bves monolayers. In contrast to the parental and C-Bves cells, t-Bves cells with disrupted endogenous Bves trafficking do not appear to have the ability to form a confluent epithelial cell layer. Instead, the t-Bves cells proliferated in disorganized clusters (Figure 16D, E & F). T-Bves appear to be unable to form cell-cell contacts as demonstrated by the lack of TER above baseline measurements.

In addition to these results in a human corneal epithelial cell line, c-Bves also appears to alter the morphology of a cancer line, Lim 2405. Figure 17 shows a phase contrast micrograph of the parental cancer line and the C-Bves transfected line, both at a moderate cell density. The parental cancer line exhibits a mesenchymal phenotype, and is unable to form well-organized layers. In contrast, the stably transfected C-Bves Lim 2405 line appears to be more epithelial, and form a monolayer.

Altered Cell Morphology

Cells were stained for ZO1 on polycarbonate inserts after TER measurement. Both parental and C-Bves monolayers have complete cell-cell contact revealed by ZO1 localization in a wire mesh pattern (Figure 18). Immuno-fluorescence staining of the t-Bves samples after TER assay reveals a lack of ZO1 at the cell membrane. Furthermore, there is no cell membrane localization of the other adhesion junction protein such claudins, e-cadhereins, or B-catenins at the cell membrane (results not shown). The results indicate that Bves is required for initiation of epithelial cell-cell contact formation

and modulation of the barrier function in an epithelial monolayer. In addition to the increased TER, c-Bves cells exhibited increased cell density within its monolayer after cell layer confluence.

We verified that cell number is increased in c-Bves HCE by measuring the internuclear distances, which is significantly shorter in c-Bves monolayer than in the parental line (Figure 18B). However, we only noted this increase in cell density after 1 week of growth after reaching full confluence. We found that this was the waiting period required in order for the monolayer TJ to fully develop. It appears that both the parental and c-Bves have similar cell density with reaching full confluence, but the C-Bves cell density further increases after reaching full confluence. We quantified this difference by measuring 100 nuclei-nuclei spacings for each cell line grown on three different transwell membranes. HCE cells expressing c-Bves had an average cell spacing of 10.5 microns with a standard deviation of 1.8 microns. The parental HCE line had an average cell-cell spacing of 12.2 with a standard deviation of 2.2microns. This measurement shows that cells over-expressing Bves are more densely packed at confluence ($p < 0.05$). These results are summarized in Figure 18.

Altered Cytoskeleton

Due to our variation on the changes in the cell shape, we hypothesized that the cytoskeletal structure in the stably transfected cells were altered. Subconfluent cultures were analyzed for both microfilament organization and intermediate filaments. Phalloidin staining of cells revealed the stress fibers in both C-Bves and parental cells (Figure 19)**.** In contrast, t-Bves cells do not exhibit stress fibers.

For analysis on intermediated filaments, immunofluorescence staining for cytokeratin and vimentin were carried out (Figure 20). C-Bves and parental cells exhibit fluorescence for cytokeratin (Figure 20A and B) while vimentin fluorescence was minimal (Figure 20D and E). Conversely, t-Bves cells stained positively for vimentin (Figure 20F) but not for cytokeratin (Figure 20C). These findings indicate that cytoskeletal organization (microfilaments and intermediate filaments) differ and the t-Bves cells expresses a mesenchymal marker, vimentin.

Altered cell growth in soft agar assay

The loss of Bves localization at the cell membrane appears to induce HCE cells to expression vimentin, a mesenchymal phenotype marker, while the parental and C-Bves both express cytokeratin, which is an indicator of epithelial phenotype. To further investigate changes of HCE phenotype with alteration in Bves, soft agar assays were carried which determines the ability of cell to proliferate (colony formation) within a 3-dimensional matrix. Typically, cells with mesenchymal phenotype are more capable of colony formation within a 3-dimensional growth matrix. The t-Bves cells exhibit the greatest number of colonies after 2 weeks (Figure 21C). The C-Bves cells have the lowest number of colonies (Figure 21A), and the parental HCE cells were intermediate in the number of colonies (Figure 21B). These results indicate that loss of Bves leads to transformation of epithelial cells to mesencymal cells.

The qualitative assessment of the soft agar images was verified using Image Pro Plus to count the cell colonies formed in 6 different wells for each cell line. We found that the t-Bves line had an average colony density of 99.3 ±17.8 colonies/cm^2, whereas

the parental line had a density of 72.5 ±12 colonies/cm^2, and the c-Bves line was 20.2±8.9 colonies/cm^2 (Figure 21). Statistical analysis of these results verify that t-Bves had improved proliferation in soft agar over the parental line, and in comparison, c-Bves had a decreased ability to survive ($p<0.05$).

Altered cellular motility

The results above strongly indicate that Bves regulates the transition between epithelial and mesenchymal phenotype. Another phenotypic difference between epithelial and mesenchymal cells is cellular motility. We have previously reported an increase in cellular migration in HCE cells treated with morpholinos to knock-down Bves expression using cell culture wounding assay (Ripley, Chang et al. 2004). The wounding assay measures migration of cells in the contexts of an organized monolayer. Since, t-Bves cells do not form a monolayer, we measured the distances traveled during the random movements of individual cells. Time-lapse light phase microscopy was carried out on groups of individual cells, and their movement was analyzed.

Analysis of the time-lapse footage showed that t-Bves cells were more motile than either the parental or c-Bves cell lines. Representative images in Figure 22 show that t-Bves cells exhibit a spread morphology, with spindle-like filopodia used for movement, in contrast to parental and c-Bves cells which appear to be more rounded and lack projections. Average individual cell migration for t-Bves was 2.8 ±0.7 microns/hr, parental HCE 1.5 ±0.6 microns/hr, and c-Bves 0.4 ± 0.2 microns/hr that is summarized in the bottom graph in Figure 23. Statistical analysis showed that the cell migration rate of

t-Bves was significantly greater than the parental line, and c-Bves migration rate was significantly lower than parental HCE ($p<0.05$).

Discussion

In this report we have demonstrated that over-expression of truncated Bves, leads to a functional loss of Bves by disrupting endogenous Bves trafficking to the cell membrane. The resulting cell phenotype exhibits the characteristics of a cell that has undergone epithelial-mesenchymal transition. Dominant negative cells expressing t-Bves are not able to form a confluent monolayer due to a lack cell-cell contacts. When grown to high density, these cells become disorganized, and do not like to come in contact with other cells. When cells do come in contact, they pile up briefly, and then slough off. In addition, they have undertaken fibroblast morphology exhibiting spindle-like projections much like filopodia. These cells exhibit increased motility and have become invasive, acquiring the ability to proliferate within a 3-dimensional nutrient matrix (soft agar). Mesenchymal phenotypic change is also confirmed by the expression of the mesenchymal cell-specific intermediate filament network component vimentin, instead of the normal keratins expressed by corneal epithelial cells.

In contrast, c-Bves stably transfected HCE have enhanced epithelial characteristics over the parental epithelial cell line. Immuno-fluorescence shows that c-Bves is properly trafficked to the cell membrane, which exhibits a wire-mesh pattern in cell monolayers at cell junctions. This confers greater epithelial sheet integrity by both increased monolayer resistance and greater, more organized cell packing. These cells exhibit epithelial morphology, and epithelial cell markers such as keratins. In addition

cell motility is decreased and cell proliferation in an agar 3-d growth matrix is diminished. We have shown that this phenomenon is not an artifact of this corneal epithelial cell line, as preliminary results in a cancer line, Lim2405, also exhibit an increase in epithelial phenotypic characteristics. The parental Lim 2405 line is unable to form a well-organized monolayer, whereas the c-Bves over-expressing Lim 2405 line forms very regular, confluent sheets.

The mechanisms for downstream molecular interaction of Bves are not fully understood, but these results appear to be in part due to Bves' role in modulating TJ formation. Our findings suggest that the loss of proper trafficking of Bves to the cell membrane induces cell changes similar to those used to characterize EMT including an increase in cell motility, whereas over-expression of Bves enhances epithelial characteristics and decreases cell motility.

Ackowledgments

We thank Sai-han Presley for her work as this project's primary cell technician and Elizabeth Dworska for her role as a supporting cell technician. This work was sponsored in part by NIH grants: EY 13593, EY 13451, HL 07751, and by a Vanderbilt University discovery grant.

References

Andree, B., T. Hillemann, et al. (2000). "Isolation and characterization of the novel popeye gene family expressed in skeletal muscle and heart." Dev Biol 223(2): 371-82.

Araki-Sasaki, K., Y. Ohashi, et al. (1995). "An SV40-immortalized human corneal epithelial cell line and its characterization." Invest Ophthalmol Vis Sci 36(3): 614-21.

Bates, R. C. and A. M. Mercurio (2005). "The epithelial-mesenchymal transition (EMT) and colorectal cancer progression." Cancer Biol Ther 4(4): 365-70.

Greenburg, G. and E. D. Hay (1982). "Epithelia suspended in collagen gels can lose polarity and express characteristics of migrating mesenchymal cells." J Cell Biol 95(1): 333-9.

Greenburg, G. and E. D. Hay (1986). "Cytodifferentiation and tissue phenotype change during transformation of embryonic lens epithelium to mesenchyme-like cells in vitro." Dev Biol 115(2): 363-79.

Hanahan, D. and R. A. Weinberg (2000). "The hallmarks of cancer." Cell 100(1): 57-70.

Hirohashi, S. (1998). "Inactivation of the E-cadherin-mediated cell adhesion system in human cancers." Am J Pathol 153(2): 333-9.

Osler, M. E., M. S. Chang, et al. (2005). "Bves modulates epithelial integrity through an interaction at the tight junction." J Cell Sci 118(Pt 20): 4667-78.

Reese, D. E. and D. M. Bader (1999). "Cloning and expression of hbves, a novel and highly conserved mRNA expressed in the developing and adult heart and skeletal muscle in the human." Mamm Genome 10(9): 913-5.

Reese, D. E., M. Zavaljevski, et al. (1999). "bves: A novel gene expressed during coronary blood vessel development." Dev Biol 209(1): 159-71.

Ripley, A. N., M. S. Chang, et al. (2004). "Bves is expressed in the epithelial components of the retina, lens, and cornea." Invest Ophthalmol Vis Sci 45(8): 2475-83.

Ripley, A. N., M. E. Osler, et al. (2006). "Xbves is a regulator of epithelial movement during early Xenopus laevis development." Proc Natl Acad Sci U S A 103(3): 614-9.

Stoker, M. (1989). "Effect of scatter factor on motility of epithelial cells and fibroblasts." J Cell Physiol 139(3): 565-9.

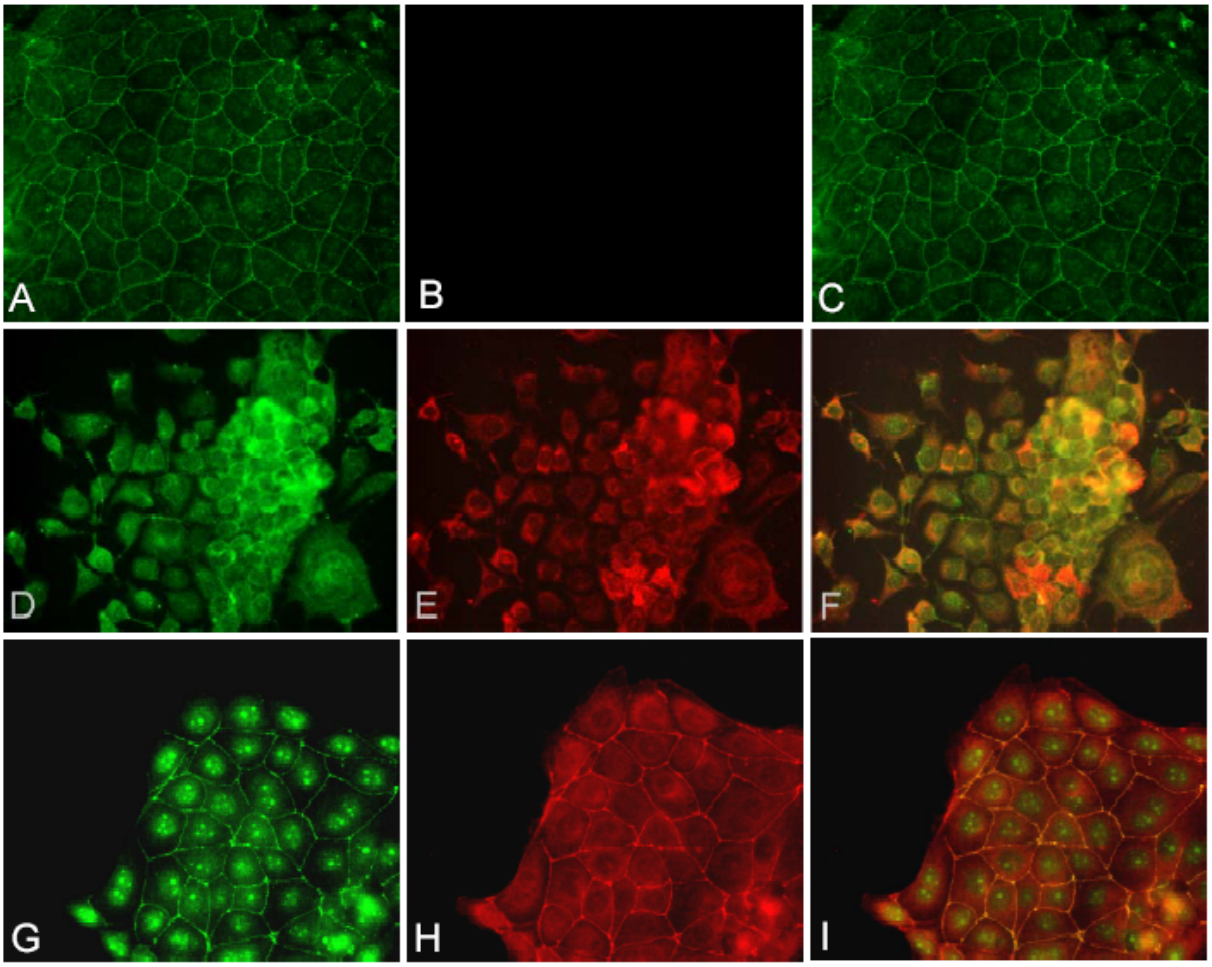

Figure 16 Immuno-fluorescence staining for Bves (green) and Flag (red) in parental HCE (A,B,C), t-Bves (D, E, F) and c-Bves (G,H,I). Parental cells exhibit endogenous Bves staining at cell junctions (A). However, cells expressing t-Bves exhibit disrupted localization of endogenous Bves (D) and have a decreased ability to establish and formation of a monolayer (F). In C-Bves cells Bves is properly trafficked to the cell membrane (I). The free edge of a C-Bves epithelial sheet was shown to emphasize that Bves is expressed at cell junctions and is not localized at the free edges of cells.

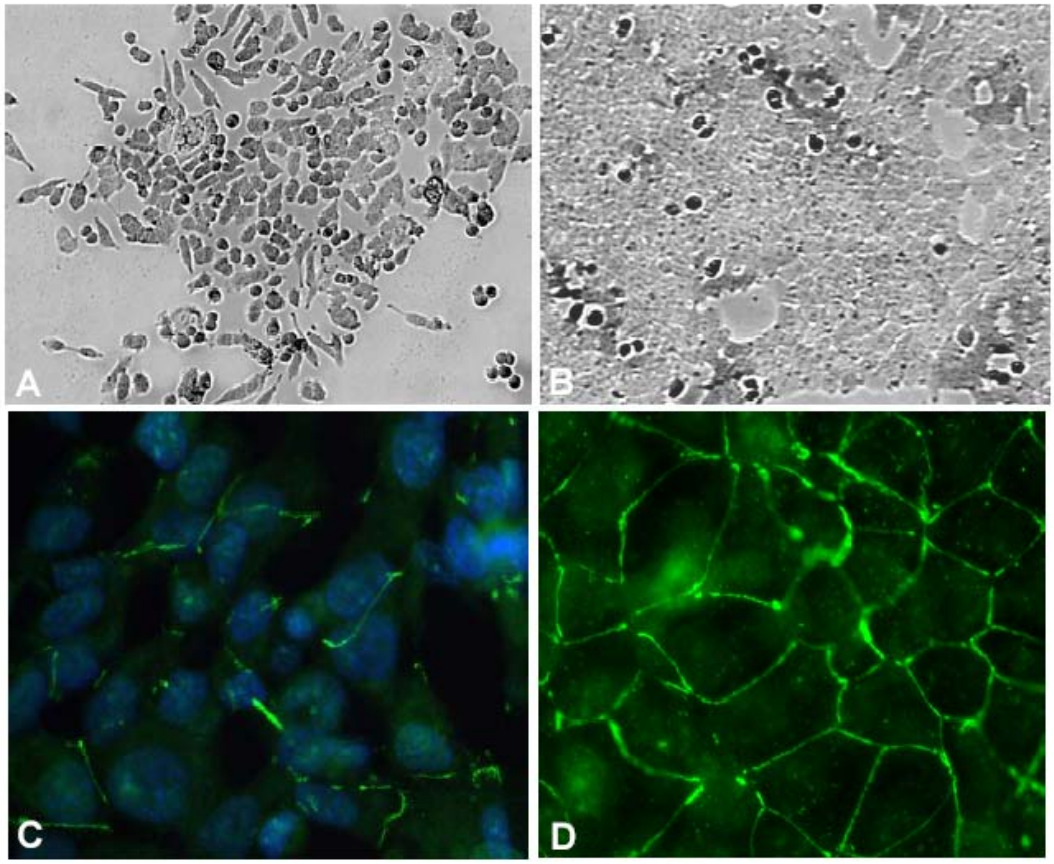

Figure 17. Phase contrast images of Lim 2405 cancer cells (A) and c-Bves Lim 2405 cells. C-Bves Lim 2405 cells form a contiguous monolayer with a regular epithelial phenotype, where as the parental cancer line exhibits a mesenchymal fibroblast-like phenotype, which does not form monolayers. In C and D, Bves is stained in green. This staining shows that there is a low baseline level of Bves expression in the cancer line (C). The over-expressing line expresses Bves that localizes to the cell membrane (D).

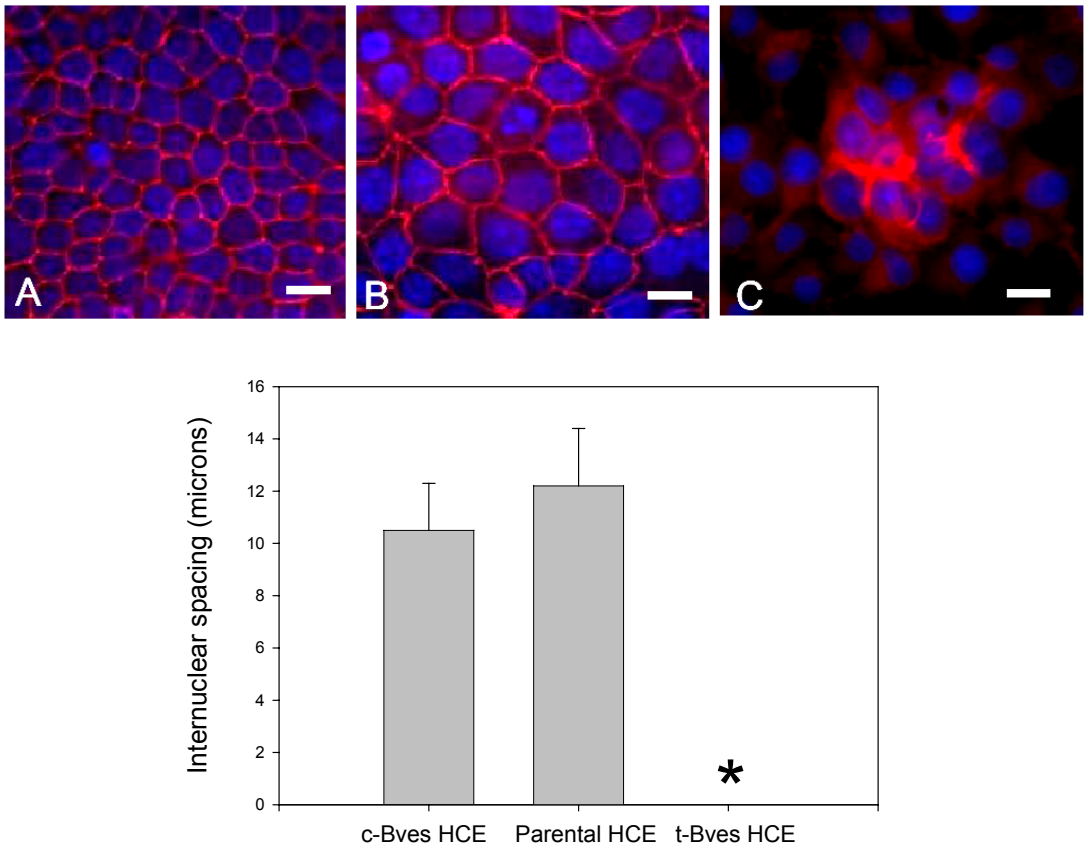

Figure 18. Immuno-fluorescence staining of ZO-1 in c-Bves cells (A), parental HCE (B) and t-Bves cells (C). Cells over expressing Bves (A) exhibit increased cell density. Truncated Bves cellsScale bar is 10 microns.. c-Bves HCEs exhibit significantly closer cell packing at confluence than parental HCEs, with > 20% decrease in the measured internuclear distances. ($p<0.05$). Mean + standard deviation (N=3). * No internuclear spacing results were tabulated for this line because the cells clump together.

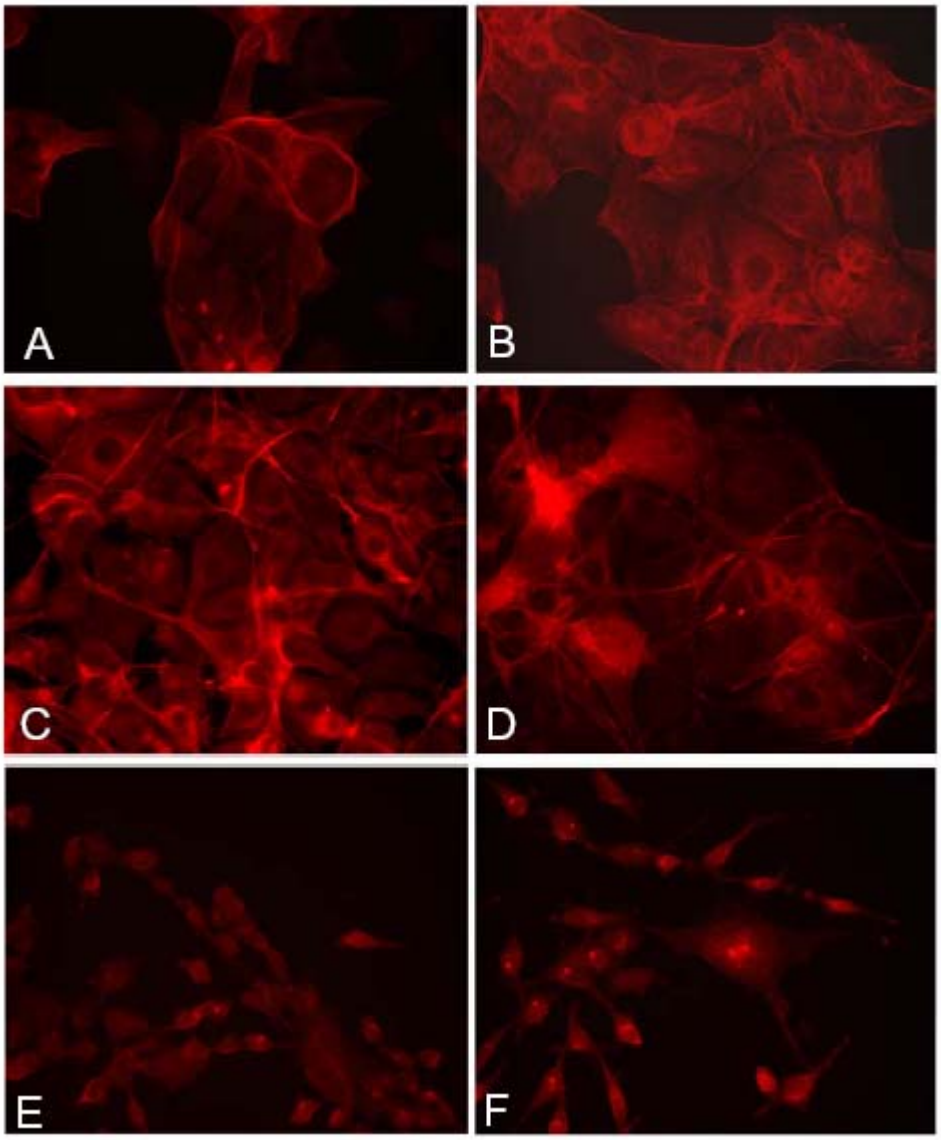

Figure 19 Immuno-fluorescence staining for actin using TRITC pahlloidin (red). Parental (A,B), and c-Bves cells (C,D)show the presence of of actin stress fibers, whereas t-Bves (E, F) cells lack stress fibers, and exhibit little cytoskeletal organization.

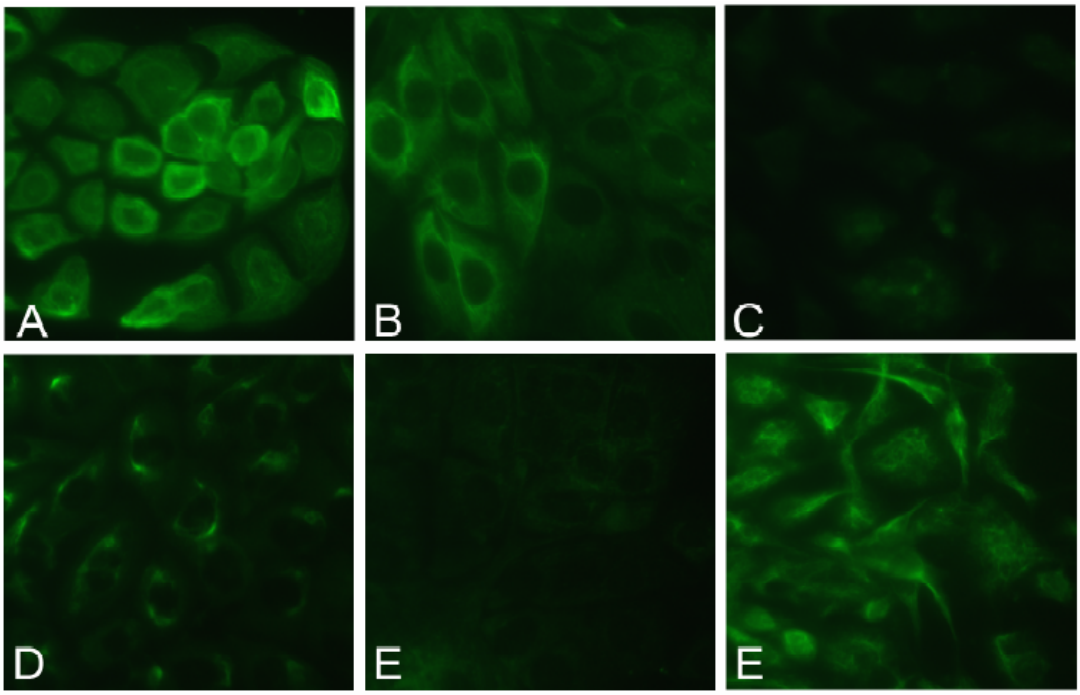

Figure 20. Immuno-fluorescence staining of c-Bves (A,D), HCE (B,E), and t-Bves (C,E) cells for cytokeratin (A,B,C) and vimentin (D,E,F). Cytokeratin is detected in c-Bves (A) and parental (HCE) cells (B), but not vimentin (D,E). Conversely, vimentin is detected in t-Bves cells (E), but not cytokeratin (C). These results indicate that t-Bves cells have untaken a mesenchymal phenotype.

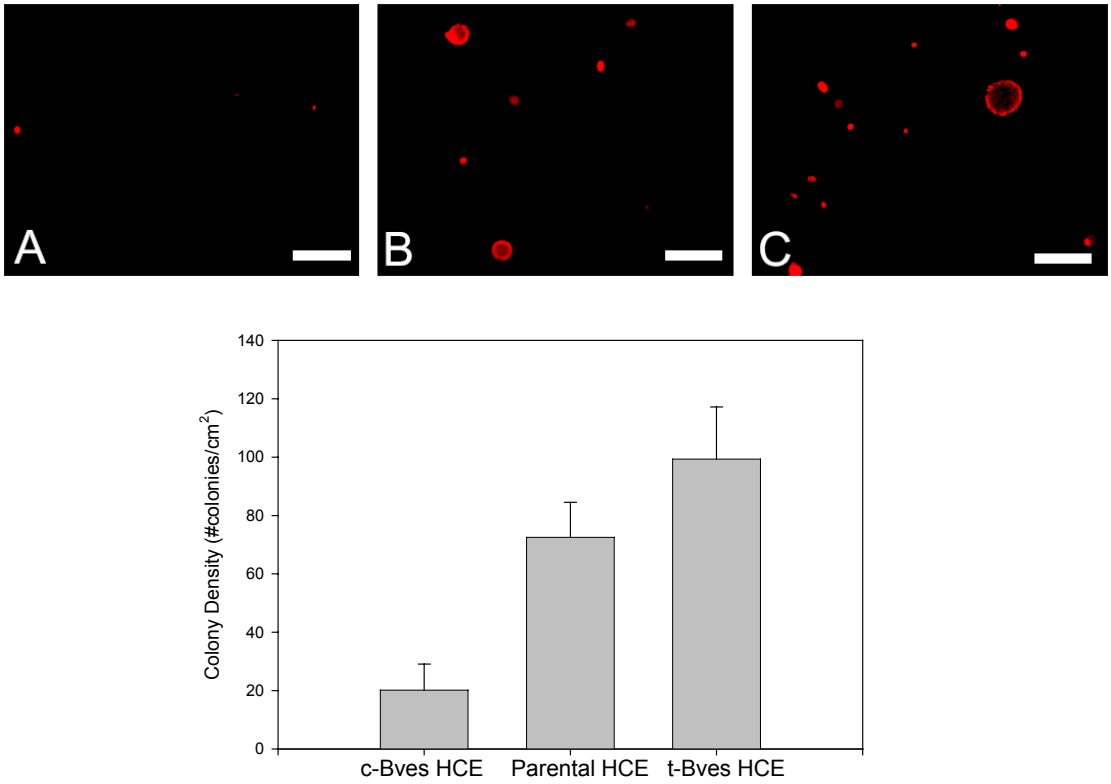

Figure 21. Low power fluorescence microscopy imaging colony formation by c-Bves (A), parental HCE (B), and t-Bves (C) cells after 2 weeks in soft agar (0.5%). Soft agar cultures were stained using a vital dye (cell-tracker red). Cells with disrupted Bves trafficking (C) have greatest capacity to proliferate within the soft agar, while cells over-expressing Bves (A) proliferated least. Scale bar is 500 microns. Density of cell colonies growing in soft agar (0.5%) after 2 weeks (N=6). There was a statistically significant increase in t-Bves HCE colony proliferation over parental HCE, and a statistically significant decrease in c-Bves cells ($p<0.05$).

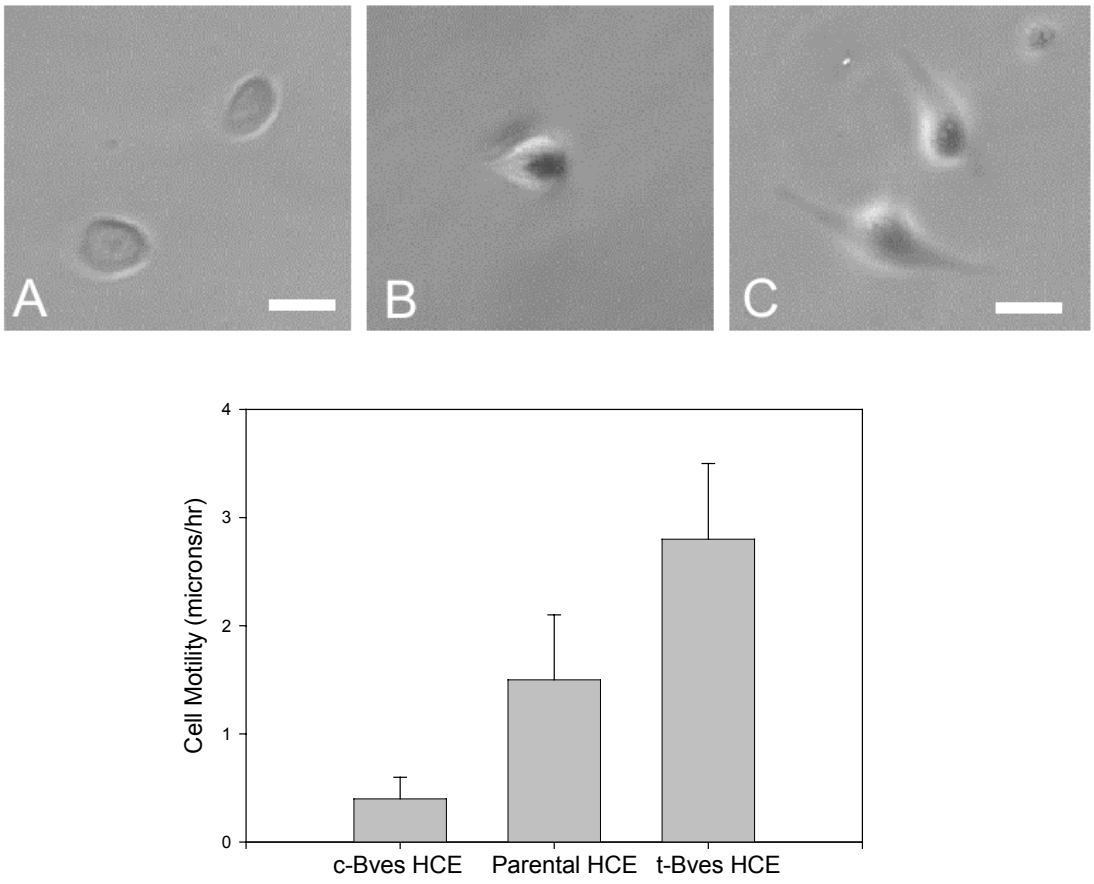

Figure 22. Time-lapse light microscopy for 20 hr on heated stage was preformed 3 days after seeding on plastic culture dishes. At low cell density, c-Bves cells (A) and parental HCE (B) appear are rounded, and ,t-Bves cells (C) appear small and fibroblast like with spindly processes. Scale bar is 20 microns. Cell motility rates of HCE cell lines. The t-Bves cell displayed the greatest motility and the c-Bves cells least. For each cell (n=10 for each cell line), the speed of locomotion was calculated by the average change in position of center of the cell in each video frame over 20 hrs. Mean ± standard deviation.

CHAPTER VI

DISCUSSION AND FUTURE WORK

The goal of any wound healing technology is to treat injured tissue so that it becomes contiguous, stable, and that it regains full function as soon as possible. In essence, at the end of wound healing the tissue should be returned to the state it was in before it was injured. In corneal wound healing, there are increased challenges such as scarring and loss of clarity. Past approaches to restoring the ocular surface involved multiple surgery procedures. In an effort to develop an easy to administer, non-surgical method to promote wound healing, we have developed a cell carrier approach to delivering corneal stem cells to severely damaged corneas.

We have evaluated a cell culture model of corneal wound healing that showed an acceleration of wound closure times when exogenous cells were applied to the interior of wounds. We found that a relatively small amount of cells, 5,000-10,000 cells per square centimeter, seeded within wounds significantly decrease time of total wound closure.

In working with various materials as cell carriers, Polydimethylsiloxane (PDMS) proved to have the most desirable traits for use as cell delivering contact lenses. PDMS was amenable to surface modification by passive protein adsorption or alternatively by plasma treatment activation and covalent coupling of molecules to its surface. In transfer experiments, autoclaved and surface coated PDMS allowed for both celll attachment and cell migration to both ECM and wounded corneas. We found that fibronectin was the most promising surface coating for both cell transfer and for protecting healthy epithelial cells from removal. We also found that post micropatterns increased transfer efficiency

to ECM such as matrigel. However, in our organ culture model system, micropatterns were found to have a less pronounced effect. PDMS contact lenses without surface features were able to transfer primary corneal epithelial cells to damaged corneal regions as shown in confocal images. However, after culture in a perfusion chamber, fewer cells remained attached to the cornea. This is indicative of poor attachment to corneal ECM, a major stumbling block to a re-epithelialization application.

There are a number of future studies that may be conducted to further investigate the effect of individual corneal stem cell delivery to corneal wounds. In the original design of this study, we planned to take optimized cell transfer contact lenses and apply autologous primary cells to corneal wounds in vivo. This would have allowed for us to evaluate how cells might transfer from a contact lens that has some degree of movement on the surface of the cornea. We hypothesize that even with lens movement, at least some exogenously applied cells would make it to the wounded cornea, and according to preliminary data, even a small amount of well adhered cells on the interior of wounds can accelerate healing. However due to time, and funding constraints, in vivo work was outside the scope of this dissertation.

Future studies assessing transferred cell adhesion to wound ECM are needed in order to improve contact lens design for cell retention. After cells can be transferred, retained and grown to confluent sheets in place on the cornea, then functional testing must be completed. In order to assess the function of a cornea healed by individual cell transfer, barrier properties should be confirmed by diffusion studies and corneal clarity should be assessed by light transmission. Histology and immuno-fluorescence staining should be used to confirm corneal epithelial layer stratification, and proper cell layer

phenotype through keratin type specific stains, and proper expression of cell junction proteins.

CHAPTER VII

PROTECTION OF RESEARCH SUBJECTS AND SOCIETAL IMPLICATIONS

Protection of Research Subjects

No living animals were used in these studies. As an alternative, an appropriate culture model was established. Prior to euthanasia, animals were treated in accordance with the ARVO Resolution on the Use of Animals in Research and Vanderbilt institutional guidelines. Animals were housed in the Central Animal Facility in Medical Center North. After euthanasia, and confirmed death by the attending veterinarian, ocular globes were harvested for corneal isolation.

Societal Implications

Corneal wound healing disorders are collectively a significant cause of blindness in the United States, and have an even greater impact worldwide. Current methods for treating delayed or slow corneal healing fail to actively re-epithelialize the cornea, and therefore risk complications such as corneal perforation. There is a growing population of patients who will be susceptible to deficient corneal healing that would benefit from new devices and methods to accelerate corneal wound healing.

APPENDIX A

ROLE OF THE STUDENT IN THE MANUSCRIPT

The first two manuscripts, and the fourth, is work conceived, experimentally undertaken and written primarily by Christopher Pino. Min Chang conceived the third manuscript, and Christopher Pino primarily conducted experiments. For all work, Elizabeth Dworska was involved in the upkeep of cell lines used. Frederick Haselton provided experimental and technical advice, and served as the final editor for all manuscripts. Dr Franz Baudenbacher provided lithography and microfabrication advice for the fourth manuscript. Dr Prasad Shastri provided some materials and surface coating trouble- shooting. Dr Tran provided clinical information and critical feedback for literature review of corneal wound healing.

APPENDIX B

PDMS AS A CELL GROWTH SURFACE

Cell attachment to untreated PDMS surfaces has been contested in the literature, however, several investigators have reported successful cell culture (Mata, Boehm et al. 2002). PDMS is made up of a chain of silicon that has two methyl groups. These methyl groups make the surface of PDMS highly hydrophobic, which means that it strongly repels water. A measure of hydrophobicity, surface contact angle (SCA), can be measured by placing a bead of deionized water on PDMS. Materials that are hydrophilic have low SCA and those that are hydrophobic have SCA of >70°. Many researchers have measured PDMS to have a SCA of 108°. Despite many advantages of PDMS' material properties, its hydrophobic nature translates into poor wettability, which is a significant problem for cell attachment. Previous studies suggest that cell adhesion is maximized on surfaces with moderate SCA from 60° to 80° (Lee, Park et al. 2003), which is an intermediate hydrophobic/hydrophilic property.

In order to make PDMS more amenable to cell attachment, the surface can be modified either by hydrophilization of PDMS or by surface coating with adhesive proteins. Several investigators have reported treating with oxygen-based plasma to reduce hydrophobicity of PDMS. The chemical structure of PDMS is a chain of silicon interconnected by oxygen with two methyl groups attached to silicon. Experimental evidence indicates that PDMS is made more hydrophilic when oxidized in plasma because oxygen in the form of hydrophilic silanol groups (Si-OH) replace hydrophobic

methyl groups ($Si\text{-}CH_3$) at the surface (Morra, Occhiello et al. 1990). However, PDMS surfaces treated by oxygen plasma do not remain hydrophilic permanently. Mobile, low-molecular weight monomers are able to migrate from the bulk of the PDMS to the air-surface interface causing hydrophobic recovery a few hours following plasma treatment. To retain the hydrophilic nature of plasma treated PDMS, several investigators have found that storage in water reduces the rate of hydrophobic recovery (Ng, Gitlin et al. 2002; Lee, Park et al. 2003)

In order to better characterize the Sylgard 184 (Dow Corning) and Silastic elastomer (Dow Corning) that were surface modified for use in transfer experiments, goniometry was used to evaluate each formulation of PDMS. Goniometry is a standard method to measure surface contact angle, which is an indicator of a surface's hydrophobiticy. Drops of deionized water was placed on untreated Sylgard 184, plasma treated Sylgard 184 within an hour of treatment and plasma treated Sylgard 184 that was allowed to recover, and then sterilized by autoclave treatment for 30 minutes (Figure 23).

Silastic MDX4-4210 Medical Grade Elastomer, also made by Dow Corning, is a two-part kit with a dimethyl siloxane monomer base and a curing agent. This formulation is dimethylvinyl-terminated. We tested medical grade Silastic because it has already been used in biomedical applications, and has known host inertness. This makes it a good candidate for cell transfer contact lenses made for future use. We treated it in the same way as Sylgard 184 previously, and found that Silastic is slightly more hydrophobic. Plasma treatment was found to decrease surface hydrophobicity shown by lower SCA (Figure 24). In Figure 25, we summarized SCA data for all PDMS types.

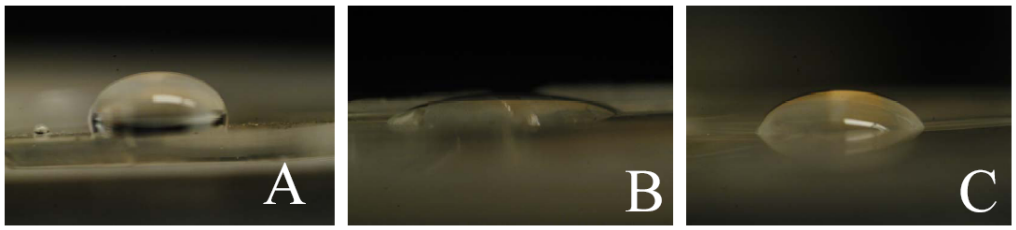

Figure 23. Drops of de-ionoized water on untreated (A), air plasma treated (B), and plasma recovered then autoclaved (C), Sylgard 184.

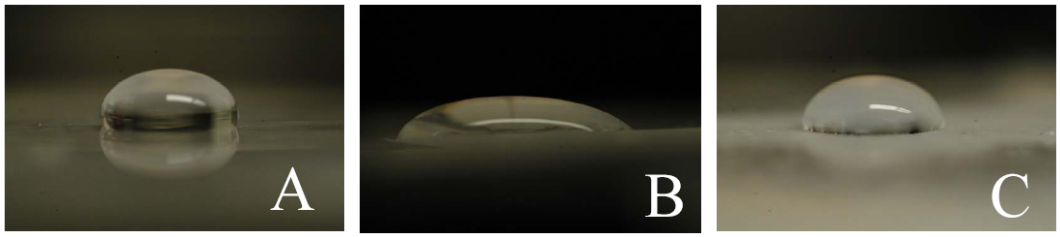

Figure 24. Drops of de-ionoized water on untreated (A), air plasma treated (B), and plasma recovered then autoclaved (C), Silastic.

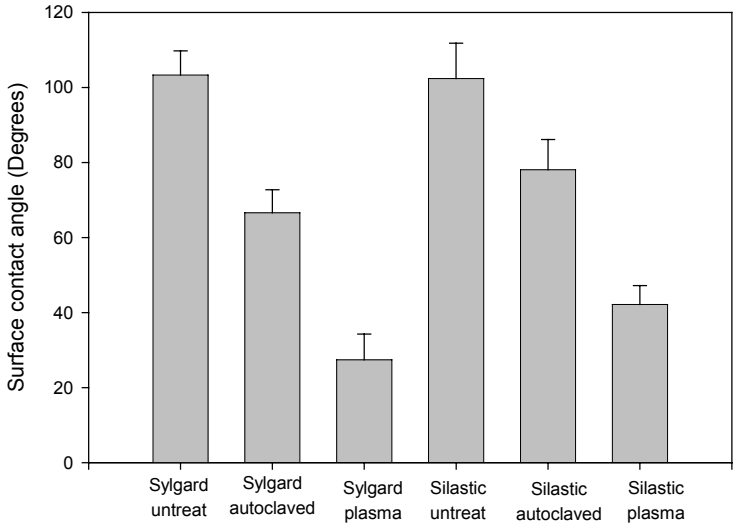

Figure 25. Surface contact angle measurements of Sylgard and Silastic PDMS formulations.

APPENDIX C

METHOD TO PRODUCE PRECISE AND REPRODUCIBLE EPITHELIAL WOUNDS FOR IN VITRO STUDIES OF CORNEAL WOUND HEALING

Christopher J. Pino[1]

Jesse H. Shaver[2]

Min S. Chang[3]

Frederick R. Haselton[1,3]

[1]Biomedical Engineering

[2]Molecular Physiology and Biophysics

and

[3]Ophthalmology and Visual Sciences

Vanderbilt University

Nashville, Tennessee

Address for Correspondence:
Rick Haselton
Box 1510 Station B
Vanderbilt University
Nashville TN, 37235, USA
(615) 322-6622 office
(615) 343-7919 fax
rick.haselton@vanderbilt.edu

Abstract

In this report, we describe a precision drill apparatus for making circular wounds in cultured epithelial monolayers and cultured corneas. Cultures of corneal epithelial cells were grown on standard tissue culture polystyrene coated with collagen, and maintained until confluence. Using a micromanipulator as a drill press, spinning teflon chisel-like drill bits were then lowered through epithelial cell layers to create wounds. Wounds were imaged, and cultured until completely closed. Maximum epithelial front migration speed and average wound closure rate were quantified by analysis of images obtained by time-lapse microscopy. To test wounding reproducibility in three separate experimental trials, different sets of cultures were wounded with the same drill bit. In these trials, wounds were an average of 8.66 mm^2 ± 0.36 (N = 16), 8.86 mm^2 ± 0.18 (N = 16), and 8.85 mm^2 ± 0.05 (N = 16). These wounds took an average of 7 days to completely close with an average of 1.19 mm^2 of closure per day. Though fairly constant, wound closure rate was greatest within the first 24 hours, and lowest just before complete closure. In wounding cultured corneas, both wound depth and wound area were controlled. Superficial epithelial wounds, ~6 mm in diameter, healed completely in five days. Partial thickness stromal wounds were created by micromanipulator positioning to a depth of 0.250 mm. The resulting average depth of stroma removed was 0.27 mm ± 0.05 (N=6), as determined by histology. These corneas also exhibited full coverage of the wounds by superficial epithelium in five days. Direct comparison of the same size wounds in monolayers and organ-culture cornea systems show that corneas heal 2-3 times faster. This epithelial drill is a promising new approach to make precise and reproducible wounds in both cultured monolayers and corneas.

Introduction

Corneal injuries are common, as ocular trauma accounts for over one million patient visits each year in the U.S. (Nash and Margo 1998) or 3.15 in 1,000 of the general population (McGwin and Owsley 2005). Many corneal abrasions are quick to heal, however wounds greater than 2 mm in diameter may persist, and can lead to ulcerations and corneal perforation (Reim, Kottek et al. 1997). Both in vitro and in vivo approaches have been used to study corneal wounds greater than 2 mm including cell culture monolayers, organotypic cultures, organ cultures or in vivo wound healing assays. The most common method for creating wounds for assays is by scratching (Gottrup, Agren et al. 2000). Strip wounds are created by scraping a strip in a cell culture monolayer, cell layers on an organotypic raft, or corneal tissue with either a pipette tip (Cha, O'Brien et al. 1996) or razor blade (Burk 1973). However, because the wounding tips or blades are at most hundreds of microns, the resulting strip wounds are narrow and close quickly, and therefore are not well suited to study large area abrasions. In organ culture and in vivo corneas the epithelium is commonly cut with a circular trephine, and then the epithelium is removed. This creates a large diameter wound in the cornea, which is a helpful model to study large abrasions. However, this method has no cell culture equivalent.

Other methods to remove the epithelium of corneal tissue include irradiation (laser ablation), thermal (cryoprobe) and chemical techniques (application of caustic agent), which have been used in both in vitro and in vivo models. However, these methods make poor models of abrasion wounds since they may alter the underlying extracellular matrix (ECM) of corneal stroma and basement membranes, which may further complicate the study. In addition, ablation and chemical treatment models may

cause damage to epithelial cells outside of the intended wound area, and therefore the total affected region cannot be easily determined. Because of the problems associated with the creation and measurement of wounds by these methods, the end result can be poor reproducibility.

In a recent report, a spinning drill was used to create wounds in corneal epithelium in vitro, and examined using time-lapse imaging (Hardarson, Hanson et al. 2004). However, this method was used only on organ culture corneas and the method was not described in detail, nor were the wounds well characterized. In this report we describe and characterize a simple method to create precise and reproducible wounds in cell culture monolayers and on organ culture corneal surfaces.

Materials and Methods

Epithelial drill apparatus

The drill was assembled using a rotational motor, interchangeable drill bits and a micromanipulator. We used a Mabuchi FF-130SH (Mabuchi Motor America Corp., Troy, MI) rotational shaft motor, powered by a 9V battery. This small and inexpensive DC motor may be operated from 0-9V DC, with either a battery power supply or a suitable AC adaptor. Our drill assembly featured a 40 ohm in-line resistor to decrease voltage across motor terminals from 9V to 3V @ ~40mA. At this power the drill rotates at ~5,000 RPM, as measured by a rotary encoder and an oscilloscope. Interchangeable blade drill bits shaped like chisel points were custom cut and smoothed by standard machining techniques. The bits were slip fit onto the motor shaft, and the motor was

mounted on a Drummond micromanipulator (Marzhauser MM33, Catalogue #3-000-024) for fine control over the x, y and z positioning.

Machining of interchangeable drill bits

Teflon cylindrical stock was used to create bits. Teflon ® was selected for its inertness and low coefficient of friction. The bits were machined on a lathe. First, the stock was turned down to approximately 4mm diameter for a length of 10mm. Then the end of the stock was faced and center-drilled using a drill bit that was just slightly smaller than the DC motor shaft (for this motor, < 2mm). The slight undersize allowed for a compression fit on the DC motor shaft. The depth of the center drill hole is not critical, but should be at least long enough to assure stable and repeatable mounting and centering on the DC motor shaft after repeated removals for cleaning. A hole depth of 4mm worked well. The 10mm long bit blank was mounted on the DC motor, which was used as a micro-lathe. The DC motor was secured in a small tooling vice and placed under a microscope to monitor the machining. The cylindrical profile of the micro-bit tip was thinned using light cutting passes until the desired epithelial diameter was reached. In order to create a chisel point, the bit was fixed in place so that rotation on the shaft would not occur. The edges of the tip were cut away under the microscope using a surgical scalpel to form a sharp chisel-point (Figure 27). In addition, to prevent wear of the bit and scratching of the plastic culture dishes, the tip was coated with a thin layer of polydimethylsiloxane (Sylgard 184, Dow Corning). The PDMS was mixed in a 10:1 ratio of monomer to curing agent, chilled to increase its viscosity, brushed onto the Teflon bits, and cured quickly in oven at 60-100°C.

Wounding cell culture monolayers

An immortalized human cornea epithelial cell line (HCE-SV40 cells) developed by Araki-Sasaki (Araki-Sasaki, Ohashi et al. 1995), was seeded at 100 cells/cm^2 on 21 cm^2 tissue culture dishes coated with Collagen I (B.D. Biosciences). Cells were fed with defined keratinocyte serum free media (Gibco/Invitrogen, Grand Island, NY) and maintained for over 3 days, to insure confluence and recovery from trypsinization. Once the dishes were ready for wounding, the drill bits were autoclaved and affixed to the motor shaft in a sterile laminar flow hood. The height adjustment screw of the micromanipulator was used to slowly lower the spinning drill bit down to the cell surface. Removed cells were washed away in sterile phosphate buffered saline (PBS). Culture media was changed every day after wounding. Wounds were viewed using a Nikon Eclipse TE2000U inverted microscope (Nikon USA, Melville, NY), and images were recorded with a Hamamatsu C7780 CCD (Hamamatsu Corporation, Bridgewater, NJ) and Nikon D100 (Nikon USA, Melville, NY) cameras every 24 hours.

Time-Lapse Microscopy

For selected wounds, time-lapse microscopy was used to follow the wound-healing progression for up to 48 hours. During these measurements, a stage incubator was used to supply CO_2 and steady heat to maintain the temperature at 37° and Image Pro Plus 5 (Media Cybernetics) controlled time-lapse image acquisition at one-hour intervals.

In separate studies of individual cell migration rates, well plates were seeded with cells at low density (< 5,000 cells/cm^2). Three days after trypsinization, individual cells were imaged hourly by time-lapse microscopy for 24 hours.

Wounding Organ Culture Corneas

Fresh tissue samples were obtained from euthanized animals that were used for other research at Vanderbilt University in accordance with IUCAC guidelines. Rabbit, goat or pig eyes were enucleated and transported in sterile PBS with 1% antibiotic. In preliminary experiments it was noted that fresh, intact globes were the best candidates for precision wounding because they had higher intraocular pressure, which provided a less compliant and more stable wounding surface. Care was taken not to rupture the globe during enucleation and corneas were wounded within an hour of enucleation. Because movement during wounding causes varied, imprecise wound areas, globes were immobilized in test tube holders during wounding. The spinning drill was positioned with a micromanipulator and lowered using the micromanipulator's fine adjustment until just touching the corneal surface. In order to create superficial wounds, an additional 50-micron fine adjustment advancement was used to remove epithelium. In studies of partial thickness stromal wounds, a portion of the underlying corneal stroma was removed by advancing the micromanipulator an addition travel of 250 microns.

In globes with low intraocular pressure greater drill depth was required to insure epithelial removal from compliant corneas. We estimate that an additional drill advancement of up to 500 microns was required to make ~250-micron partial thickness wounds in some cases. After wounding, corneas were isolated by cutting the sclera to

form a corneal button. A millimeter rim of the sclera was kept all around the cornea button. This scleral ring is advantageous in organ culture as it slows swelling and helps to maintain corneal clarity and integrity. Before imaging, the corneal surface was washed with PBS containing 1% antibiotic to remove cell debris, then sodium fluorescein in PBS (25 mg/ml) was applied to visualize wound regions. After 30 seconds, excess fluorescein was washed off with PBS, and the corneas were placed on clear domes for imaging. Fluorescein was excited by using a bulb with a maximum emission peak in the near UV at 377nm, and fluorescence images were captured with a Nikon D100 camera coupled to a Zeiss surgical microscope. No emission filter was used. Corneas were washed in PBS following imaging and placed into 6 well plates for culture on agar plugs. Dulbeco's Minimum Essential Medium (DMEM), supplemented with 5% fetal bovine serum (FBS) was used to culture the corneas for up to a week. Fluorescein images of the wound region were taken every 24 hours.

Analysis of wound area, depth and healing rate

All image analysis was done using the Image Pro software package (IPP version 5.0, Media Cybernetics, Silver Spring, MD). Images were calibrated using a stage micrometer. Before analysis, each image was contrast enhanced by boosting the contrast to 75% and adjusting the overall brightness so that the background pixels had zero values. Using Image Pro's measurement tools, the automated free hand tool was used to identify the wound perimeter for both wounded cell culture monolayers and corneas. Image Pro reported the area of these regions in square microns, which were converted into corresponding areas in square millimeters. All initial wound areas and subsequent

wound healing areas were entered into Excel (Microsoft Office) spreadsheets for statistical analysis. In order to calculate average wound closure rate for each period, the wound diameter at the end of a time interval was subtracted from the initial wound diameter.

To determine the maximum epithelial front migration for wound healing in monolayer cultures, individual cells of the leading wound edge were selected for tracking. Migration speed was calculated by measuring cell center-to-center movement from one time-lapse point to the next, and the maximum movement was reported.

Epithelial stromal wound depth was quantified by subtracting the stromal thickness at the wound margin from the stromal thickness in the center of the wound after tissue fixation and sectioning.

Regression fit of in vitro wound healing area

In order to estimate the change in wounds area over the duration of healing, data points were fit with a linear regression curve whose slope is the wound closure rate.

Equation 1. Linear empirical curve fit of wound healing

$A(t) = A_o - (\text{Closure Rate}) \times (\text{time})$

It has been long established that epithelial wound closure is a process of coordinated cell movement, where cells on the wound margin spread and migrate into the wound void. Therefore, our mathematical model was developed to predict in vitro wound closure based solely on healing by cell migration from the wound margin. The assumption of the model is that the affect of cell division on wound healing is small in

comparison to the contribution from cell migration, and that cell migration will be driven by passive diffusion throughout wound healing.

Equation 2: Empircal curve fit assuming uniform cell migration from the wound margin

$$A(t) = \pi[R_0 - V_f(t)]^2$$

This empirical formula is based on the observation that the circular wounds are closing with a constant epithelial front speed, V_f, where R_0 initial wound radius, and t is the time of elapsed wound healing in days. Using the wound healing data, the epithelial front speed can be solved for, and can be compared between model systems and with individual cell migration rates.

Results

Cell culture wounds for longitudinal healing studies

In three separate trials a ~3.3mm drill bit produced wounds of 8.66 mm^2 ± 0.36 (N = 16), 8.86 mm^2 ± 0.18 (N = 16), and 8.85 mm^2 ± 0.05 (N = 16) in epithelial monolayers grown on Petri dishes coated with collagen. These wounds took an average of 7 days to completely close. Wound closure rate was fairly constant around 1.2 mm^2 per day. However, the greatest wound healing was observed in the first 24 hours (1.5 mm^2), with decreasing healing rate just before wound closure (day 6, <0.5 mm^2). Maximum epithelial front velocity within the first 24 hours exceeded 0.3 mm/day. Average epithelial front velocity over the duration of wound healing was 0.2 mm/day.

Similar healing rate parameters were found for wounds produced with larger and smaller drill bits. Bits of ~2.5mm in diameter produced wounds of 5.04 mm^2 ± 0.6 (N=16), and 4.99 mm^2 ± 0.44 (N=16), and bits with diameters of ~6mm created wounds of 31.06 mm^2 ± 3.10 (N = 9), 30.28 mm^2 ± 1.40 (N = 9) and 28.32 mm^2 ± 0.34 (N = 9). In the worst cases, standard deviations of wounds areas were around 10% of the average, and in the best cases, as low as 0.5%.

Individual corneal epithelial cell migration

Individual immortalized human corneal epithelial cells are active, locomotive cells, which are similar to primary epithelial cells in many respects (Araki-Sasaki, Ohashi et al. 1995). According to the analysis of time-lapse images of cell migration, these cells had an average migration rate of 8 microns per hour (0.19 mm/day), and maximal speeds of over 25 microns per hour (0.60 mm/day). These values are consistent with a previously published migration rate of 9 microns per hour for this cell line (Zhao, McCaig et al. 1997).

Superficial corneal wounds

Superficial wounds of 23.8 mm^2 ± 0.8 (N=4) were produced using 5.5 mm bits on pig cornea. Sodium fluorescein staining, as shown in Figure 31, was used to visualize wound areas for measurement. These wounds healed completely after 5 days, with an average epithelial front velocity of 0.6 mm/day.

Wounds of 6.16 mm^2 ± 0.6 (N=16) were produced using the 2.5 mm drill bit on fresh rabbit corneas. These wounds healed completely in 3 days, with an average

epithelial front velocity of 0.48 mm/day. These findings are consistent with a previous report by Hardarson et al for organ cultured corneas with wounds of 2-3mm which healed in 2-4 days (Hardarson, Hanson et al. 2004). Similar results were obtained for other types of organ culture corneas including goat and dog corneas (data not shown).

Partial thickness stromal wounds

Precise stromal wounds of 0.27 mm ± 0.05 (N=6) in depth were created in pig corneas by lowering the epithelial drill an additional 0.25 mm beyond superficial contact with the cornea. Wound depths were quantified in histological sections by measuring the stromal thickness in the central wound region, and the stromal thickness at the wound margin (Black bars in Figure 32). The average stromal thickness at the wound margin was 0.78 mm ± 0.08 (N=6). After partial thickness stromal wounding, the average stromal thickness in the center of the wound was 0.50 mm ± 0.06 (N=6). Like the superficial wounds of 5.5mm, partial stromal wounds of the same area healed completely in 5 days. There was no statistical difference in the epithelial coverage rate between superficial and stromal wounds.

Discussion

Using the equation $A(t) = \pi[R_0 - V_f(t)]^2$ to fit wound closure data, we solved for epithelial front migration speed V_f for different sized wounds in monolayers and organ culture cornea. The calculated migration speed for monolayer wounds was 0.20 mm/ day which is very similar to the average random walk migration speed for individual cells of this cell line (0.19 mm/day). The wound area equation appears to be a good regression fit

because it exhibits a second order curve shape that is consistent with the wound area data where wound area decreases the most rapidly early on during the healing process, and slows just before wound closure. In addition, the predictive value of this model is high, when V_f is set to 0.19 mm/day and compared to the data from 3.3mm diameter wounds $\{A(t) = \pi[1.67 - 0.192(t)]^2 (\text{mm}^2)\}$, the R^2 value is over 0.98, which is better than the linear regression R^2 of 0.96. For organ-cultured corneas, the epithelial migration speed was 0.48mm/day, approximately two and a half times as fast as monolayer closure.

Though in vitro and organ culture wound healing rates of corneal epithelium and corneal cell lines have been reported previously, this is the first report of using a precision drill apparatus for making similar sized wounds in different model systems. When we directly compare wound closure rates, we found that organ culture corneas heal more quickly than do monolayer cell culture wounds. Our results of wound closure in organ cultured corneas match previously reported rates for wounds created mechanically with a drill where 2-3mm in diameter wounds took 2 days to heal (Hardarson, Hanson et al. 2004). However, organ culture cornea wound healing rates are slower than reported in vivo healing rates, for example in rabbit eyes where 6 mm diameter wounds healed completely in less than 2 days (Watsky 1999). Though monolayer healing and organ culture healing of the same size wounds may not exhibit the same healing rates, we have characterized the wounds, making it possible to extrapolate wound healing rate from one model system to the next. From our results we estimate that organ culture healing of wounds greater than 2mm in diameter is twice as fast as monolayer healing, and according to published rates, healing in vivo is twice as fast as organ culture healing.

Our epithelial drill may also enable new experiments into partial thickness stromal injuries, which could include stromal remodeling and epithelial/stromal interactions. However, as noted in the methods section, high intraocular pressure of the eye is important for partial thickness wounding because pressure insures that the cornea does not comply during wounding. In these experiments we did not measure intraocular pressure before or during wounding, however we proceeded based on feel. When the cornea complied we continued drill travel until there was resistance against the drill, marking the start of applied wound depth. Future studies using this technique may opt for a way to control intraocular pressure, such as a canulated syringe, so that for each cornea the same range of travel of the drill can be used.

We have demonstrated the reproducibility of using a drill mounted on a micromanipulator to create precise wound areas in both corneal wound healing and cell culture models. This method may have future application in creating superficial and partial stromal circular wounds in vivo.

Acknowledgments

We thank Elizabeth Dworska, for her work as this project's primary cell technician. This work was sponsored in part by a NIH training grant HL 07751 and a Vanderbilt University Discovery Grant.

References

Araki-Sasaki, K., Y. Ohashi, et al. (1995). "An SV40-immortalized human corneal epithelial cell line and its characterization." Invest. Ophthalmol. Vis. Sci. 36(3): 614-621.

Buisson, A. C., J. M. Zahm, et al. (1996). "Gelatinase B is involved in the in vitro wound repair of human respiratory epithelium." J Cell Physiol 166(2): 413-26.

Burk, R. R. (1973). "A factor from a transformed cell line that affects cell migration." Proc Natl Acad Sci U S A 70(2): 369-72.

Cha, D., P. O'Brien, et al. (1996). "Enhanced modulation of keratinocyte motility by transforming growth factor-alpha (TGF-alpha) relative to epidermal growth factor (EGF)." J Invest Dermatol 106(4): 590-7.

Gottrup, F., M. S. Agren, et al. (2000). "Models for use in wound healing research: a survey focusing on in vitro and in vivo adult soft tissue." Wound Repair Regen 8(2): 83-96.

Hardarson, T., C. Hanson, et al. (2004). "Time-lapse recordings of human corneal epithelial healing." Acta Ophthalmol Scand 82(2): 184-8.

McGwin, G., Jr. and C. Owsley (2005). "Incidence of emergency department-treated eye injury in the United States." Arch Ophthalmol 123(5): 662-6.

Nash, E. A. and C. E. Margo (1998). "Patterns of emergency department visits for disorders of the eye and ocular adnexa." Arch Ophthalmol 116(9): 1222-6.

Reim, M., A. Kottek, et al. (1997). "The Cornea Surface and Wound Healing." Progress in Retinal and Eye Research 16(2): 183-225.

Watsky, M. A. (1999). "Loss of fenamate-activated K+ current from epithelial cells during corneal wound healing." Invest Ophthalmol Vis Sci 40(7): 1356-63.

Zhao, M., C. D. McCaig, et al. (1997). "Human corneal epithelial cells reorient and migrate cathodally in a small applied electric field." Curr Eye Res 16(10): 973-84.

Figures

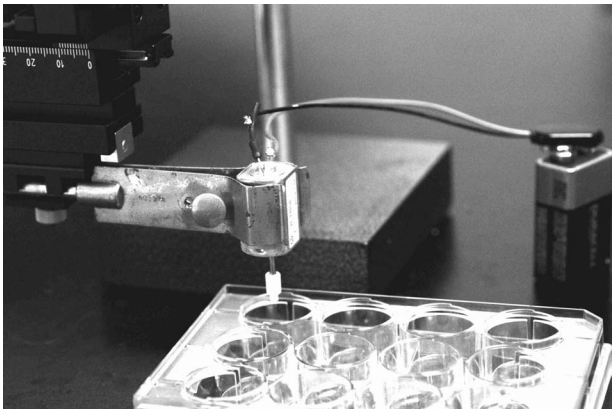

Figure 26. The epithelial drill apparatus consists of an interchangeable drill bit and a motor positioned using a micromanipulator.

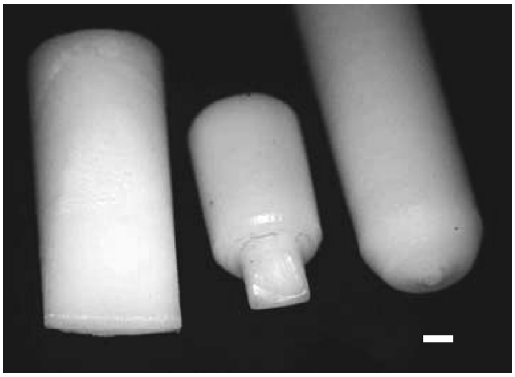

Figure 27. 5.5mm, 3mm and 0.5 mm Teflon drill bits. Scale bar 1mm.

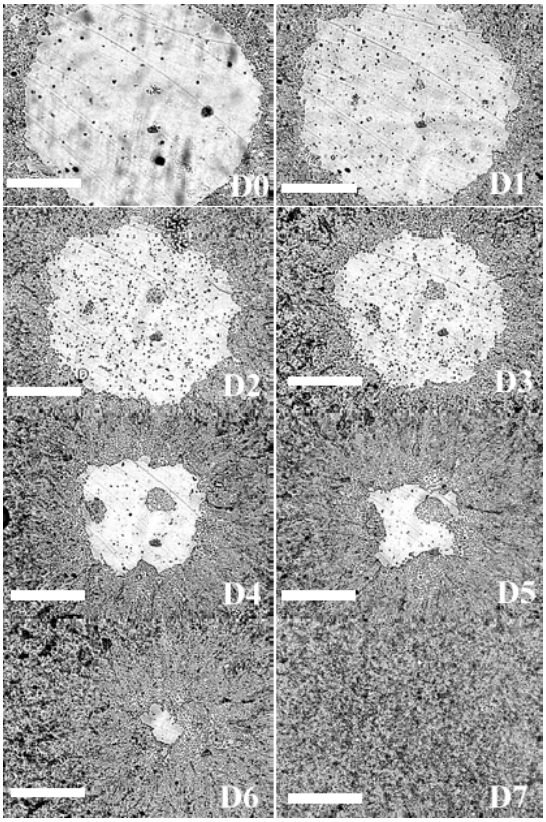

Figure 28. Healing progression of a 3mm diameter wound over 7 days. Initial wound is shown in the top left image, followed by day 1, day 2, day 3, day 4, day 5, day 6 and day 7 images. Scale bar is 1mm.

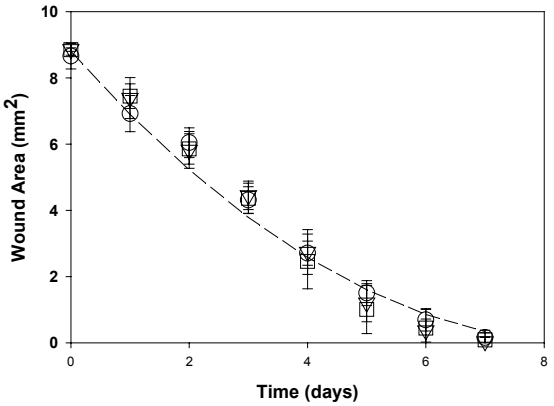

Figure 29. Three separate wound healing trials for wounds produced with a 3.3mm bit (8.8 mm^2). Average wound area is plotted as a function of time. The dashed line is the best fit migration model.

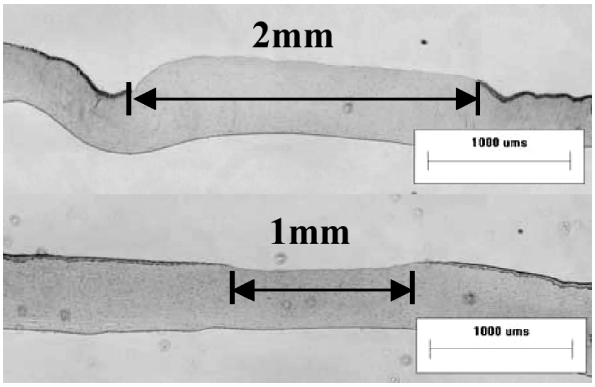

Figure 30. A superficial epithelial wound in a cultured rabbit cornea was created by epithelial drill with a 2mm drill bit (top). After 24 hours, an identical superficial wound heals partially (bottom).

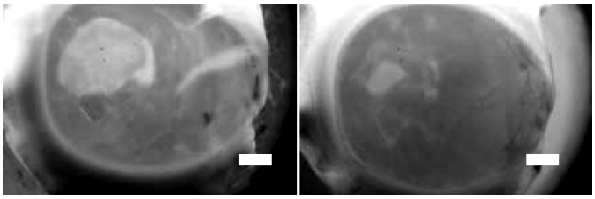

Figure 31. A superficial epithelial wound in a cultured pig cornea was created by epithelial drill with a 5.5mm drill bit (left). After 48 hours, the cornea heals partially (right). The scale bar is 2mm.

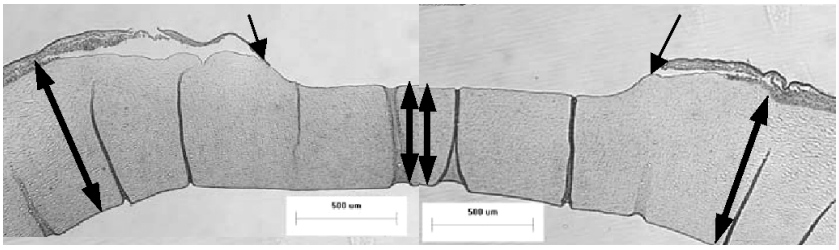

Figure 32. Partial thickness stromal wounds were created in pig cornea. The left wound margin (top); and right wound margin (bottom) show both removal of epithelium and a portion of the stroma in the wounded region. The black bars shown, denote measurements for stromal thickness. The striations seen are wrinkles introduced by fixation and embedding in paraffin.

BIBLIOGRAPHY

Ali, Z. and M. S. Insler (1986). "A comparison of therapeutic bandage lenses, tarsorrhaphy, and antibiotic and hypertonic saline on corneal epithelial wound healing." Ann Ophthalmol **18**(1): 22-4.

Amagai, M., V. Klaus-Kovtun, et al. (1991). "Autoantibodies against a novel epithelial cadherin in pemphigus vulgaris, a disease of cell adhesion." Cell **67**(5): 869-77.

Anderson, R. A. (1977). "Actin filaments in normal and migrating corneal epithelial cells." Invest Ophthalmol Vis Sci **16**(2): 161-6.

Andree, B., T. Hillemann, et al. (2000). "Isolation and characterization of the novel popeye gene family expressed in skeletal muscle and heart." Dev Biol **223**(2): 371-82.

Araki-Sasaki, K., Y. Ohashi, et al. (1995). "An SV40-immortalized human corneal epithelial cell line and its characterization." Invest. Ophthalmol. Vis. Sci. **36**(3): 614-621.

Araki-Sasaki, K., Y. Ohashi, et al. (1995). "An SV40-immortalized human corneal epithelial cell line and its characterization." Invest Ophthalmol Vis Sci **36**(3): 614-21.

Arias, A. M. (2001). "Epithelial mesenchymal interactions in cancer and development." Cell **105**(4): 425-31.

Aucoin, L., C. M. Griffith, et al. (2002). "Interactions of corneal epithelial cells and surfaces modified with cell adhesion peptide combinations." Journal of Biomaterials Science-Polymer Edition **13**(4): 447-462.

Balda, M. S., C. Flores-Maldonado, et al. (2000). "Multiple domains of occludin are involved in the regulation of paracellular permeability." J Cell Biochem **78**(1): 85-96.

Bates, R. C. and A. M. Mercurio (2005). "The epithelial-mesenchymal transition (EMT) and colorectal cancer progression." Cancer Biol Ther **4**(4): 365-70.

Ben Osman, N., A. Jeddi, et al. (1995). "[The cornea of diabetics]." J Fr Ophtalmol **18**(2): 120-3.

Bishop, A. L. and A. Hall (2000). "Rho GTPases and their effector proteins." Biochem J **348 Pt 2**: 241-55.

Brand, T. (2005). "The Popeye domain-containing gene family." Cell Biochem Biophys **43**(1): 95-103.

Brewitt, H. (1979). "Sliding of epithelium in experimental corneal wounds. A scanning electron microscopic study." Acta Ophthalmol (Copenh) **57**(6): 945-58.

Burk, R. R. (1973). "A factor from a transformed cell line that affects cell migration." Proc Natl Acad Sci U S A **70**(2): 369-72.

Cha, D., P. O'Brien, et al. (1996). "Enhanced modulation of keratinocyte motility by transforming growth factor-alpha (TGF-alpha) relative to epidermal growth factor (EGF)." J Invest Dermatol **106**(4): 590-7.

Chen, Z., W. H. Evans, et al. (2006). "Gap junction protein connexin 43 serves as a negative marker for a stem cell-containing population of human limbal epithelial cells." Stem Cells **24**(5): 1265-73.

Chuck, R. S., A. Behrens, et al. (2001). "Microkeratome-based limbal harvester for limbal stem cell transplantation: preliminary studies." American Journal of Ophthalmology **131**(3): 377-378.

Cotsarelis, G., S. Cheng, et al. (1989). "Existance of slow cycling limbal epithelial basal cells that can be preferentially stimulated to proliferate: implications on epithelial stem cells." Cell **57**: 201-209.

Crosson, C. E., S. D. Klyce, et al. (1986). "Epithelial wound closure in the rabbit cornea. A biphasic process." Invest Ophthalmol Vis Sci **27**(4): 464-73.

Datiles, M. B., P. F. Kador, et al. (1983). "Corneal re-epithelialization in galactosemic rats." Invest Ophthalmol Vis Sci **24**(5): 563-9.

Deutsch, J., D. Motlagh, et al. (2000). "Fabrication of microtextured membranes for cardiac myocyte attachment and orientation." J Biomed Mater Res **53**(3): 267-75.

DiAngelo, J. R., T. K. Vasavada, et al. (2001). "Production of monoclonal antibodies against chicken Pop1 (BVES)." Hybrid Hybridomics **20**(5-6): 377-81.

Evans, M. D., G. A. McFarland, et al. (2005). "The response of healing corneal epithelium to grooved polymer surfaces." Biomaterials **26**(14): 1703-11.

Fagerholm, P. (2000). "Wound healing after photorefractive keratectomy." J Cataract Refract Surg **26**: 4328-447.

Feenstra, R. P. and S. C. Tseng (1992). "What is actually stained by rose bengal?" Arch Ophthalmol **110**(7): 984-93.

Fischbarg, J., J. Hernandez, et al. (1985). "The mechanism of fluid and electrolyte transport across corneal endothelium: critical revision and update of a model." Curr Eye Res **4**: 351.

Furuse, M., K. Fujita, et al. (1998). "Claudin-1 and -2: novel integral membrane proteins localizing at tight junctions with no sequence similarity to occludin." J Cell Biol **141**(7): 1539-50.

Furuse, M., T. Hirase, et al. (1993). "Occludin: a novel integral membrane protein localizing at tight junctions." J Cell Biol **123**(6 Pt 2): 1777-88.

Garrod, D., M. Chidgey, et al. (1996). "Desmosomes: differentiation, development, dynamics and disease." Curr Opin Cell Biol **8**(5): 670-8.

Gipson, I. K. (1992). "Adhesive mechanisms of the corneal epithelium." Acta Ophthalmol Suppl(202): 13-7.

Gipson, I. K., S. Spurr-Michaud, et al. (1989). "Reassembly of the anchoring structures of the corneal epithelium during wound repair in the rabbit." Invest Ophthalmol Vis Sci **30**(3): 425-34.

Gonzalez-Mariscal, L., A. Betanzos, et al. (2003). "Tight junction proteins." Prog Biophys Mol Biol **81**(1): 1-44.

Gottrup, F., M. S. Agren, et al. (2000). "Models for use in wound healing research: a survey focusing on in vitro and in vivo adult soft tissue." Wound Repair Regen **8**(2): 83-96.

Greenburg, G. and E. D. Hay (1982). "Epithelia suspended in collagen gels can lose polarity and express characteristics of migrating mesenchymal cells." J Cell Biol **95**(1): 333-9.

Greenburg, G. and E. D. Hay (1986). "Cytodifferentiation and tissue phenotype change during transformation of embryonic lens epithelium to mesenchyme-like cells in vitro." Dev Biol **115**(2): 363-79.

Grueterich, Scheffer, et al. (1996). "Human limbal progenitor cells expanded on intact amniotic membrane ex vivo." Archives of Ophthalmology **120**(6): 783-791.

Grueterich, Scheffer, et al. (2002). "Human limbal progenitor cells expanded on intact amniotic membrane ex vivo." Archives of Ophthalmology **120**(6): 783-791.

Gumbiner, B., T. Lowenkopf, et al. (1991). "Identification of a 160-kDa polypeptide that binds to the tight junction protein ZO-1." Proc Natl Acad Sci U S A **88**(8): 3460-4.

Gumbiner, B. M. (1996). "Cell adhesion: the molecular basis of tissue architecture and morphogenesis." Cell **84**(3): 345-57.

Haik, B. G. and M. L. Zimny (1977). "Scanning electron microscopy of corneal wound healing in the rabbit." Invest Ophthalmol Vis Sci **16**(9): 787-96.

Hanahan, D. and R. A. Weinberg (2000). "The hallmarks of cancer." Cell **100**(1): 57-70.

Hanna, C., D. S. Bicknell, et al. (1961). "Cell turnover in the adult eye." Archives of Ophthalmology **65**: 695.

Hardarson, T., C. Hanson, et al. (2004). "Time-lapse recordings of human corneal epithelial healing." Acta Ophthalmol Scand **82**(2): 184-8.

Haskins, J., L. Gu, et al. (1998). "ZO-3, a novel member of the MAGUK protein family found at the tight junction, interacts with ZO-1 and occludin." J Cell Biol **141**(1): 199-208.

Hirohashi, S. (1998). "Inactivation of the E-cadherin-mediated cell adhesion system in human cancers." Am J Pathol **153**(2): 333-9.

Huttenlocher, A., M. Lakonishok, et al. (1998). "Integrin and cadherin synergy regulates contact inhibition of migration and motile activity." J Cell Biol **141**(2): 515-26.

Inoue, K., S. Kato, et al. (2001). "Ocular and systemic factors relevant to diabetic keratoepitheliopathy." Cornea **20**(8): 798-801.

Kaufman, H. E. (1998). The Cornea. Boston, Butterworth-Heinemann.

Kenney, M. C. and M. Chwa (1990). "Abnormal extracellular matrix in corneas with pseudophakic bullous keratopathy." Cornea **9**(2): 115-21.

Kenyon, K. and S. Tseng (1989). "Limbal autograft transplantation for ocular surface disorders." Ophthalmology **96**: 709-23.

Kenyon, K. and S. Tseng (1989). "Limbal autograft transplantation for

ocular surface disorders." Ophthalmology **96**: 709-23.

Kim, J. and S. Tseng (1995). "Transplantation of preserved human amniotic membrane for surface reconstruction in severely damaged rabbit corneas." Cornea **14**: 473-484.

Knight, R. F., D. M. Bader, et al. (2003). "Membrane topology of Bves/Pop1A, a cell adhesion molecule that displays dynamic changes in cellular distribution during development." J Biol Chem **278**(35): 32872-9.

Koizumi, N., T. Inatomi, et al. (2001). "Cultivated corneal epithelial stem cell transplantation in ocular surface disorders." Ophthalmology **108**(9): 1569-1574.

Kourenkov, V., O. Mytiagina, et al. (1999). "Stimulating re-epithelialization after photorefractive keratectomy." J Refract Surg **15(2 suppl)**: S234-7.

Kuriana, P., B. Kasibhatlaa, J. Dauma, C.A. Burnsb, M. Moosac, K.S. Rosenthald, J.P. Kennedya (2003). "Synthesis, permeability and biocompatibility of tricomponent

membranes containing polyethylene glycol, polydimethylsiloxane and polypentamethylcyclopentasiloxane domains." Biomaterials **24**: 3493–3503.

Larouche, K., S. Leclerc, et al. (2000). "Expression of the alpha 5 integrin subunit gene promoter is positively regulated by the extracellular matrix component fibronectin through the transcription factor Sp1 in corneal epithelial cells in vitro." J Biol Chem **275**(50): 39182-92.

Le Sage, N., R. Verreault, et al. (2001). "Efficacy of eye patching for traumatic corneal abrasions: a controlled clinical trial." Ann Emerg Med **38**(2): 129-34.

Lee, J. N., C. Park, et al. (2003). "Solvent compatibility of poly(dimethylsiloxane)-based microfluidic devices." Anal Chem **75**(23): 6544-54.

Liesegang, T. J., L. J. Melton, 3rd, et al. (1989). "Epidemiology of ocular herpes simplex. Incidence in Rochester, Minn, 1950 through 1982." Arch Ophthalmol **107**(8): 1155-9.

Lim, J. J. and H. H. Ussing (1982). "Analysis of presteady-state Na+ fluxes across the rabbit conreal endothelium." J Membr Biol **65**: 187.

Mata, A., C. Boehm, et al. (2002). "Growth of connective tissue progenitor cells on microtextured polydimethylsiloxane surfaces." J Biomed Mater Res **62**(4): 499-506.

Matsuzaka, K., X. F. Walboomers, et al. (2003). "The attachment and growth behavior of osteoblast-like cells on microtextured surfaces." Biomaterials **24**(16): 2711-9.

McGwin, G., Jr. and C. Owsley (2005). "Incidence of emergency department-treated eye injury in the United States." Arch Ophthalmol **123**(5): 662-6.

Meller, D., V. Dabul, et al. (2002). "Expansion of conjunctival epithelial progenitor cells on amniotic membrane." Exp Eye Res **74**(4): 537-45.

Merrett, K., C. M. Griffith, et al. (2003). "Interactions of corneal cells with transforming growth factor beta 2-modified poly dimethyl siloxane surfaces." Journal of Biomedical Materials Research Part A **67A**(3): 981-993.

MolecularProbes (2003). "Follow that cell." BioProbes(44).

Monge, S., A. Mas, et al. (2003). "Improvement of silicone endothelialization by treatment with allylamine and/or acrylic acid low-pressure plasma." Journal of Applied Polymer Science **87**(11): 1794-1802.

Monier-Gavelle, F. and J. L. Duband (1995). "Control of N-cadherin-mediated intercellular adhesion in migrating neural crest cells in vitro." J Cell Sci **108 (Pt 12)**: 3839-53.

Morra, M., E. Occhiello, et al. (1990). "The characterization of plasma-modified polydimethylsiloxane interfaces with media of different surface energy." Clin Mater **5**(2-4): 147-56.

Nagafuchi, A. (2001). "Molecular architecture of adherens junctions." Curr Opin Cell Biol **13**(5): 600-3.

Nagasaki, T. and J. Zhao (2003). "Centripetal Movement of Corneal Epithelial Cells in the Normal Adult Mouse." Invest. Ophthalmol. Vis. Sci. **44**(2): 558-566.

Nakamura, M., N. Sato, et al. (1997). "Fibronectin facilitates corneal epithelial wound healing in diabetic rats." Exp Eye Res **64**(3): 355-9.

Nash, E. A. and C. E. Margo (1998). "Patterns of emergency department visits for disorders of the eye and ocular adnexa." Arch Ophthalmol **116**(9): 1222-6.

Ng, J. M., I. Gitlin, et al. (2002). "Components for integrated poly(dimethylsiloxane) microfluidic systems." Electrophoresis **23**(20): 3461-73.

Nichols, B., C. R. Dawson, et al. (1983). "Surface Features of the conjunctiva and the cornea." Invest Ophthalmol Vis Sci **24**: 570.

Nishida, K., M. Yamato, et al. (2004). "Functional bioengineered corneal epithelial sheet grafts from corneal stem cells expanded ex vivo on a temperature-responsieve cell culture surface." Transplantation **77**(3): 379-385.

Ohashi, Y., M. Matsuda, et al. (1988). "Aldose reductase inhibitor (CT-112) eyedrops for diabetic corneal epitheliopathy." Am J Ophthalmol **105**(3): 233-8.

Osler, M. E., M. S. Chang, et al. (2005). "Bves modulates epithelial integrity through an interaction at the tight junction." J Cell Sci **118**(Pt 20): 4667-78.

Pahlitzsch, T. and P. Sinha (1985). "The alkali burned cornea: electron microscopical, enzyme histochemical, and biochemical observations." Graefes Arch Clin Exp Ophthalmol **223**(5): 278-86.

Pan, Z., W. Zhang, et al. (2002). "Transplantation of corneal stem cells cultured on amniotic membrane for corneal burn: experimental and clinical study." Chin Med J (Engl) **115**(5): 767-9.

Pellegrini, G., O. Golisano, et al. (1999). "Location and clonal analysis of stem cells and their differentiated progeny in the human ocular surface." J Cell Biol **145**(4): 769-82.

Pellegrini, G., R. Ranno, et al. (1999). "The control of epidermal stem cells (holoclones) in the treatment of massive full-thickness burns with autologous keratinocytes cultured on fibrin." Transplantation **68**(6): 868-79.

Pellegrini, G., C. E. Traverso, et al. (1997). "Long-term restoration of damaged corneal surfaces with autologous cultivated corneal epithelium." The Lancet **349**(9057): 990-993.

Pino, C. J., F. R. Haselton, et al. (2005). "Seeding of corneal wounds by epithelial cell transfer from micropatterned PDMS contact lenses." Cell Transplant **14**(8): 565-71.

Quantock, A. J., N. Koizumi, et al. (2002). "Limbal stem cell deficiencies and ocular surface reconstruction." Optometry Today(July 12th): 27-30.

Reese, D. E. and D. M. Bader (1999). "Cloning and expression of hbves, a novel and highly conserved mRNA expressed in the developing and adult heart and skeletal muscle in the human." Mamm Genome **10**(9): 913-5.

Reese, D. E., M. Zavaljevski, et al. (1999). "bves: A novel gene expressed during coronary blood vessel development." Dev Biol **209**(1): 159-71.

Reim, M., A. Kottek, et al. (1997). "The cornea surface and wound healing." Progress in Retinal and Eye Research **16**(2): 183-225.

Ripley, A. N., M. S. Chang, et al. (2004). "Bves is expressed in the epithelial components of the retina, lens, and cornea." Invest Ophthalmol Vis Sci **45**(8): 2475-83.

Ripley, A. N., M. E. Osler, et al. (2006). "Xbves is a regulator of epithelial movement during early Xenopus laevis development." Proc Natl Acad Sci U S A **103**(3): 614-9.

Rosenberg, M. E., T. M. Tervo, et al. (2000). "Corneal structure and sensitivity in type 1 diabetes mellitus." Invest Ophthalmol Vis Sci **41**(10): 2915-21.

Sanchez-Thorin, J. C. (1998). "The cornea in diabetes mellitus." Int Ophthalmol Clin **38**(2): 19-36.

Sariri, R. and R. Sabbaghzadeh (2001). "Competitive adsorption of proteins on hydrogel contact lenses." Clao J **27**(3): 159-62.

Schermer, A., S. Galvin, et al. (1986). "Differentiation-related expression of a major 64K corneal keratin in vivo and in culture suggests limbal location of corneal epithelial stem cells." J. Cell Biol. **103**(1): 49-62.

Schwab, I. R. and R. R. Isseroff (2000). "Bioengineered Corneas -- The Promise and the Challenge." N Engl J Med **343**(2): 136-138.

Shimazaki, J., M. Aiba, et al. (2002). "Transplantation of human limbal epithelium cultivated on amniotic membrane for the treatment of severe ocular surface disorders." Ophthalmology **109**(7): 1285-1290.

Soong, H. K. (1987). "Vinculin in focal cell-to-substrate attachments of spreading corneal epithelial cells." Arch Ophthalmol **105**(8): 1129-32.

Soong, H. K., B. Dass, et al. (1990). "Effects of cytochalasin D on actin and vinculin in cultured corneal epithelial cells." J Ocul Pharmacol **6**(2): 113-21.

Stevenson, B. R., J. D. Siliciano, et al. (1986). "Identification of ZO-1: a high molecular weight polypeptide associated with the tight junction (zonula occludens) in a variety of epithelia." J Cell Biol **103**(3): 755-66.

Stoker, M. (1989). "Effect of scatter factor on motility of epithelial cells and fibroblasts." J Cell Physiol **139**(3): 565-9.

Tseng, S. C., P. Prabhasawat, et al. (1998). "Amniotic membrane transplantation with or without limbal allografts for corneal surface reconstruction in patients with limbal stem cell deficiency." Arch Ophthalmol **116**(4): 431-41.

Tsubota, K., Y. Satake, et al. (1999). "Treatment of Severe Ocular-Surface Disorders with Corneal Epithelial Stem-Cell Transplantation." N Engl J Med **340**(22): 1697-1703.

van Kooten, T. G., J. F. Whitesides, et al. (1998). "Influence of silicone (PDMS) surface texture on human skin fibroblast proliferation as determined by cell cycle analysis." J Biomed Mater Res **43**(1): 1-14.

Vascotto, S. G. and M. Griffith (2006). "Localization of candidate stem and progenitor cell markers within the human cornea, limbus, and bulbar conjunctiva in vivo and in cell culture." Anat Rec A Discov Mol Cell Evol Biol **288**(8): 921-31.

Vracko, R. and E. P. Benditt (1972). "Basal Lamina:the scaffold for orderly cell replacement. Observations on regeneration of injured skeletal muscles and capillaries." J Cell Biology **55**: 406.

Wada, A. M., D. E. Reese, et al. (2001). "Bves: prototype of a new class of cell adhesion molecules expressed during coronary artery development." Development **128**(11): 2085-93.

Waterman-Storer, C. M., W. C. Salmon, et al. (2000). "Feedback interactions between cell-cell adherens junctions and cytoskeletal dynamics in newt lung epithelial cells." Mol Biol Cell **11**(7): 2471-83.

Watsky, M. A. (1999). "Loss of fenamate-activated K+ current from epithelial cells during corneal wound healing." Invest Ophthalmol Vis Sci **40**(7): 1356-63.

Weaver, V. M., O. W. Petersen, et al. (1997). "Reversion of the malignant phenotype of human breast cells in three-dimensional culture and in vivo by integrin blocking antibodies." J Cell Biol **137**(1): 231-45.

Weene, L. E. (1985). "Recurrent corneal erosion after trauma: a statistical study." Ann Ophthalmol **17**(9): 521-2, 524.

Wiederholt, M., T. J. Jentsch, et al. (1985). "Electrical sodiumcarbonate symport in cultured corneal endothelial cells." Pflugers Arch **405**: S167.

Zhao, M., C. D. McCaig, et al. (1997). "Human corneal epithelial cells reorient and migrate cathodally in a small applied electric field." Curr Eye Res **16**(10): 973-84.